ANALYSIS OF CIRCULAR PLATE WITH TUNABLE FREQUENCY

BY

SYED NOH BIN SYED ABU BAKAR

A thesis submitted in fulfilment of the requirement for the degree of Doctor of Philosophy in Engineering

Kulliyyah of Engineering
International Islamic University Malaysia

AUGUST 2015

ABSTRACT

The study of plate with tunable frequency becomes an important study as it aids for more effective design of plate for the use of devices such as resonator (i.e. SJAs, speakers) or energy harvesting devices. This study explored on idea of a structure which its frequency may be tuned through the application of electrical means alone. This idea would eliminate the needs of extra mechanical structure in certain transportation such as aircraft. A circular plate is tuned through attaching a piezoceramic annular plate at the edge of a circular plate. By controlling the voltage applied to the piezoceramic annular plate, thus the radial load, the fundamental frequency of the circular plate may be tuned. The analysis is performed by using finite different method which coded through MATLAB®. The study is divided into two major parts. First part is the study of circular plate buckling problem in order to obtain the limit of radial load that may be applied by using attached piezoceramic annular plate. This will provide an information on significant radial load. Second part is the study of circular plate vibration problem which aim to look at the feasibility of using attached piezoceramic annular plate in tuning the circular plate frequency. For both, buckling and vibration problems, a parametric study was also performed. Results on vibration problem showed that the radial load applied through attached piezoceramic annular plate gave a significant range of frequency tuning for most configuration reported. Parametric study for buckling problem showed that the inner radius has a significant influence in critical buckling voltage except for the case of annular plate is thicker than the circular plate. Also, it is found that for inner radius far enough from the outer radius, the circular thickness only influence the critical buckling voltage when the circular plate has thickness near the annular plate or smaller. Lastly, the critical buckling voltage increases as the annular thickness increases regardless the annular plate is thicker or thinner than the circular plate. On the other hand, parametric study for vibration problem showed that the fundamental frequency is independent of the radius if the annular plate has equal thickness as the circular plate. While the similar may be conclude for the case where the annular is thicker than the circular plate but only for the if the inner radius is less than half of the outer radius. The fundamental frequency reduces rapidly as the inner radius became larger than half of the outer radius. For the case where the annular plate is thinner than the circular plate, the fundamental frequency increases with the change of the inner radius.

خلاصة البحث

المعادلة المسيطره التي تحكم اللوحة الدائرية و الحلقية للمادة المتجانسة قد تم استحداثها. المعادلات المسيطره قابلة للتطبيق عند الالتواء و مشاكل الاهتزاز خارج الطائرة. و أجريت دراسة على اللوحة الدائرية مع التردد الانضباطي. ويتحقق ضبط تردد من خلال ربط اللوحة الحلقيه بيزو السيراميك على حافة الصفيحة الدائرية. عن طريق التحكم في الجهد المطبق على اللوحة الحلقي بيزو السيراميك ، وبالتالي فإن تحميل شعاعي ، ويمكن ضبطها تواتر الأساسية من لوحة دائرية. يتم دراستها دراسة التواء من اللوحة الدائرية مع اللوحة الحلقية بيزو السيراميك و تعلق على حافته لإظهار جدوى هذه الفكرة. أظهرت النتائج من خلال التحكم في تطبيق الجهد ، وعموما الحمل التواء من اللوحة الدائرية تغيرت مما يدل على جدوى الأسلوب في التردد الأساسي من خلال ضبط تطبيق الحمولة الشعاعية عبر اللوحة الحلقي بيزو السيراميك. وهناك مشكلة من الاهتزاز من لوحة دائرية أن اللوحة الحلقي بيزو السيراميك تعلق على حافته تحت حمولة شعاعي و درس أيضا. ومن المعروف أن وتيرة الأساسية يذهب إلى الصفر في التواء الحمل. اللوحة دائرية حالة و حلقي سمك متساوون في 0.3 ملم يظهر تردد الأساسية لتكون قادرة على ضبط ما يصل إلى 0 هرتز. ومع ذلك ،لسمك مختلف، هو أنه أظهر أن تكوين لوحة الحلقي يلعب دورا هاما في فعالية تحميل شعاعي المطبقة في ضبط التردد الأساسي. أكبر عرض أو سمكا من لوحة الحلقي سيعطي التغيير أكثر أهمية في التردد الأساسي في تأثير الحمل شعاعي تطبيقها. ويرجع ذلك إلى الجهد القسرية من لوحة بيزو السيراميك القيد.

APPROVAL PAGE

The thesis of Syed Noh Bin Syed Abu Bakar has been approved by the following:

_____
Waleed Fekry Faris
Supervisor

_____
Sany Izan Ihsan
Co-Supervisor

_____
Yulfian Aminanda
Internal Examiner

_____
Ahmad Kamal Ariffin
External Examiner

_____
Mohamed B. Trabia
External Examiner

_____
Hassan Ahmed Ibrahim
Chairman

DECLARATION

I hereby declare that this dissertation is the result of my own investigations, except where otherwise stated. I also declare that it has not been previously or concurrently submitted as a whole for any other degrees at IIUM or other institutions.

Syed Noh Bin Syed Abu Bakar

Signature ..... Date 9th July 2015

INTERNATIONAL ISLAMIC UNIVERSITY MALAYSIA

DECLARATION OF COPYRIGHT AND AFFIRMATION OF FAIR USE OF UNPUBLISHED RESEARCH

ANALYSIS OF CIRCULAR PLATE WITH TUNABLE FREQUENCY

Affirmed by Syed Noh Bin Syed Abu Bakar.

……. 9th July 2015

Signature Date

ACKNOWLEDGEMENTS

First and foremost, gratitude and appreciation is for Allah, the Most Merciful and Most Compassionate for granting me a precious opportunity to complete this work and granted me health and strength for the realization of this endeavor.

I would like to gratefully thank my supervisor, Dr. Waleed Fekry Faris for his scholarly guidance and tireless effort in assisting me in this very work. Truly this work shall not be completed without his continuous encouragement and support.

I would like to thank also to my co-supervisor, Dr Sany Izan Ihsan for his motivation and guidance in keeping me going with the works. With his assistance I manage to complete this thesis. I believe that without him, completion of this thesis will much harder.

I would also like to thank to Dr. Mostafa Abdalla for his motivation and assistance and always making himself available for any help during my time at TU Delft, Holland. Not to forget also my colleagues at the Kulliyyah of Engineering, IIUM especially Dr. Hanafi and Dr. Raihan for offering to hear and share all problems and challenges of PhD student. Also to all others, whether academic and non-academic staff for assistance and for keeping asking me on my completion of study.

This work would not be possible without the scholarship provided by the Government of Malaysia and International Islamic University Malaysia throughout the study period.

Of course, I owe the greatest debt of gratitude to my beloved wife, Dr Nurul Yaqeen, for her patience, support, understanding, assistance and prayer throughout my study, especially during the three years period in Delft, Holland. It would surely be impossible for me to complete this work without her contribution. Also gratitude to my sons – Luqman, Iqbal and Qutb for making my life very exciting and lively. Not to forget my deepest gratitude to my beloved late mother, Hjh. Sharifah Salmah S.D. Abbas and father, Syed Abu Bakar Syed Mohamad for their love and prayers

I wish to express my appreciation and thanks to those who provided their time, effort and support for this project. To the members of my dissertation committee, thank you for sticking with me.

TABLE OF CONTENTS

LIST OF TABLES

LIST OF FIGURES

LIST OF SYMBOLS

N_0	Applied Radial Load
V	Applied Voltage
$D^{(a)}$	Bending Stiffness of Annular Plate
$D^{(b)}$	Bending Stiffness of Bimorph Circular Plate
$D^{(s)}$	Bending Stiffness of Isotropic Solid Circular Plate
κ_{22}	Circumferential Curvature
θ	Circumferential Direction/Angle
N_{22}	Circumferential Load
e_{22}	Circumferential Strain
e_{22}^0	Circumferential Strain at Mid-surface
s_{ij}^E	Compliance Constants at Constant Electric Field
ρ	Density of Isotropic Plate
ρ_p	Density of Piezoceramic Plate
ϵ_{ij}^T	Dielectric Constants at Constant Stress
v_0	Displacement of Mid-surface in Circumferential Direction
u_0	Displacement of Mid-surface in Radial Direction
w_0	Displacement of Mid-surface in Thickness Direction
D_i	Electric Displacement Components
E_i	Electric Field Components
ϕ	Electric Potential
h_a	Half Thickness of Annular Plate

h	Half Thickness of Isotropic Layer/Plate
r_i	Inner Radius
r_o	Outer Radius
d_{ij}	Piezoelectric Constants
k_p	Planar Electromechanical Coupling Coefficient
ν_p	Poisson Ratio for Piezoceramic Plate
μ	Poisson ratio for the isotropic shim
κ_{11}	Radial Curvature
r	Radial Direction
N_{11}	Radial Load
e_{11}	Radial Strain
e_{11}^0	Radial Strain at Mid-surface
κ_{12}	Shear Curvature
N_{12}	Shear Load
e_{12}	Shear Strain
e_{12}^0	Shear Strain at Mid-surface
$e_{ij}^{(p)}$	Strains Components
$A^{(b)}$	Strecthing Stiffness of Bimorph Circular Plate
$\sigma_{ij}^{(p)}$	Stresses Components
$A^{(a)}$	Stretching Stiffness of Annular Plate
$A^{(s)}$	Stretching Stiffness of Isotropic Solid Circular Plate
z	Thickness Direction

h_p	Thickness of Piezoceramic Layer
q	Total Charge
E	Young coefficient for the isotropic shim

Subscript

P	piezoelectric

Supercript

(a)	Annular pieoceramic plate
(s)	Solid circular isotropic plate

CHAPTER ONE

INTRODUCTION

1.1 OVERVIEW

In this chapter, problem statement, background and motivation for the current research are presented. The chapter started with presentation of the motivation and background of the research. From the background, a problem statement is raised and a philosophy to the research solutions is presented. Then, the scope of the research is briefly explained. In order to answer the problem statement, several objectives are laid down. The approach of current study is explained in research methodology. The chapter concluded with thesis outline and the contributions of current study.

1.2 INTRODUCTION

Vehicles must consume fuel to supply the energy needed to move the vehicles and their passengers. The greater force needed to move the vehicles, the greater fuel will be consumed. One of the forces that contributed to greater fuel consumption is the aerodynamic drag. Aerodynamic drag exerts a force on the vehicles in the opposite direction from the velocity. It is known to be a principal determinant of energy consumption in the vehicles such as aircrafts because they operate at such high speeds. One flow phenomenon that contribute to increase of aerodynamic drag is known as flow separation. It is a phenomenon where the fluid flow becomes detached from the surface of the object or surface, and instead takes the forms of eddies and vortices. It is of interest many researchers to eliminate the separation or at least to delay the separation in order to reduce drag, hence reducing the fuel consumptions.

Method of separation control may be classified into passive and active approach. Passive approach is achieved by design an optimal aerodynamic shape of the vehicle body or by attaching structure such as wingtip and shark fin that may delay the flow separation. On the other side, active approach is achieved by attaching structure that may interact with the flow depending on the flow conditions. In passive approach, the structure is designed to handle flow separation for certain range of velocity. Outside this range the approach may be ineffective or even may be negatively influence the flow past the objects (i.e. create larger drag). On the other hand, active approach is more beneficial since it interacts with the flow depending on the flow conditions. Even better, with the advancement of current sensor-actuator technology and computer technology, the system may be designed to adapt to the surrounding automatically without the interference of human.

One of the examples of the concepts in active flow control is steady injecting momentum and removing mass from the boundary layer (near surface flow field). Typical example of researches in steady injection of momentum is by continuous blowing, known as surface-tangential blowing. While it may found way to production aircraft but it plagued by technical complexity and additional weight resulting from plumbing systems. Meanwhile a typical example of removing mass is by continuous suction. Similar to blowing, suction also has complex piping systems and also add weight. However, in recent years, there is an emergence of new technology that combined the concepts of injecting and removing which is known as synthetic jet actuator (SJA). An SJA also known as a zero-net-mass but non-zero momentum fluid flux generated by an oscillating structure such as a piezo-oscillator.

Research work on SJAs has shown great potential of using SJA in active control of boundary layer separation in order to reduce the drag and increase the efficiency of

aerodynamic devices. The SJA consists of an oscillated boundary (i.e. electrically oscillated membrane and moving piston) located at the bottom of a small cavity which has an orifice in the face opposite the membrane.

Many research works have shown that the actuation frequency of the SJA plays a significant role in optimum separation control. Since for moving vehicles, the speed of the vehicles is changing throughout the travelling course, the flow regime or pattern also changing. Therefore, in order to have an optimum design of SJA, there is need to design an SJA that its actuation frequency may be tuned depending on the vehicle speed.

For an SJA that its oscillating boundary is a piezoceramic plate, the plate frequency may be tuned by several ways. Some of the researchers have showed that the natural frequencies may be control via shunt circuit (Davis & Lesieutre, 2000; Hagood & Flotov, 1991). However, there is limited range of frequency that may be tuned depending on the shunt circuit properties such as the capacitance. On the other hands there are also some researchers that showed how the in-plane load influenced the natural frequencies (Hebert & Lesieutre, 1998; Hu, et al., 2007; Lesieutre & Davis, 1997). Their study was limited to either on beam structure or by using complicated mechanical structure to provide the in-plane load.

1.3 PROBLEM STATEMENT AND ITS SIGNIFICANTS

Given the background of the study from the previous introduction, one would question whether the range of the tunable frequency may be broadened by using applied in-plane load without having complicated mechanical structure. To answer this question, one aims to study the idea of applying in-plane loads via electrical means in controlling the natural frequencies, therefore eliminating complicated mechanical structure. By eliminating the needs of mechanical structure, one would expect reduces in weight

and/or size of a structure. For industry that put significant effort in reducing weight and size such as aerospace industry, the benefit of reducing weight and size would present a significant contribution.

To achieve the aim, one would study the effects of the in-plane load to natural frequency of a circular plate. The in-plane load is provided by using piezoceramic material as part of the circular plate structure. The piezoceramic material is used as a medium to provide the in-plane load through applied voltage.

1.4 RESEARCH PHILOSOPHY

SJA has emerged as an interesting method in controlling separation. However, it still did not found its way to actual application in aircraft industry or in any aerodynamics related devices. One of the issue related in designing an actuator as SJA is the effectiveness of its application in wide range of flow conditions. One of the factors that influence the effectiveness SJA is the frequency of the vortex trains that are produced by SJA. The frequency of the vortex trains are influenced by the frequency of the vibrating boundary that produced the vortex trains. Therefore, broadening the operating frequency of the vibrating boundary will also improve the performance of the SJA.

For SJA that the vibrating boundary is a piezoceramic plate, one may control the frequency via shunt circuit or apply in-plane load. While shunt circuit application limited to narrow frequency band depending on the passive design of the shunt circuit, the application of in-plane load riddle with complicated mechanical structure. It is desirable that the complicated mechanical structure may be removed while the frequency range may be broadened. The issue may be resolved if the in-plane load may be produced through electrical means. One way to produce the in-plane load is by using

piezoceramic materials since the piezoceramic material has ability to convert electrical current to mechanical strains.

1.5 RESEARCH SCOPE

In current study, one would study vibration of circular plate structure under the influence of in-plane load. As part of the circular plate piezoceramic material is used as the medium of conversion of electrical voltage to mechanical strains (thus in-plane load).

This study is conducted through numerical method called Finite Difference Method. However, variables such as electric distributions and the in-plane loads are derived analytically. The derived variables are used with combination with the classic governing equations that govern a circular plate buckling and vibration problem to complete the numerical study. The obtained governing equations in FDM formulation is coded in MATLAB®. The validity of the MATLAB® code is validated by comparing the ability of the code to produced results for problems in available literatures.

1.6 RESEARCH OBJECTIVES

The specific objectives of this study are:

i. Formulate equations and load distributions that govern vibration problem of a circular plate with applied intermediate radial load using piezoceramic.
ii. Develop and validate finite difference code.
iii. Apply the finite difference code for buckling and vibration problem of circular plate with applied intermediate radial load.

iv. Determine the influence of intermediate in-plane load from electrical means to the natural frequency.

1.7 RESEARCH METHODOLOGY

The research methodology is summarized in the following chart.

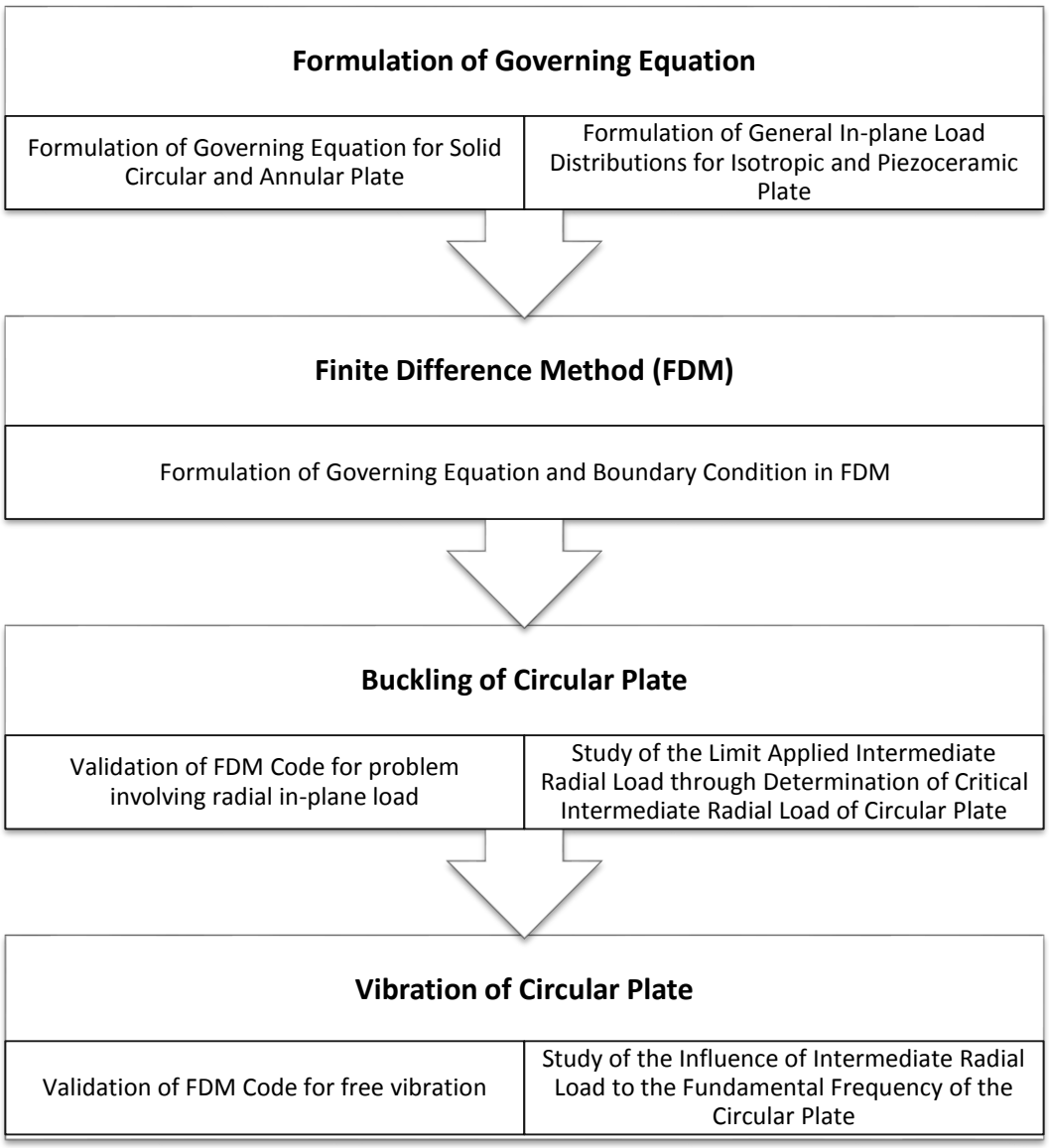

In order to achieve the objective one would approaches the circular plate problem numerically by using finite difference method that is coded in MATLAB. In

brief, one would first formulate the required load distributions and governing equations that governed a circular plate and an annular plate. Next, the formulated governing equations are converted into FDM formulations. Later the FDM formulation is coded in MATLAB and validated with the available case from literature. Once validated, the code is used to study the buckling and vibration of circular plate under application of intermediate radial load. First the buckling study is done to study the limitation of the plate structure. Then, the vibration study is performed to show the influence of the in-plane load to the natural frequency.

The formulation of the required expression and equations is explained in detail as in Chapter 3. Here is brief explanation on the formulation. First, fundamental assumptions are laid out. Secondly, the equations and expressions that involved in circular plate study are formulated. The formulation is divided into two parts which are formulation for solid circular plate and formulation for annular plate. In each parts, one starts with the definition of strain-mechanical displacement and constitutive equation. This follows with the derivation of general expression of force and moment resultants. The force resultants are used for deriving the expression of applied in-plane radial load. On the other hand, the definition of bending stiffness is obtained from moment resultants. The formulation continues with deriving expression of in-plane radial load for current study. Then, the governing equations for buckling and vibration are defined. Third part of the formulation is defining the boundary conditions that appear in this dissertation.

Next step is converting the formulations into finite difference expressions. In formulation of FDM, one starts with the treatment at the center of solid circular plate. Next is applying FDM to governing equations and boundary conditions. Lastly, the

equations in FDM are transformed in matrix form. The theoretical of circular plate vibration and buckling is explained and the formulation is developed.

After formulating the expressions and equations in finite difference, the formulation is coded in MATLAB®. The code is validated by using existing problem in literature for both buckling and vibration of circular plate. Two problems are chosen which are an annular plate buckling due to the uniform compression at both its edges and buckling/wrinkling due to tensional load at its inner edge while its outer edge is free from loading. The main purpose is to show the FDM may handle the different type of in-plane load which one is constant throughout the plate while the other vary with radius. While the analysis is done for validating purpose, the two examples are also chosen to show the different of the stresses (thus the in-plane loads) distribution throughout the annular plates which is difference due to different nature of applied load and it may be dependent on the radius. These validations are done at the beginning of Chapter 4. On vibration part, another two examples chosen which are free vibration of clamped circular plate and influence of radial edge load to free vibration of clamped circular plate. Both examples should be suffice to show that the coded FDM is able to solve free vibration problem involving radial in-plane load. These validations are shown in early part of Chapter 5.

Once the FDM code is validated, it is ready to be used as tool to analyze circular plate problem. First, one would focus on study of circular plate buckling provide limitation of the size of the intermediate radial load that may be applied to the circular plate structure (last part of Chapter 4). The intermediate buckling load is realized by application of annular piezoceramic plate.

Lastly, problem of circular plate free vibration is studied (Chapter 5). First, the free vibration analysis is done without the effects of the in-plane load. Later, a circular

plate vibration analysis also done to see the effects of the in-plane load on the fundamental frequency.

1.8 OVERVIEW OF THESIS

1.8.1 Thesis Outline

This thesis is organized as follows:

i. Chapter 2 provides the literature review on the related topics of current thesis.

ii. Chapter 3 provides the formulation that required in current study such as distribution of in-plane loads, governing equations and boundary conditions. This chapter also provided the FDM formulation. The finite difference method is applied to the formulated governing equations and boundary conditions. Issues involving FDM, such as treatment at the center of the plate, are also discussed.

iii. In Chapter 4, a problem of circular plate buckling due to the intermediate radial load is presented FDM code is validated. In early of this chapter, the FDM code is first validated. Two existing problems are solved by formulated FDM and the results are compared with the existing results for buckling. This also served as evident that the FDM code able to handle involving in-plane load.

iv. In Chapter 5, a problem of circular plate free vibration is presented. The validation of FDM code for free vibration of circular plate is also presented in this chapter.

v. Chapter 6 summarizes the results of this thesis and outlines directions for future research.

1.8.2 Summary

The main objective of current works is to propose a frequency tunable plate structure. This will benefit not only for SJAs but also for devices such as vibration damping/absorber, energy harvester and resonator which may comprise such plate structure. Therefore, the contributions of the research described in this PhD thesis are the following:

i. Equations that govern vibration of a circular plate with applied intermediate radial load are formulated. Radial load distributions for the circular plate structure are derived. It is shown that the radial load in the annular region is radius depending while at solid circular plate region the radial load is constant.

ii. A finite different code for the vibration problem of the circular plate structure with applied intermediate radial load has been developed and validated.

iii. The developed finite different code for a circular plate structure vibration problem is able to predict the effect of in-plane load, applied via electrical, to the natural frequency.

CHAPTER TWO

LITERATURE REVIEW

2.1 OVERVIEW

Background, motivation and some early work in topic that related to research in this thesis is presented in current chapter. Due to large number of publication available in the area of plate study, it is impossible to review all of them. Therefore, only works that related to current study are presented here.

The review started with review the potential application of the proposed structure which served as the motivation of current study. In the following section, a review on methods of vibration control is presented. This follows with section reviews on the topic of buckling, particularly on the buckling where there is in-plane load distribution across the plate which is not constant. After that, plate theories are presented which will review the plate theory involving annular and piezoceramic plate. Lastly, since current study use finite different method as a tool to solve the problem, a review on the method is also presented.

2.2 INTRODUCTION

In modern day, mechanical behavior of a structure such as vibration is not only seen as a negative structural behavior that an engineer wishes to eliminate but also to manipulate it. If one manages to manipulate the behavior, it may be channel to a much more effective application rather than just waste it.

As an example is the area of energy harvesting involving vibrating structure. In such application, the vibrating structure becomes the natural structure to be harvest.

Particularly of interest in the area is the application of piezoceramic material in the energy harvester devices. The device structure takes the advantage of the ability of the piezoceramic to convert mechanical energy to electrical energy and store it for future usage (Ottman, et al., 2002; Roundy, et al., 2003; Zheng, et al., 2009).

Another example of area that need to manipulate the vibration of a structure is in vibration damping. A vibration damper that exploits the advantage of piezoceramic material has a mechanism similar to the energy harvesting devices. The piezoceramic structure is embedded or attached to the vibrating structure. The piezoceramic structure is attached to a circuit where the mechanical energy (the vibration) is shunted to the circuit. The devices that exploit the piezoceramic material are active vibration damping devices. The passive vibration damping devices are useful for certain range of frequency only since the dampers works best at its resonance frequency. As for the active vibration damper, the range may be broaden by designing shunt circuit that may be tuned. Reports such as, not restricted to, report by Moheimani (Moheimani, 2003) and, Hagood and Flotov (Hagood & Flotov, 1991) show the ability of the shunt circuit to active vibration damper.

There are also reports that show the application of vibrating devices in flow control such as a review paper by Gad-el-Hak and Bushnell (1991). In their review, they discuss on the separation phenomena, its governing equation, and its control methods - both passive and active. There are many devices developed that exploit vibration in flow control such as SJA (Mittal, Rampunggoon, & Udaykumar, 2001; You & Moin, 2007), fliperon (D. Greenblatt & I. J. Wygnanski, 2000; Veldhuis & Jagt, 2010; Zhou & Wygnanski, 2001), ribbon (David Greenblatt & Israel J. Wygnanski, 2000) and fluidic oscillator (Gregory, Sullivan, Raman, & Raghu, 2004). Glezer and Amitay (2002) have highlighted in their review paper that the actuation frequency of SJA may directly

influence to the separation flow. Raju et. al. (2008) also suggest similar conclusion from their simulation works. In a more recent review by Glezer (2011), he discussed two control strategies that are related to actuation frequency. One where the actuation frequency is coupled with the natural shedding frequency and the other is at the actuation frequency higher than the natural shedding frequency which lead to the altercation of the body aerodynamic shapes. Regardless of the strategies, one may conclude that the control of the actuation frequencies plays significant role in performance of SJA. In fact, Amitay and Glezer (2002) have performed an experimental study on the role of the actuation frequency in SJA which led to the similar conclusion.

Energy harvester, vibration damper and separation flow control are some of the examples that exploits vibration control. As briefly explain in previous paragraphs, it is understood that there are needs in controlling the vibration parts of the devices (i.e. tuning resonant frequency) in order to improve their performance.

2.3 VIBRATION CONTROL

Area of vibration attracts many researcher into it either to exploit it or to avoid it. In automotive design, a designer will try to avoid vibration that may affect the passenger as well as to cut off the noise induced by vibration. However, in designing devices such as resonator, a designer exploit the vibration. Furthermore, it is sometime desired to operate the resonator at its resonant frequency.

Although resonant frequently normally associates with harm, for devices such as energy harvesting devices, synthetic jet actuators and vibration absorber devices, it is desired that the devices to operate at its resonant frequency. The response of a structure is at its maximum when the resonant frequency is reached. This is beneficial since the less power needed to operate at this resonant. As noted by Cattafesta III and

Sheplak (2011), one of the main issues that need to be addressed for design of an SJA is the necessity of the device to operate near its resonance frequency. Meanwhile, in energy harvesting devices, ones may harvest more energy if the ambient frequency is equal to the resonant frequency of the devices. However, ambient frequency may change by time or environment conditions. Therefore, research in tuning frequency, particularly resonant frequency, is so much important. Zhu et. al. (2010) have reviewed tuning strategies for beam energy harvester.

There are many reports on application of shunt circuit to control vibration of structure consist of piezoelectric material (Adams, et al., 1998; Corr & Clark, 2006; Davis & Lesieutre, 2000; Hagood & Flotov, 1991; Muriuki & Clark, 2007; Tylikowski, 2001). Inductor, resistor and/or capacitor are a typical element that combined to form a typical shunt circuit. This shunt circuit may be exploit with piezoceramic material to shunt mechanical energy (vibration) away by electrical means. The characteristics of piezoceramic that convert mechanical energy to electrical energy make this mechanism possible. Therefore, this provides a mechanism of vibration control by exploiting a piezoceramic material.

Coupling coefficients of a piezoceramic shows how efficient is the conversion between electrical and mechanical energy by the piezoceramic. Obviously, it is ideal that the coupling coefficients to be unity. However, the highest available piezoceramic coupling coefficients is 0.7. Although the original piezoceramic material may be hardly made to the ideal condition, it has been shown that device consist of piezoceramic may have coupling coefficient higher than its active material (i.e. piezoceramic material). This can be done by applying in-plane load (Hebert & Lesieutre, 1998; Lesieutre & Davis, 1997).

2.3.1 Shunt Circuit

In electronics, devices that allows electric current to pass around another point in the circuit are called shunts. Therefore circuits that allows electric current that induced by vibration of piezoceramic devices to pass through another point in the circuit is known as shunt circuit. Inductor, capacitor and/or resistor is the typical electronic element to be combined to form the shunt circuit. The application of shunt circuit in vibration control of piezoceramic devices is reviewed by Lesieutre (1998) and, Ahmadian and DeGuilio (2001).

Davis and Lesieutre (2000), have developed and demonstrated a tunable solid-state piezoelectric vibration absorber and an active tuning method. They showed that the plate frequency may be tuned by connecting a bimorph circular plate consist of piezoelectric layer to a capacitive shunt circuit.

Later, Tylikowski (2001) has analyzed, by numerical simulation, vibrating annular plate excited by harmonic displacement of the inner plate edge. The plate is glued with patches of piezoelectric elements that capacitively shunted. Their results showed that the plate frequency is influenced by the external shunting capacity.

Hagood and Flotov (1991) have showed that passive electrical circuits means may control a structural damping mechanism. They investigated on cantilevered beam that patched with piezoelectric materials which shunted to passive electrical circuits. In their report, it is shown that the shunting circuit has influenced on the frequency of the shunted piezoelectric structure. Thus lead to their suggestions that the damping mechanism of a structure comprises of piezoceramic material may be controlled or manipulated by passive electrical means through shunt circuit.

Corr and Clark (2006) have investigated the piezoceramic actuators coupled with switching shunts to determine the similarities between mechanical and

piezoceramic variable stiffness members. The authors showed that a Type I mechanical spring (structural member consists of two springs in parallel: a primary spring and a secondary spring that can continuously vary its stiffness from zero to a maximum stiffness) is similar to a piezoceramic actuator used with a capacitance ladder shunt circuit. It was also shown that a Type II mechanical spring (structural member is also constructed of two springs in parallel except the variable spring is replaced with a spring that is either clamped or free) is similar to a piezoceramic actuator used with a switching ground shunt circuit. Also, a third type of variable stiffness structural member (Type III mechanical spring) is introduced so that the piezoceramic actuator used with a switching resistor/inductor shunt circuit could also have a mechanical spring counterpart. The type III is defined as the like the type II mechanical spring with the only different is that the secondary spring is no longer just freed or clamped at fixed point, but it can also be compressed or elongated such that the clamping point can be varied.

Muriuki and Clark (2007) provides insight into the design, analysis and operation of a cantilever beam resonator that is driven electrically. The study is based on an analytical model of the beam and experimental testing. The papers shows a method for using a shunt capacitance on a piezoelectric resonator to change the frequency of a vibrating cantilevered beam. The cantilevered beam consist of piezoelectric layer on top of an aluminum layer. The piezoelectric layer is design to have three parts which will act as sensor, actuator and a passive part. The capacitive shunt circuit is connected to the passive part as a way to provide control to the beam stiffness.

2.3.2 In-plane Load

Lesieutre and Davis (1997) have identified a class of device which its apparent coupling coefficient can, in principal, approach 1.0, a limit that corresponds to perfect electromechanical energy conversion. The device exploits the use of the destabilizing mechanical pre-loads to counter inherent stiffness. Their experiment verified the trend of increasing coupling with pre-load, with 40% increase in apparent coupling coefficient observed for pre-load of about 50% of the buckling load. The authors also defined two alternative device coupling coefficients from energy considerations; an 'apparent' coupling coefficient that treats the destabilizing pre-load as a reduction in stiffness, and a 'proper' coupling coefficient that explicitly treats the pre-load as a source of mechanical work on the device.

Hebert and Lesieutre (1998) the authors verifies and extend the works of Lesieutre and Davis (1997). Their works focus on application of trilaminar beams and disks. It is shown that the in-plane loads are capable of significantly changing the natural frequency and coupling coefficients of trilaminar devices. In the studies of trilaminar disks, they successfully applied 23% of the buckling load which corresponds to a frequency decrease of 13% and coupling coefficient increase of 15%. In their experimental work, the pre loads are mechanically applied. They also suggest that by exploiting this work, it might be possible to reduce size while maintaining the lower frequency characteristic of a larger device. Thus might decrease the size, weight and cost of some piezoelectric transducer. As mention in this paper, the methods of applying the load and the transducer geometry are remain an issue to be addressed.

Hu et. al. (2007) has studied the feasibility and characteristics of adjusting the resonant frequency of a piezoelectric bimorph by applying an axial preload. In their experiment, the preload is applied mechanically. The application of their study is for

energy harvesting. There are researchers that have already been able to design a harvesting structure with a very low natural frequency, which suitable for scavenging energy from a low-frequency ambient vibration. However, the variation of frequency of ambient vibrations may require a device with adjustable frequency so that strong interaction can happen between the bimorph natural frequency and the external driving frequency.

Bokaian (1988) has reported a study of the influence of a constant axial compressive load on natural frequencies and mode shapes of a uniform single-span beam with ten different combinations of end conditions. Their analytical results indicate that the variation of normalized natural frequency with normalized axial force is exactly the same for pinned- pinned, pinned-sliding and sliding-sliding beams and can be expressed in a closed form. The closed-form expression could be used for a beam with any kind of end conditions when the beam vibrates in a high mode. Their results indicate that the effect of end constraints on natural frequency of a beam is significant only in the first few modes. For higher modes, mode shapes of all beams approach multi-sine waves.

Deolasi and Datta (1997) have performed and experimental study on rectangular plate transverse vibration with periodic tensile loading. For a certain combinations of parameters, beams or plates may undergo resonant transverse vibration when subjected periodic axial or in-plane load. This is known as dynamic instability or parametric instability or parametric resonance. The pulsating component of the periodic in-plane load is called the parametric excitation, and the transverse response of the plate under parametric excitation is called the parametric response. They observed that the natural frequencies and the boundaries of the instability regions of the plate are considerably influenced by the nature of the edge loading. They studied parametric instability

characteristics of rectangular plates with nearly concentrated periodic tensile loading at various locations on the two opposite edges by means of experiments.

Rammerstorfer (1977) has investigated on the possibility of increasing first natural frequency and buckling load of plates by optimal fields of initial stresses. The results obtained by means of gradient methods. He observed that a suitably distributed initial stresses allow an improvement of the dynamical behavior, i.e., an increase of the fundamental frequency, and render higher buckling loads without a consumption of additional material or stronger materials, while the shape of the plate, i.e., constant thickness, is not changed. Though, in his conclusion he posed a question on how to achieve the optimal stresses. He did proposed a way by exploiting a plastic deformation which reported by his earlier works.

Li et. al. (2006) report that a novel tunable vibration absorber (TVA) has been developed for active absorption of vibrations in vibrating structures. The newly developed TVA is composed of a piezoceramic sensori-actuator suspended in a mounting frame by two flexible beams connected to axial ends of the sensori-actuator. The sensori-actuator provides the axial load that will affects the frequency. In this work, they demonstrated that the tunability of natural frequency as high as 12% and sensibility of vibrations as good as a commercial accelerometer.

In a more recent study in frequency tuning for energy harvester, Chen et. al. (2012) proposed a device that exploited the application of in-plane load in tuning frequency. They found that the energy from the harvester increases while its resonance frequency decreases when the pre-stress increasing.

2.4 BUCKLING

Analysis of buckling problem is classic structure problem. The general purpose of carrying such analysis is to avoid loading a structure beyond its buckling load, particularly for load bearing structure. The problem has been extensively studied by many researchers and many analytical results are available in many classical or contemporary books. Since current thesis deal with problem circular plate subjected to intermediate load, first the review on intermediate buckling load is presented and followed with review of circular/annular plate buckling problem which involve in-plane stress distribution in radial direction.

2.4.1 Intermediate Load Buckling

Plate problem with intermediate load buckling has been reported by Xiang et. al. (2003), Yu (2003), Wang et. al. (2004) and Aung and Wang (2005). Xiang et. al. (2003) reported on elastic buckling of rectangular plates subjected to both intermediate and end uniaxial loads. Their solution procedure involves the use of the Levy approach, the domain decomposition technique, and the state-space concept. Yu (2003) has reported in his Master's thesis a similar problem but extend the problem for plastic buckling. Later, Wang et. al. reported on problem of elastic buckling of rectangular plates subjected to intermediate and end uniaxial in-plane loads, whose direction is parallel to two simply supported edges. They solved by decomposing the plate into two subplates at the location where the intermediate uniaxial load acts. Each subplate buckling problem is solved exactly using the Levy approach and the two solutions brought together by matching the continuity equations at the separated interface.

Aung and Wang (2005) reported on elastic buckling problem of a circular plate subjected to both intermediate and edge radial loads. The stability criteria, in the form

of transcendental equations, are derived as a function of the location of the intermediate load and the ratio of the magnitudes of the intermediate load and the edge load.

However, in the aforementioned reports, the authors only considered only constant distribution of the in-plane stress (thus the in-plane load) or stress free throughout the plate. In most practical condition which involve intermediate load acting on a plate, in one of the sub-plate normally will have a length (or radial) dependent distribution. This is due to the different size of load acting at its edges.

2.4.2 Annular Plate Buckling

Since in this thesis, only circular (or annular) plate is concerned, the review of buckling problem which involve in-plane load distribution varied with radial for circular/annular plate is presented here.

As early as 1960, Mansfield (1960) considered the buckling of an infinite plate supported along two concentric circles and subjected to a uniform radial compression, or tension, along the inner circle. The solution is also applicable to a similarly loaded finite annular plate if there is a member of the requisite tensile stiffness supporting the outer circle. Though, in his report, the stress distribution throughout the plate is assumed to be uniform.

For annular plate buckling problem with stress distribution varying throughout the plate, to one knowledge, the exact analytical solution is yet to exist. However, there are reports using asymptotic methods such as perturbation method and matric compound method in solving such problems (Sheng-li and Ai-shu, 1984; Li Shi-rong, 1992; Fu and Waas 1992; Coman & Haughton, 2006a and Coman & Haughton, 2006b). Sheng-li and Ai-shu (1984) have reported on the problem of unsymmetrical buckling of an annular thin plate under the action of in-plane pressure and transverse load. They

used the method of multiple scales that is similar to what Kiang (1980) used in his analysis. They showed the application of their analysis for circular plate subjected to the in-plane radial pressures that uniformly distributed over the plate boundaries ($N_{11} = N_{22} = N$ and $N_{12} = 0$) and also subjected to uniform pressure that acts on the plate surface. The plate is clamped along its boundary. Their asymptotic solution shows excellent agreement with the exact analytical solution.

Li Shi-rong (1992) has reported on study of the axisymmetric nonlinear vibration and thermal buckling of a uniformly heated isotropic plate with a completely clamped outer edge and a fixed rigid mass along the inner edge. He used both parametric perturbation technique and finite different method to obtain the nonlinear response of the plate-mass system and the critical temperature in the mid plane at which the plate is in buckled state.

Fu and Waas (1992) have reported the buckling of polar and rectilinearly orthotropic annuli subjected to internal or external pressure loading without restriction to axisymmetric buckling modes. The buckling analyses were performed in both the polar orthotropic and rectilinearly orthotropic cases by the Rayleigh-Ritz method. Their results also concluded that the unwarranted assumption of axisymmetry actually produces non-minimum buckling loads.

Coman and Haughton (2006a) have investigate a pre-stressed annular thin film subjected to a uniform displacement field along its inner edge. The plate is free at the outer edge while simply supported at the inner edge. They applied the compound matrix method to solve the problem numerically. They also did WKB analyses to complement their results. Later, they have used the compound matrix method to solve annular plate buckling/wrinkling problems (Coman and Haughton 2006b). They compare their results with the existing results from other literatures. They also compare their results with

approximate method such as the Galerkin technique. Their annular plate is free at outer edge and simply supported at inner edge with a tensional force is uniformly applied at the inner edge. As a compliment of the Coman and Haughton's works, recently, Jillella and Peddieson (2012) investigated further on wrinkling of thin circular plates. However their approach is based on the imperfection methods and solved numerically with the aid of the finite different method.

2.5 PLATES MODEL/THEORY

2.5.1 Piezoceramic Plate

In a similar case as modeling homogeneous isotropic plate, a piezoceramic plate also may be modeled by Classical Plate Theory (CPT) which in accordance to Kirchhoff's hypotheses. Further, as reported by Adelman and Stavsky (1980), composite plate consist of piezoceramic may be modeled based on CPT. In their report, they have developed a plate-type theory for the flexural extensional vibratory response and static voltage deformation of heterogeneous piezoelectric circular transducer element. In their formulation the localized electroelastic governing equations are converted to globalized plate equations which directly describe the geometry of the media while indirectly accounting for the local variations in composition, polarization, etc.

In other works, such as by Sekouri, Hu and Ngo (2004), Prasad et. al. (2006) and Brissaud (2006) also used the CPT to modeled their piezoceramic plate. Sekouri, Hu and Ngo (2004) compared their analytical results with the experimental one which showed good agreement. Prasad et. al. (2006) performed analysis of unimorph plate by using Lumped Element Method, but modeled their plate based on CPT. In their analysis, a finite-element (FE) analysis of the structure is performed to validate whether Classical

Laminate Plate Theory (which based on CPT) is appropriate to model their plate and found their results to be in good agreement between the two results. Brissaud (2006) did analysis for bimorph plate, but as similar to Adelman and Stavsky (1980), their results of formulation shows that the analysis of the non-symmetric and symmetric circular bimorphs reduced to the determination of the global flexural rigidity and the global Poisson ratio of the structure. Therefore the actual bimorph is then equal to a homogeneous circular plate.

However, for more accurate analysis of plate problem, particularly for composite plate analysis such as unimorph or bimorph plate, the shear effects that influence the through thickness variables may need to be taken account. For example, Fernandes and Pouget (2001a) have presented an accurate modeling of single-layered piezoelectric plates. Their plate formulation is based on the variational methods which accounts for the piezoelectricity. The through thickness variables are approximate to accounts the shear effects and a refinement of the electric potential. Their shear effects is model by sine function. The computed electromechanical quantities' distributions through the thickness showed a good agreement with the results computed by finite element and a simplified model which does not accounts the shear effects. Later, they further showed that their model gave better accuracy compared to the plate model based on CPT (Fernandes and Pouget, 2003).

In modeling piezoceramic plate, one important issue that need to give attention is the electric potential distribution within the plate. According to Wang et. al. (2001), many researchers assumed the distribution of the electric potential to be uniform in the longitudinal direction of the piezoelectric actuator and linear in its thickness direction. This assumption may violate the Maxwell static electricity equation. Therefore, in their paper they proposed that the electric potential distribution to be quadratic variation in

thickness direction. Their formulation satisfies the Maxwell static electricity equation. They compared their proposed distribution with analysis done by Finite Element Analysis, which shows good agreement.

Later, Huang et. al. (2004) and Huang (2005) have presented an analysis of circular bimorph plate by analytical analysis, numerical and experimental measurement. In their analysis, similar to Wang et. al. (2001), they modeled their plate by using CPT and assumed the electric potential distributions to varied by quadratic law in thickness direction. They compared their analytical results with the results from Finite Element Analysis as well as experimental works. Their results showed that their analytical results have an excellent agreement with both Finite Element Analysis and experimental results.

2.5.2 Annular Plates

Theory in modelling an annular plate is the same as modelling a solid circular plate. Therefore, any theory of CPT or shear deformation theory or variation method may be used in annular plate analysis. In fact, in cases where there is discontinuity in ring shape boundary for a circular plate, the circular plate may be divide into two regions which is annular region and circular region. Example of such problem is the problem analyzed by Aung and Wang (2005) in their report of a circular plate buckling problems due to intermediate radial edge. However, in their report, they only analyzed cases where the in-plane loads are uniformly distributed in both annular and solid circular region. However, one would argue that in many practical condition, if there is an intermediate radial load acting on a circular plate, the in-plane load distribution will vary in radial direction. This is due to the fact that the different boundary constraint at inner and outer radius of the annular region.

There are many papers, (Fraser, 1975; Kiang, 1980; Jia-qi & Bing-guo, 1981 and Fu-ru, 1982, 1984) that study on annular plate problem such that the stress distribution (thus the in-plane load) is not uniform or varies in radial direction. Fraser (1975) has reports on bending of a radially pre-stressed annular plate by tilting a central rigid inclusion. Since the inclusion is truly rigid, the stress distribution throughout the annular plate is not uniform. In such cases, the analytical solution is not available. In this report, he used the method of matched asymptotic expansion to find the approximate expression for the applied couple as a function of the small angle of rotation of the rigid inclusion. Later, Kiang (1980) has showed applications of perturbation method in problems of bending of annular and circular thin plates. The thin plates are under combined action of lateral loading and in-plane forces. In this analysis, he consider the case of $N_{11} > 0, N_{12} > 0$ that is the radial force and circumferential force which act on the in- plane are tensile forces, and the shearing force is simply small. He first solved for general case of the plates bending problem but then gave three examples;

a. Circular plate with rigid inclusion in its center. The radial tension develop due to the rotation of the inclusion. The in plane loads are assumed as $N_{11} = N_{12} = N$ and $N_{12} = 0$.

b. Similar to (a.) but the in plane loads are assumed as $N_{11} = N_{12} = N(r)$ and $N_{12} = 0$.

c. Circular plate submitted to lateral load depending on radius $(q = q(r))$ as well as radial and circumferential load depending on radius ($N_{11} = N_{12} = N(r)$ and $N_{12} = 0$). The boundary conditions are simply supported or built in.

Jia-qi and Bing-guo (1981) has reported on annular thin plates unsymmetrical bending problem through application of the method of multiple scales. They used the same method used by Kiang (Kiang, 1980) except they consider the case of $N_{11} = N_{11}(r), N_{22} = 0$ and $(N_{12})^2 = 0$. They showed example of the analysis on an annular plate with rigid body inclusion which rotates in small angle. In this example the radial load is constant, $N_{11} = N_0$. Fu-ru (1982, 1984) has reported on unsymmetrical bending of elastic flexible annular and circular thin plates under various supporting conditions. In his report (Fu-ru, 1982), he solved the problem for general case while in his other report (Fu-ru, 1984) he extended his study to the case of the tensile force acting on its boundary is zero which has been lacked from his first report (Fu-ru, 1982). For the latter case, the asymptotic approximation of solution obtained at the boundary where the tensile force acts should be singular. He used the singular perturbation methods to solve the problems. He claimed that the method may be applied to thin plate bending problem with any other smooth boundary or under other supports showed in the reports. However, all the reports above are analysis restricted to static problem such as analysis of bending problems.

For buckling or vibration problem that involve in-plane stress distribution, there are several interesting reports involving asymptotic method which discussed under previous subsection (Subsection 2.4).

2.6 FINITE DIFFERENT METHOD (FDM)

As discussed in subsection 2.4 and 2.5, analytical solution of plate involving distributed in-plane load are, to one knowledge, is yet to exist. Therefore, one reduced to choose method of solving the problem through numerical method.

Finite Different Method (FDM) is easy and simple numerical method to be implemented. Due to this reason, author chosed the FDM as a method to solve the problem. Application of FDM in the plate problem field is not new and being used in various plate problems including plate vibration (Raju, 1966; Aksu & Ali, 1976; Mukhopadhyay, 1978; and Darus & Tokhi, 2004) and buckling/instability (Tani & Yamaki, 1981; Spencer & Surjanhata, 1986a, 1986b; Cohen, 1992; and Pawlus, 2006, 2011). There are some that proposed improvement of the FDM such as one reported by Ergun and Kumbasar (2011), which they shows that some plate bending problems which have not been solved without computer may be analyzed in this method by hand.

One of the issue that may be raised when dealing with circular plate or differential equations involving polar coordinate is the singularity at center of the plate or at $r = 0$. Some researchers proposed extra condition for the origin which would give a non-singular solution at the origin (Mohseni & Colonius, 2000). However, Lai (2002) has proposed a very simple way to treat this problem which is by shifting a grid a half mesh away from the origin and incorporating the symmetry constraint of Fourier coefficients. This approach also does not need to use one sided difference approximation (i.e. backward difference approximation) at the origin, thus maintain the accuracy of central different approximation. The similar approach also reported by Mohseni and Colonius (2000).

2.7 SUMMARY

It is known that there are devices such as SJA where its vibrating part has influence in its performance. For such devices, the design of its vibrating part so that it may be controlled to its best performance is required. There are several ways in controlling vibration such as by using shunt circuit and applying in-plane load. As an addition to

controlling vibration through electrical means by using shunt circuits, current thesis looks into possibility in application of in-plane loads via electrical means. This is realize by using piezoceramic material.

As an excessive in-plane load may results the plate structure to buckle, a buckling analysis will also be conducted. However, here, focus will be given on buckling due to intermediate radial load particularly for condition where its in-plane load varies with radius.

Current problem will be solved using FDM as it is simple numerical tools. Since at the center of circular plate numerically will give singularity problem, there is a special treatment needed to avoid it. In current work, the treatment at the center of the plate is follow the work of Lai (2002).

The formulation of governing equation is based on Classical Plate Theory with extra assumption for plate involving piezoceramic material. The general procedure of the formulation follows the works of Huang (2005).

CHAPTER THREE

FORMULATION OF THE CIRCULAR PLATE GOVERNING EQUATION

3.1 OVERVIEW

In this chapter the general formulation of the circular and annular plate is presented. The chapter starts with laying down the fundamental assumptions in formulating governing equations. This follows by defining related variables such as the loads distribution and electrical distributions that will be used throughout the study. The governing equation that will be used throughout this dissertation is provided in this chapter. The chapter closed by formulating the governing equations in finite different form.

3.2 INTRODUCTIONS

Current study is involving study of solid circular plate vibration with influence of intermediate radial in-plane load. In such problem, the solid circular plate may be divided into two regions; i.e. a smaller solid circular plate and annular plate such in Figure 3.1. The boundary where the smaller solid circular and annular plate are separated is the boundary where the radial load is applied. This load may be realized by heating up the annular region or by using material such as piezoceramic as source of the radial load. In current analysis, the annular region is made of piezoceramic and the smaller solid annular region is made of alloy (representing homogeneous, isotropic material). As certain voltage applied to the piezoceramic annular plate, the annular plate may expand or contract thus applying radial load to the solid circular plate.

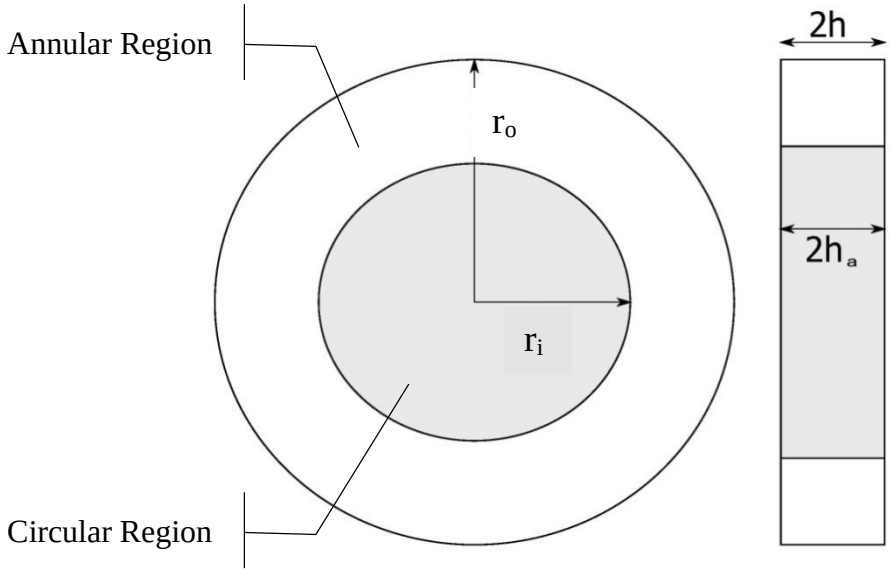

Figure 3.1 Circular plate with two sub-region

This chapter is dedicated on formulating all equations and expressions that required in the study. First, fundamental assumptions are laid out. In general, the Kirchoff's assumptions are used with additional assumptions for piezoceramic material.

Secondly, the equations and expressions that involved in circular plate study are formulated. As explained before, in current study the circular plate can be viewed as a circular plate having two regions or plates (as in Figure 3.1). Therefore, one divide the formulation into two parts which are formulation for solid circular plate and formulation for annular plate. In each parts, one starts with the definition of strain-mechanical displacement and constitutive equation. This follows with the derivation of general expression of force and moment resultants. The force resultants are used for deriving the expression of applied in-plane radial load. On the other hand, the definition of bending stiffness is obtained from moment resultants. The formulation continues with deriving expression of in-plane radial load for current study. Then, the governing equations for buckling and vibration are defined.

Third part of the formulation is defining the boundary conditions that appear in this dissertation. And the formulation is concluded with formulation of FDM. In formulation of FDM, one starts with the treatment at the center of solid circular plate. Next is applying FDM to governing equations and boundary conditions. Lastly, the equations in FDM are transformed in matrix form.

3.3 ASSUMPTIONS

In the present analysis the cylindrical polar coordinate is adopted. The origin of the coordinate is located at the center of the circular. The radius and the thickness of the solid circular plate are denoted by r_i and $2h$, respectively. While the outer radius and thickness of the ring are denoted by r_o and $2h_a$, respectively. The inner radius of the annular plate is equal to the circular plate's radius, r_i. Notes also that the thickness of the annular plate may not necessarily be equal to the thickness of the solid circular plate.

3.3.1 Kirchhoff Asumptions

In most practical applications, the ratio of a circular plate radius to the thickness is more than ten where the plate is considered to be a thin plate. For a thin plate, Kirchhoff's hypotheses may be applied and the shear deformation and rotatory inertia can be omitted. The Kirchhoff hypothesis assumed:

i. The thickness of the plate is small compared to its lateral dimensions, i.e. h≪ R.

ii. The middle plane of the plate does not undergo in-plane deformation. Thus, the midplane remains as the neutral plane after deformation or bending.

iii. The displacement components of the midsurface of the plate are small compared to the thickness of the plate.

iv. The influence of transverse shear deformation is neglected. This implies that the plane cross sections normal to the midsurface remain normal to the midsurface even after deformation or bending. This assumption implies that the transverse shear strains, e_{13} and e_{23} , are negligible and 1, 2, and 3 are referred to r, θ and z.

v. The transverse normal strain e_{33} under transverse loading can be neglected. The transverse normal stress, σ_{33} , is small and hence can be neglected compared to the other components of stress.

These assumptions results in the reduction of a three-dimensional plate problem to a two-dimensional problem. Any plate bending theory based on these assumptions is referred to as Classical Plate Theory or Kirchhoff's Plate Bending Theory.

3.3.2 Additional Assumptions related to Piezoceramic Material

The assumption of electric field is constant across the thickness of piezoelectric layer violates the Maxwell static electricity equation. Wang et. al. (2001) proposed that the electric potential varies in thickness of piezoelectric layer by a quadratic law, which satisfies the Maxwell static electricity equation. This assumption will provide full coupling effect of the piezoelectric layer on the host plate. Therefore in the present analysis, in addition to the Kirchhoff's assumptions for thin plate, the following additional assumptions are made (Huang, 2005; Huang, et al., 2004):

vi. the electric potential is assumed to varies with the thickness by the square law, i.e. $\phi = \phi_0 + \phi_1 z + \phi_2 z^2$ where ϕ_0, ϕ_1 and ϕ_2 are constants, and

vii. the electric displacement is assumed to be constant with respect to the plate thickness, i.e. $\partial D_3 / \partial z = 0$.

3.4 THE ISOTROPIC CIRCULAR PLATE FORMULATION

Most of the expressions in the following section may be found in typical books discussing theory of plate. However, for complete discussion it showed here as reference in subsequent sections and chapters.

3.4.1 Strains-Mechanical Displacements Relationship

Define the mechanical displacement in r, θ and z as u, v and w, where these displacements are a function of space and time, i.e. $u = u(r, \theta, z, t)$. The mechanical displacement can be defined as (Reddy, 1999):

$$u = u_0 - z\left(\frac{\partial^2 w_0}{\partial r^2}\right) \tag{3.1}$$

$$v = v_0 - z\frac{1}{r}\left(\frac{\partial w_0}{\partial \theta}\right) \tag{3.2}$$

$$w = w_0 \tag{3.3}$$

where u_0, v_0 and w_0 is the mechanical displacement of the mid-surface. The strain-mechanical displacement relations are:

$$
\begin{aligned}
e_{11} &= \frac{\partial u}{\partial r} \\
&= \frac{\partial u_0}{\partial r} - z\frac{\partial^2 w_0}{\partial r^2} \\
&= e_{11}^0 + z\kappa_{11}
\end{aligned} \tag{3.4}
$$

$$
\begin{aligned}
e_{22} &= \frac{u}{r} + \frac{1}{r}\frac{\partial v}{\partial \theta} \\
&= \frac{u_0}{r} + \frac{1}{r}\frac{\partial v}{\partial \theta} - \frac{z}{r}\left(\frac{\partial w_0}{\partial r} - \frac{1}{r}\frac{\partial^2 w_0}{\partial \theta^2}\right) \\
&= e_{22}^0 + z\kappa_{22}
\end{aligned} \tag{3.5}
$$

$$
\begin{aligned}
e_{11} &= \frac{1}{2}\left(\frac{1}{r}\frac{\partial u}{\partial \theta} + \frac{\partial v}{\partial r} - \frac{v}{\theta}\right) \\
&= \frac{1}{2}\left(\frac{1}{r}\frac{\partial u_0}{\partial \theta} + \frac{\partial v_0}{\partial r} - \frac{v_0}{\theta}\right) - \frac{z}{r}\left(\frac{\partial^2 w_0}{\partial r \partial \theta} - \frac{1}{r}\frac{\partial w_0}{\partial \theta}\right) \\
&= e_{22}^0 + \frac{z}{2}\kappa_{12}
\end{aligned} \tag{3.6}
$$

where e_{ij}^0 is the in-plane strains and κ_{ij} is the curvature.

3.4.2 Constitutive Equations

The variation of stress throughout the thickness for isotropic circular plate, derived from the constitutive equation of stress and strain and the Kirchhoff assumptions, lead to a completely defined law which are

$$
\sigma_{11}^{(s)} = \frac{E}{\left(1-\mu^2\right)}\left(e_{11}^0 + z\kappa_{11} + \mu\left(e_{22}^0 + z\kappa_{22}\right)\right) \tag{3.7}
$$

$$
\sigma_{22}^{(s)} = \frac{E}{\left(1-\mu^2\right)}\left(e_{22}^0 + z\kappa_{22} + \mu\left(e_{11}^0 + z\kappa_{11}\right)\right) \tag{3.8}
$$

$$
\sigma_{12}^{(s)} = \frac{E}{2\left(1+\mu\right)}\left(e_{12}^0 + z\kappa_{12}\right) \tag{3.9}
$$

where E and μ the Young coefficient and Poisson ratio for the isotropic shim, respectively and superscript (s) denotes the isotropic material.

3.4.3 Force and Moment Resultants

The stress for an isotropic plate are given by Equation (3.7) to (3.9). The force resultants and moment resultants may be determined from

$$N_{11} = \int_{-h}^{h} \sigma_{11} dz \;\; ; \;\; N_{22} = \int_{-h}^{h} \sigma_{22} dz \;\; \text{and} \;\; N_{12} = \int_{-h}^{h} \sigma_{12} dz \tag{3.10}$$

$$M_{11} = \int_{-h}^{h} \sigma_{11} z dz \;\; ; \;\; M_{22} = \int_{-h}^{h} \sigma_{22} z dz \;\; \text{and} \;\; M_{12} = \int_{-h}^{h} \sigma_{12} z dz \tag{3.11}$$

where h is the plate half thickness (i.e. $h = h_a$ for annular plate and $h = h + h_p$ for bimorph). Let h is the half thickness of the isotropic circular plate. Substituting Equation (3.7) to (3.9) into Equation (3.10) to (3.11) will lead the following expression, which are the force resultant and moment resultant for an isotropic plate

$$\begin{aligned} N_{11} &= \int_{-h}^{h} \sigma_{11} dz \\ &= A_{11}^{(s)} e_{11}^{0} + A_{12}^{(s)} e_{22}^{0} \\ &= A^{(s)} \left(e_{11}^{0} + \mu e_{22}^{0} \right) \end{aligned} \tag{3.12}$$

$$\begin{aligned} N_{22} &= \int_{-h}^{h} \sigma_{22} dz \\ &= A_{12}^{(s)} e_{11}^{0} + A_{11}^{(s)} e_{22}^{0} \\ &= A^{(s)} \left(e_{22}^{0} + \mu e_{11}^{0} \right) \end{aligned} \tag{3.13}$$

$$\begin{aligned} N_{12} &= \int_{-h}^{h} \sigma_{12} dz \\ &= A_{66}^{(s)} e_{11}^{0} \end{aligned} \tag{3.14}$$

where $A^{(s)} = Eh/\left(1-\mu^2\right)$, $A_{11}^{(s)} = A^{(s)}$, $A_{22}^{(s)} = \mu A^{(s)}$ and $A_{66}^{(s)} = Eh/\left(1-\mu\right)$ and

$$
\begin{aligned}
M_{11} &= \int_{-h}^{h} \sigma_{11} z dz \\
&= D_{11}^{(s)} \kappa_{11} + D_{12}^{(s)} \kappa_{22} \\
&= D^{(s)} \left(\kappa_{11} + \mu \kappa_{22} \right)
\end{aligned} \tag{3.15}
$$

$$
\begin{aligned}
M_{22} &= \int_{-h}^{h} \sigma_{22} z dz \\
&= D_{11}^{(s)} \kappa_{22} + D_{12}^{(s)} \kappa_{11} \\
&= D^{(s)} \left(\kappa_{22} + \mu \kappa_{11} \right)
\end{aligned} \tag{3.16}
$$

$$
\begin{aligned}
M_{12} &= \int_{-h}^{h} \sigma_{12} z dz \\
&= D_{66}^{(s)} \kappa_{12}
\end{aligned} \tag{3.17}
$$

where $D^{(s)} = 2Eh^3 \Big/ \left(3\left(1-\mu^2\right) \right)$, $D_{11}^{(s)} = D^{(s)}$, $D_{22}^{(s)} = \mu D^{(s)}$ and $D_{66}^{(s)} = Eh^3 \Big/ \left(3\left(1-\mu\right) \right)$.

3.4.4 General Governing Equation of Circular Plate

The Governing equation may be derived using Hamilton's principle (Reddy, 1999). For simplicity, the derivation is not shown here. The detailed derivation for circular plate governing equation may be referred to Faris' dissertation (Faris, 2003). The general governing equation for a plate problem may be written as

$$
-\frac{1}{r}\left[\frac{\partial}{\partial r}\left(rN_{11} \right) + \frac{\partial N_{12}}{\partial \theta} - N_{22} \right] + I_0 \frac{\partial^2 u_0}{\partial t^2} = 0 \tag{3.18}
$$

$$
-\frac{1}{r}\left[\frac{\partial}{\partial r}\left(rN_{12} \right) + \frac{\partial N_{22}}{\partial \theta} - N_{12} \right] + I_0 \frac{\partial^2 v_0}{\partial t^2} = 0 \tag{3.19}
$$

$$
\begin{aligned}
&-\frac{1}{r}\left[\frac{\partial}{\partial r}\left(rM_{11} \right) - \frac{\partial M_{22}}{\partial r} + \frac{1}{r}\frac{\partial^2 M_{22}}{\partial \theta^2} + \frac{2}{r}\frac{\partial}{\partial r}\left(r\frac{\partial M_{12}}{\partial \theta} \right) \right] \\
&-\frac{1}{r}\frac{\partial}{\partial r}\left(rN_{11}\frac{\partial w_0}{\partial r} + N_{12}\frac{\partial w_0}{\partial \theta} \right) - \frac{1}{r^2}\frac{\partial}{\partial \theta}\left(N_{22}\frac{\partial w_0}{\partial \theta} + rN_{12}\frac{\partial w_0}{\partial r} \right) \\
&-q + I_0 \frac{\partial^2 w_0}{\partial t^2} = 0
\end{aligned} \tag{3.20}
$$

where N_{ij} and M_{ij} is the force and moment resultants derived in subsections 3.2.4 to 3.2.6, q is the lateral load/pressure and I_0 is defined as

$$I_0 = \int_{-h/2}^{h/2} \rho dz \tag{3.21}$$

In this study, the in-plane vibration is assumed to be negligible so that the final terms of Equation (3.18) and (3.19) can be dropped. Furthermore the effect of lateral load/pressure, q is also not considered in current study.

Substituting the bending moments expressions into Equation (3.20) will results the governing equation for buckling and vibration of a circular plate. The expression in terms of deflection w is as follows

$$\begin{aligned} D\nabla_r^4 w - \frac{1}{r}\frac{\partial}{\partial r}\left(rN_{11}\frac{\partial w}{\partial r} + N_{12}\frac{\partial w}{\partial \theta}\right) - \frac{1}{r^2}\frac{\partial}{\partial \theta}\left(N_{22}\frac{\partial w}{\partial \theta} + rN_{12}\frac{\partial w}{\partial r}\right) \\ + I_0\frac{\partial^2 w}{\partial t^2} = 0 \end{aligned} \tag{3.22}$$

where D, N_{11}, N_{22} and N_{12} represents the bending stiffness, radial load, circumferential load and shear load for circular plates which may be of the isotropic or piezoceramic that have been derived in subsequent section. In the present analysis, the shear in-plane load is assumed to be negligible while the radial and circumferential in-plane load may be varied with radial direction.

$$N_{11} = N_{11}(r) \;\; ; \;\; N_{22} = N_{22}(r) \;\text{ and }\; N_{12} = 0 \tag{3.23}$$

Under this condition, the governing equation may be rewritten as

$$D\nabla_r^4 w - N_{11}\frac{\partial^2 w}{\partial r^2} - \left(\frac{N_{11}}{r} + \frac{\partial N_{11}}{\partial r}\right)\frac{\partial w}{\partial r} - \frac{N_{22}}{r^2}\frac{\partial^2 w}{\partial \theta^2} + I_0\frac{\partial^2 w}{\partial t^2} = 0 \tag{3.24}$$

Noting that

$$\left(\frac{N_{11}}{r}+\frac{\partial N_{11}}{\partial r}\right)=\frac{N_{22}}{r} \tag{3.25}$$

which lead to the following equation

$$D\nabla_r^4 w-N_{11}\frac{\partial^2 w}{\partial r^2}-N_{22}\left(\frac{1}{r}\frac{\partial w}{\partial r}-\frac{1}{r^2}\frac{\partial^2 w}{\partial \theta^2}\right)+I_0\frac{\partial^2 w}{\partial t^2}=0 \tag{3.26}$$

The biharmonic operator, ∇_r^4 is defined as

$$\begin{aligned}\nabla_r^4 \equiv{}& \frac{\partial^4}{\partial r^4}+\frac{2}{r}\frac{\partial^3}{\partial r^3}-\frac{1}{r^2}\frac{\partial^2}{\partial r^2}+\frac{2}{r^2}\frac{\partial^4}{\partial r^2\partial\theta^2}\\ &+\frac{1}{r^3}\frac{\partial}{\partial r}-\frac{2}{r^3}\frac{\partial^3}{\partial r\partial\theta^2}+\frac{1}{r^4}\frac{\partial^4}{\partial\theta^4}+\frac{4}{r^4}\frac{\partial^2}{\partial\theta^2}\end{aligned} \tag{3.27}$$

Let $w(r,\theta)=w_n(r)\cdot\cos(n\theta)$, where from here $w_n(r)$ will be denoted as w_n unless stated otherwise. Thus after dividing by bending stiffness D

$$\begin{aligned}&\frac{\partial^4 w_n}{\partial r^4}+\frac{2}{r}\frac{\partial^3 w_n}{\partial r^3}-\left(\frac{1}{r^2}+\frac{2n^2}{r^2}\right)\frac{\partial^2 w_n}{\partial r^2}+\left(\frac{1}{r^3}+\frac{2n^2}{r^3}\right)\frac{\partial w_n}{\partial r}+\left(\frac{n^4}{r^4}-\frac{4n^2}{r^4}\right)w_n\\ &-\frac{N_{11}}{D}\frac{\partial^2 w_n}{\partial r^2}-\frac{N_{22}}{D}\left(\frac{1}{r}\frac{\partial w_n}{\partial r}-\frac{n^2}{r^2}w_n\right)+\frac{I_0}{D}\frac{\partial^2 w_n}{\partial t^2}=0\end{aligned} \tag{3.28}$$

where n is the nodal diameter. The distributions of the radial and circumferential load will be discussed in next subsection.

3.4.5 In-plane Load Distributions

For a nonlinear problems, the Equation (3.18) to (3.20) are coupled. However for certain a weakly nonlinear problems or weakly coupled problem, the equations may be uncoupled thus linearized. This is the problems that is being considered in the present study. First we assumed that the pre-buckling state to be axisymmetric such that $u=u(r)$ and $v=0$. For such case, the Equation (3.4) - (3.6) for strains becomes

$$e_{11} = \frac{du}{dr} \;\; ; \;\; e_{22} = \frac{u}{r} \;\; \text{and} \;\; e_{12} = 0 \tag{3.29}$$

Under this assumption, the in-plane load can be rewritten as

$$\begin{aligned} N_{11}^{(s)} &= \frac{Eh}{\left(1-\mu^2\right)}\left(e_{11}^0 + \mu e_{22}^0\right) \\ &= \frac{Eh}{\left(1-\mu^2\right)}\left(\frac{du_s}{dr} + \mu\frac{u_s}{r}\right) \end{aligned} \tag{3.30}$$

$$\begin{aligned} N_{22}^{(s)} &= \frac{Eh}{\left(1-\mu^2\right)}\left(e_{22}^0 + \mu e_{11}^0\right) \\ &= \frac{Eh}{\left(1-\mu^2\right)}\left(\frac{u_s}{r} + \mu\frac{du_s}{dr}\right) \end{aligned} \tag{3.31}$$

If the radial displacement u_s is known then the load distribution is also known. Substitute Equation (3.30) to (3.31) into the Equation (3.18) will lead to a Cauchy-Euler differential equation.

$$-\frac{1}{r}\left[\frac{\partial}{\partial r}\left(rN_{11}^{(s)}\right) + \frac{\partial N_{12}^{(s)}}{\partial\theta} - N_{22}^{(s)}\right] + \overbrace{I_0\frac{\partial^2 u_0}{\partial t^2}}^{\approx 0} = 0$$

$$\frac{\partial}{\partial r}\left(rN_{11}^{(s)}\right) + \frac{\partial N_{12}^{(s)}}{\partial\theta} - N_{22}^{(s)} = 0 \tag{3.32}$$

$$\frac{du_s^2}{\partial r^2} + \frac{1}{r}\frac{du_s}{dr} - \frac{1}{r^2}u_s = 0 \tag{3.33}$$

Note that the in-plane inertia term is assumed to be negligible and u_s is the radial displacement for an annular plate. The general solution of the Equation (3.33) is

$$u_s = \frac{C_3}{r} + C_4 r \tag{3.34}$$

where the coefficients C_3 and C_4 are determined from boundary conditions.

For a solid circular plate, the first terms of Equation (3.34) may produce singularity at the center of the plate. To avoid the singularity problem, the first term should be omitted thus the solution for a solid circular plate may be written as

$$u_s = C_4 r \tag{3.35}$$

If one substitute Equation (3.35) into the in-plane load expression as,

$$\begin{aligned} N_{11}^{(s)} &= \frac{Eh}{\left(1-\mu^2\right)}\left(e_{11}^{0(s)} + \mu e_{22}^{0(s)}\right) \\ &= \frac{Eh}{\left(1-\mu^2\right)}\left(\frac{du_s}{dr} + \mu\frac{u_s}{r}\right) \\ &= A_{11}^{(s)}\frac{du_s}{dr} + A_{12}^{(s)}\frac{u_s}{r} \\ &= C_4\left(A_{11}^{(s)} + A_{12}^{(s)}\right) \end{aligned} \tag{3.36}$$

$$\begin{aligned} N_{22}^{(s)} &= \frac{Eh}{\left(1-\mu^2\right)}\left(e_{22}^{0(s)} + \mu e_{11}^{0(s)}\right) \\ &= \frac{Eh}{\left(1-\mu^2\right)}\left(\frac{u_s}{r} + \mu\frac{du_s}{dr}\right) \\ &= A_{12}^{(s)}\frac{du_s}{dr} + A_{11}^{(s)}\frac{u_s}{r} \\ &= C_4\left(A_{11}^{(s)} + A_{12}^{(s)}\right) \end{aligned} \tag{3.37}$$

where $A_{11}^{(s)}$ and $A_{22}^{(s)}$ are defined in subsection 3.4.3. One would see that the in-plane loads are independent of radius and uniformly distributed across the plate. In addition, the radial in-plane load is equal to circumferential in-plane load.

The constant C_4 is determined by the boundary condition of the plates. The determination of these constants is shown in the following chapters.

3.5 THE PIEZOCERAMIC ANNULAR PLATE FORMULATION

3.5.1 Constitutive Equations

The strain-mechanical displacement definitions for piezoceramic plate is similar as for isotropic plate thus may be refered to Section 3.4. The linear piezoceramic constitutive equations for a piezoceramic material with crystal symmetry class C_6mm (Tiersten, 1969) can be written as:

$$\begin{Bmatrix} e_{11}^{(p)} \\ e_{22}^{(p)} \\ e_{33}^{(p)} \\ e_{23}^{(p)} \\ e_{13}^{(p)} \\ e_{12}^{(p)} \\ D_1 \\ D_2 \\ D_3 \end{Bmatrix} = \begin{bmatrix} s_{11}^E & s_{12}^E & s_{13}^E & 0 & 0 & 0 & 0 & 0 & d_{31} \\ s_{12}^E & s_{11}^E & s_{13}^E & 0 & 0 & 0 & 0 & 0 & d_{31} \\ s_{13}^E & s_{13}^E & s_{33}^E & 0 & 0 & 0 & 0 & 0 & d_{31} \\ 0 & 0 & 0 & s_{44}^E & 0 & 0 & 0 & d_{31} & 0 \\ 0 & 0 & 0 & 0 & s_{44}^E & 0 & d_{31} & 0 & 0 \\ 0 & 0 & 0 & 0 & 0 & s_{66}^E & 0 & 0 & 0 \\ 0 & 0 & 0 & 0 & d_{31} & 0 & \epsilon_{11}^T & 0 & d_{31} \\ 0 & 0 & 0 & d_{31} & 0 & 0 & 0 & \epsilon_{33}^T & d_{31} \\ d_{31} & d_{31} & d_{31} & 0 & 0 & 0 & 0 & 0 & \epsilon_{33}^T \end{bmatrix} \begin{Bmatrix} \sigma_{11}^{(p)} \\ \sigma_{22}^{(p)} \\ \sigma_{33}^{(p)} \\ \sigma_{23}^{(p)} \\ \sigma_{13}^{(p)} \\ \sigma_{12}^{(p)} \\ E_1 \\ E_2 \\ E_3 \end{Bmatrix} \tag{3.38}$$

where s_{ij}^E are the compliance constants at constant electric field, d_{ij} are the piezoelectric constants, ϵ_{ij}^T are the dielectric constants at constant stress, $e_{ij}^{(p)}$ are the strains components, $\sigma_{ij}^{(p)}$ are the stresses components, D_i are the electric displacement components and E_i are the electric field components. Also $s_{66}^E = 2s_{11}^E\left(1+\nu_p\right)$ and superscript (p) denotes for stresses/strains for piezoceramic material. From the Kirchhoff assumptions 4 and 5, the transverse shear strain and transverse normal stresses are negligible.

$$e_{23} = 0 \ ; \ e_{13} = 0 \ \text{and} \ \sigma_{33} = 0 \tag{3.39}$$

In the meanwhile, the assumption of the electric potential varies with thickness by the square law lead to the electric field component in $r-$ and $\theta-$direction to be

zero, and $E_1 = 0$ and $E_2 = 0$. This is due to the following relations of electric field and the electric potential;

$$E_1 = -\frac{\partial \phi}{\partial r} \;;\; E_2 = -\frac{1}{r}\frac{\partial \phi}{\partial \theta} \text{ and } E_3 = -\frac{\partial \phi}{\partial z} \tag{3.40}$$

As a results of these assumptions and the linear constitutive equations, e_{33} , σ_{13} , σ_{23} D_1 and D_2 also becomes zero which simplified the Equation (3.38) to

$$\begin{Bmatrix} e_{11}^{(p)} \\ e_{22}^{(p)} \\ e_{12}^{(p)} \\ D_3 \end{Bmatrix} = \begin{bmatrix} s_{11}^E & s_{12}^E & 0 & d_{31} \\ s_{12}^E & s_{11}^E & 0 & d_{31} \\ 0 & 0 & s_{66}^E & 0 \\ d_{31} & d_{31} & 0 & \epsilon_{33}^T \end{bmatrix} \begin{Bmatrix} \sigma_{11}^{(p)} \\ \sigma_{22}^{(p)} \\ \sigma_{12}^{(p)} \\ E_3 \end{Bmatrix} \tag{3.41}$$

Or if rewritten in equations and rearrange the equations as strains are the independence variables, the following equations are obtained:

$$\sigma_{11}^{(p)} = \frac{1}{s_{11}^E\left(1-\nu_p^2\right)}\left(e_{11}^0 + z\kappa_{11} + \nu_p\left(e_{22}^0 + z\kappa_{22}\right)\right) - \frac{d_{31}}{s_{11}^E\left(1-\nu_p\right)}E_3 \tag{3.42}$$

$$\sigma_{22}^{(p)} = \frac{1}{s_{11}^E\left(1-\nu_p^2\right)}\left(e_{22}^0 + z\kappa_{22} + \nu_p\left(e_{11}^0 + z\kappa_{11}\right)\right) - \frac{d_{31}}{s_{11}^E\left(1-\nu_p\right)}E_3 \tag{3.43}$$

$$\sigma_{12}^{(p)} = \frac{1}{2s_{11}^E\left(1+\nu_p\right)}\left(e_{12}^0 + z\kappa_{12}\right) \tag{3.44}$$

$$D_3 = d_{31}\left(e_{11}^0 + z\kappa_{11} + e_{22}^0 + z\kappa_{22}\right) + \epsilon_{33}^T E_3 \tag{3.45}$$

where $\nu_p = -s_{12}^E / s_{11}^E$ is the planar Poisson's ratio.

3.5.2 Distribution of Electric Field in the Annular Piezoceramic Plate

In many published literature on mechanics model for the analysis of the coupled structure, the distribution of the electric potential is assumed to be uniform in the longitudinal direction of the piezoelectric actuator and linear in its thickness direction,

which may violate the Maxwell static electricity equation. For full coupling effects of the piezoceramic layer on host plate to be considered, this issue must be taken care. Wang et. al. (2001) have proposed a formulation of electric potential, which is a quadratic variation in the thickness direction, that satisfies the Maxwell static electricity equation. In the present analysis, the electric potential is assumed to be varies with thickness by the square law as stated in subsection 3.2.1. The constant in the equation of the electric potential can be determined from the electric potential boundary conditions on the piezoceramic layer surfaces, relations of electric displacement to electric potential from linear piezoelectric constitutive equations and the assumption that the electric displacement is constant with respect to the plate thickness (refer to subsection 3.2.1). This follows the work of Huang (2005) and Huang et. al. (2004).

With polarization direction and the external voltage source connection for the annular piezoceramic plate taken into account, the electric potential boundary conditions of an annular piezoelectric of thickness $2h_a$ are:

$$\phi\big|_{z=h_a} = V \quad \text{and} \quad \phi\big|_{z=-h_a} = 0 \tag{3.46}$$

where the plate is considered to be grounded at the bottom surface.

From Equation (3.4) to (3.6) and Equation (3.42) to (3.45),

$$\begin{aligned} D_3 &= d_{31}\left(\sigma_{11}+\sigma_{22}+\epsilon_{33}^{T}E_3\right) \\ &= \frac{d_{31}}{s_{11}^{E}\left(1-\nu_p\right)}\left(e_{11}+e_{22}\right)-\left(\frac{2\left(d_{31}\right)^2-\epsilon_{33}^{T}s_{11}^{E}\left(1-\nu_p\right)}{s_{11}^{E}\left(1-\nu_p\right)}\right)E_3 \\ &= \frac{d_{31}}{s_{11}^{E}\left(1-\nu_p\right)}\left[e_{11}^{0}+e_{22}^{0}+z\left(\kappa_{11}+\kappa_{22}\right)\right]+\epsilon_{33}^{T}\left(1-\left(k_p\right)^2\right)E_3 \end{aligned} \tag{3.47}$$

where $k_p = \sqrt{\left(2\left(d_{31}\right)^2\right)/\left(\epsilon_{33}^T s_{11}^E\left(1-\nu_p\right)\right)}$ is the planar electromechanical coupling coefficient. Using the assumption that the electric displacement is constant throughout the thickness (not a function of z),

$$\frac{\partial D_3}{\partial z} = \frac{d_{31}}{s_{11}^E\left(1-\nu_p\right)}\left(\kappa_{11}+\kappa_{22}\right)+\epsilon_{33}^T\left(1-\left(k_p\right)^2\right)\frac{\partial E_3}{\partial z}$$

$$= \frac{d_{31}}{s_{11}^E\left(1-\nu_p\right)}\left(\kappa_{11}+\kappa_{22}\right)-\epsilon_{33}^T\left(1-\left(k_p\right)^2\right)\frac{\partial^2 \phi}{\partial z^2}$$

$$= 0 \tag{3.48}$$

The assumption that the electric potential ϕ varies with thickness in quadratic law ($\phi = \phi_0 + z\phi_1 + z^2\phi_2$) gave the derivative of electric field with z as $\partial^2\phi/\partial z^2 = 2\phi_2$. Substitute this equation in Equation (3.48) will lead to;

$$\phi_2 = \frac{d_{31}}{2\epsilon_{33}^T s_{11}^E\left(1-\nu_p\right)\left(1-\left(k_p\right)^2\right)}\left(\kappa_{11}+\kappa_{22}\right) \tag{3.49}$$

From electrical potential boundary condition, Equation (3.46)

$$\phi\big|_{z=h_a} = \phi_0 + \left(h+h_p\right)\phi_1 + \left(h+h_p\right)^2\phi_2 = V \tag{3.50}$$

$$\phi\big|_{z=-h_a} = \phi_0 + \left(h\right)\phi_1 + \left(h\right)^2\phi_2 = 0 \tag{3.51}$$

Solving Equation (3.50) and (3.51) simultaneously to obtain ϕ_1;

$$\phi_1 = \frac{V}{2h_a} \tag{3.52}$$

With the derived expression for ϕ_1 and ϕ_2, the electric field in z direction for annular piezoceramic plate can be written as

$$
\begin{aligned}
E_3^{(a)} &= -\frac{\partial \phi}{\partial z} \\
&= -\phi_1 - 2z\phi_2 \\
&= -\frac{V}{2h_a} - \frac{zd_{31}}{2\epsilon_{33}^T s_{11}^E \left(1-\nu_p\right)\left(1-\left(k_p\right)^2\right)}\left(\kappa_{11}+\kappa_{22}\right)
\end{aligned}
\tag{3.53}
$$

3.5.3 Force and Moment Resultants for Piezoceramic Annular Plate

The stress distribution for a piezoelectric plate is given by Equation (3.42) to (3.44) while for an isotropic plate is given by Equation (3.7) to (3.9). By using these stress distributions in addition to electric field distribution given by Equation (3.54), the force resultants and moment resultants for a piezoceramic plates may be determined from Equation (3.10) to (3.11).

3.5.3.1 Force Resultants

The radial force may be obtained as the following,

$$
\begin{aligned}
N_{11}^{(a)} &= \int_{-h_a}^{h_a} \sigma_{11}^{(p)} dz \\
&= \frac{1}{s_{11}^E\left(1-\nu_p^2\right)} \int_{-h_a}^{h_a} \left(e_{11}^0 + z\kappa_{11} + \nu_p\left(e_{22}^0 + z\kappa_{22}\right)\right) dz \\
&\quad - \frac{d_{31}}{s_{11}^E\left(1-\nu_p\right)} \int_{-h_a}^{h_a} E_3^{(a)} dz
\end{aligned}
\tag{3.55}
$$

The integration of the electric field is done by integrating Equation (3.56);

$$\begin{aligned}
&\int_{-h_a}^{h_a} E_3^{(a)} dz \\
&= \int_{-h_a}^{h_a} \left(-\frac{V}{2h_a} - \frac{z d_{31}}{2\epsilon_{33}^T s_{11}^E \left(1-\nu_p\right)\left(1-\left(k_p\right)^2\right)} \left(\kappa_{11}+\kappa_{22}\right) \right) dz \\
&= -V
\end{aligned} \tag{3.57}$$

Substitute this equation into Equation (3.55), to obtained the final form of the radial force

$$\begin{aligned}
N_{11}^{(a)} &= \int_{-h_a}^{h_a} \sigma_{11}^{(p)} dz \\
&= \frac{2h_a}{s_{11}^E \left(1-\nu_p^2\right)} \left(e_{11}^0 + \nu_p e_{22}^0\right) + \frac{d_{31}}{s_{11}^E \left(1-\nu_p\right)} V
\end{aligned} \tag{3.58}$$

$$\begin{aligned}
&= A_{11}^{(a)} e_{11}^0 + A_{12}^{(a)} e_{22}^0 + N_p \\
&= A_{11}^{(a)} \left(e_{11}^0 + \mu_A^{(a)} e_{22}^0\right) + N_p
\end{aligned} \tag{3.59}$$

where $A_{11}^{(a)} = 2h_a \big/ s_{11}^E \left(1-\nu_p^2\right)$, $A_{22}^{(a)} = 2h_a \nu_p \big/ s_{11}^E \left(1-\nu_p^2\right)$, $\mu_A^{(a)} = A_{12}^{(a)} \big/ A_{11}^{(a)}$ and $N_p = d_{31} \big/ s_{11}^E \left(1-\nu_p\right) V$. Similarly for circumferential force,

$$\begin{aligned}
N_{22}^{(a)} &= \int_{-h_a}^{h_a} \sigma_{22}^{(p)} dz \\
&= \frac{2h_a}{s_{11}^E \left(1-\nu_p^2\right)} \left(e_{22}^0 + \nu_p e_{11}^0\right) + \frac{d_{31}}{s_{11}^E \left(1-\nu_p\right)} V
\end{aligned} \tag{3.60}$$

$$\begin{aligned}
&= A_{11}^{(a)} e_{22}^0 + A_{12}^{(a)} e_{11}^0 + N_p \\
&= A_{11}^{(a)} \left(e_{22}^0 + \mu_A^{(a)} e_{11}^0\right) + N_p
\end{aligned} \tag{3.61}$$

Lastly, the shear force,

$$\begin{aligned}
N_{12}^{(a)} &= \int_{-h_a}^{h_a} \sigma_{12}^{(p)} dz \\
&= \frac{1}{2s_{11}^E \left(1+\nu_p\right)} \int_{-h_a}^{h_a} \left(e_{12}^0 + z\kappa_{12}\right) dz \\
&= \frac{h_a}{s_{11}^E \left(1+\nu_p\right)} e_{12}^0
\end{aligned} \tag{3.62}$$

$$= A_{66}^{(a)} e_{12}^{0} \tag{3.63}$$

where $A_{66}^{(a)} = h_a \big/ s_{11}^{E}\left(1+\nu_p\right)$.

3.5.3.2 Moment Resultants

The radial bending moment may be obtained as the following,

$$\begin{aligned} M_{11}^{(a)} &= \int_{-h_a}^{h_a} \sigma_{11}^{(p)} z dz \\ &= \frac{1}{s_{11}^{E}\left(1-\nu_p^2\right)} \int_{-h_a}^{h_a} \left(e_{11}^{0} + z\kappa_{11} + \nu_p \left(e_{22}^{0} + z\kappa_{22} \right) \right) z dz \\ &\quad - \frac{d_{31}}{s_{11}^{E}\left(1-\nu_p\right)} \int_{-h_a}^{h_a} E_3^{(a)} z dz \end{aligned} \tag{3.64}$$

The integration of the electric field in the last term of Equation (3.64) is done by integrating Equation (3.65);

$$\begin{aligned} &\int_{-h_a}^{h_a} E_3^{(a)} z dz \\ &= \int_{-h_a}^{h_a} \left(-\frac{V}{2h_a} - \frac{z d_{31}}{2\epsilon_{33}^{T} s_{11}^{E}\left(1-\nu_p\right)\left(1-\left(k_p\right)^2\right)} \left(\kappa_{11}+\kappa_{22}\right) \right) z dz \\ &= -\frac{h_a^3 d_{31}}{3\epsilon_{33}^{T} s_{11}^{E}\left(1-\nu_p\right)\left(1-\left(k_p\right)^2\right)} \left(\kappa_{11}+\kappa_{22}\right) \end{aligned} \tag{3.66}$$

Substitute this equation into Equation (3.64), to obtained the final form of the radial moment

$$\begin{aligned} M_{11}^{(a)} &= \int_{-h_a}^{h_a} \sigma_{11}^{(p)} z dz \\ &= \frac{2h_a^3}{3s_{11}^{E}\left(1-\nu_p^2\right)} \left(\kappa_{11} + \nu_p \kappa_{22}\right) + \frac{h_a^3 d_{31}}{3\epsilon_{33}^{T} s_{11}^{E}\left(1-\nu_p\right)\left(1-\left(k_p\right)^2\right)} \left(\kappa_{11}+\kappa_{22}\right) \end{aligned} \tag{3.67}$$

$$\begin{aligned} &= D_{11}^{(a)} \kappa_{11} + D_{12}^{(a)} \kappa_{22} \\ &= D_{11}^{(a)} \left(\kappa_{11} + \mu_D^{(a)} \kappa_{22} \right) \end{aligned} \tag{3.68}$$

where $D_{11}^{(a)} = 2h_a^3 \big/ 3s_{11}^E\left(1-\nu_p^2\right)$, $D_{12}^{(a)} = 2h_a^3\nu_p \big/ 3s_{11}^E\left(1-\nu_p^2\right)$ and $\mu_D^{(a)} = D_{12}^{(a)} \big/ D_{11}^{(a)}$.

Similarly for circumferential moment,

$$\begin{aligned} M_{22}^{(a)} &= \int_{-h_a}^{h_a} \sigma_{22}^{(p)} z dz \\ &= \frac{2h_a^3}{3s_{11}^E\left(1-\nu_p^2\right)}\left(\kappa_{22}+\nu_p\kappa_{11}\right) + \frac{h_a^3 d_{31}}{3\epsilon_{33}^T s_{11}^E\left(1-\nu_p\right)\left(1-\left(k_p\right)^2\right)}\left(\kappa_{11}+\kappa_{22}\right) \end{aligned} \tag{3.69}$$

$$\begin{aligned} &= D_{11}^{(a)}\kappa_{22} + D_{12}^{(a)}\kappa_{11} \\ &= D_{11}^{(a)}\left(\kappa_{22} + \mu_D^{(a)}\kappa_{11}\right) \end{aligned} \tag{3.70}$$

Lastly, the shear moment,

$$\begin{aligned} M_{12}^{(a)} &= \int_{-h_a}^{h_a} \sigma_{12}^{(p)} z dz \\ &= \frac{1}{2s_{11}^E\left(1+\nu_p\right)} \int_{-h_a}^{h_a} \left(e_{12}^0 + z\kappa_{12}\right) z dz \\ &= \frac{h_a^3}{3s_{11}^E\left(1+\nu_p\right)}\kappa_{12} \end{aligned} \tag{3.71}$$

$$= D_{66}^{(a)}\kappa_{12} \tag{3.72}$$

where $D_{66}^{(a)} = h_a^3 \big/ 3s_{11}^E\left(1+\nu_p\right)$.

3.5.4 In-plane Load Distribution

Under this assumption and noting that the electric field distribution for an annular piezoelectric plate is given by Equation (3.53), the in-plane load can be rewritten as

$$\begin{aligned} N_{11}^{(a)} &= \frac{2h_a}{s_{11}^E\left(1-\nu_p^2\right)}\left(e_{11}^0 + \nu_p e_{22}^0\right) + \frac{d_{31}}{s_{11}^E\left(1-\nu_p\right)}V \\ &= \frac{2h_a}{s_{11}^E\left(1-\nu_p^2\right)}\left(\frac{du_a}{dr} + \nu_p\frac{u_a}{r}\right) + \frac{d_{31}}{s_{11}^E\left(1-\nu_p\right)}V \end{aligned} \tag{3.73}$$

$$
\begin{aligned}
N_{22}^{(a)} &= \frac{2h_a}{s_{11}^E\left(1-\nu_p^2\right)}\left(e_{22}^0+\nu_p e_{11}^0\right)+\frac{d_{31}}{s_{11}^E\left(1-\nu_p\right)}V \\
&= \frac{2h_a}{s_{11}^E\left(1-\nu_p^2\right)}\left(\frac{u_a}{r}+\nu_p\frac{du_a}{dr}\right)+\frac{d_{31}}{s_{11}^E\left(1-\nu_p\right)}V
\end{aligned}
\tag{3.74}
$$

In a similar way of determination of u_s, u_a may be determined. The solution is similar only that, since annular plate has no issue of singularity the expression of u_a can be write as

$$
u_a = \frac{C_1}{r}+C_2 r \tag{3.75}
$$

Rewrite Equation (3.30) and (3.31) in terms of C_1 and C_2,

$$
\begin{aligned}
N_{11}^{(a)} &= \frac{2h_a}{s_{11}^E\left(1-\nu_p^2\right)}\left(e_{11}^0+\nu_p e_{22}^0\right)+\frac{d_{31}}{s_{11}^E\left(1-\nu_p\right)}V \\
&= \frac{2h_a}{s_{11}^E\left(1-\nu_p^2\right)}\left(\frac{du_a}{dr}+\nu_p\frac{u_a}{r}\right)+\frac{d_{31}}{s_{11}^E\left(1-\nu_p\right)}V \\
&= A_{11}^{(a)}\frac{du_a}{dr}+A_{12}^{(a)}\frac{u_a}{r}+N_p \\
&= A_{11}^{(a)}\left(-\frac{C_1}{r^2}+C_2\right)+A_{12}^{(a)}\left(\frac{C_1}{r^2}+C_2\right)+N_p \\
&= -\frac{C_1}{r^2}\left(A_{11}^{(a)}-A_{12}^{(a)}\right)+C_2\left(A_{11}^{(a)}+A_{12}^{(a)}\right)+N_p
\end{aligned}
\tag{3.76}
$$

$$
\begin{aligned}
N_{22}^{(a)} &= \frac{2h_a}{s_{11}^E\left(1-\nu_p^2\right)}\left(e_{22}^0+\nu_p e_{11}^0\right)+\frac{d_{31}}{s_{11}^E\left(1-\nu_p\right)}V \\
&= \frac{2h_a}{s_{11}^E\left(1-\nu_p^2\right)}\left(\frac{u_a}{r}+\nu_p\frac{du_a}{dr}\right)+\frac{d_{31}}{s_{11}^E\left(1-\nu_p\right)}V \\
&= A_{12}^{(a)}\frac{du_a}{dr}+A_{11}^{(a)}\frac{u_a}{r}+N_p \\
&= A_{12}^{(a)}\left(-\frac{C_1}{r^2}+C_2\right)+A_{11}^{(a)}\left(\frac{C_1}{r^2}+C_2\right)+N_p \\
&= \frac{C_1}{r^2}\left(A_{11}^{(a)}-A_{12}^{(a)}\right)+C_2\left(A_{11}^{(a)}+A_{12}^{(a)}\right)+N_p
\end{aligned}
\tag{3.77}
$$

where $N_p = Vd_{31}\Big/\left(s_{11}^E\left(1-\nu_p\right)\right)$. Therefore the in-plane load, $N_{11}^{(a)}$ and $N_{22}^{(a)}$, are known when the boundary condition is known.

The constant C_1 and C_2 are determined by the boundary condition of the plates. The determination of these constants is shown in the following chapters.

3.6 BOUNDARY CONDITIONS

The following are some of the commonly used boundary conditions in dynamic or static problems of a plate (Reddy, 1999):

1. Clamped edge

$$u_0 = 0 \ , \ v_0 = 0 \ , \ w_0 = 0 \ \text{ and } \ \frac{\partial w_0}{\partial r} = 0 \tag{3.78}$$

2. Simply supported edge

$$u_0 = 0 \ , \ v_0 = 0 \ , \ w_0 = 0 \ \text{and} \ M_{11} = 0 \tag{3.79}$$

3. Free edge

$$N_{11} = 0 \ , \ N_{12} = 0 \ , \ V_1 = 0 \ \text{and} \ M_{11} = 0 \tag{3.80}$$

4. Edge with fixed in-plane movement (slide)

$$N_{11} = 0 \ , \ v_0 = 0 \ , \ w_0 = 0 \text{ and } \frac{\partial w_0}{\partial r} = 0 \tag{3.81}$$

where

$$V_1 = \frac{1}{2}\left[\frac{\partial}{\partial r}\left(rM_{11}\right) + \frac{\partial M_{12}}{\partial \theta} - M_{22}\right] + \frac{1}{r}\frac{\partial M_{12}}{\partial \theta} + N_{11}\frac{\partial w_0}{\partial r} + \frac{N_{12}}{r}\frac{\partial w_0}{\partial \theta} \tag{3.82}$$

$$V_2 = \frac{1}{2}\left[\frac{\partial}{\partial r}\left(rM_{12}\right) + \frac{\partial M_{22}}{\partial \theta} - M_{12}\right] + \frac{\partial M_{22}}{\partial r} + \frac{N_{22}}{r^2}\frac{\partial w_0}{\partial \theta} + \frac{N_{12}}{r}\frac{\partial w_0}{\partial r} \tag{3.83}$$

3.7 FINITE DIFFERENT METHOD

Among the most important of the numerical approaches are the method of finite differences (FD) and the finite element method (FEM). Both techniques eventually require the solution of a system of linear algebraic equations. Due to the simplicity and versatility of the FD method, the present report used it for analysis of current problems of plate. Given that relatively fine mesh is used, the FD also provides results in acceptable accuracy for most technical purposes. The current plate problem also analyzed by FEM but through an application of available FEM software such as ABAQUS. Therefore the FEM theory is not discussed here and the ABAQUS manual is referred if necessary.

The method of finite differences replace the plate differential equation and the expression defining the boundary conditions with equivalent difference equations. Therefore, the solution of the plate problems reduced to the simultaneous solution of a set of algebraic equations written for every nodes/nodal points within the plate.

In finite different formulation there are three type of expansion which is forward difference, backward difference and central difference. Since central difference is known to have better accuracy, hereafter the central difference will be used in the

formulation of any equations involved in this study. For reference, the following is the first, second, third and fourth derivatives using central difference formulation.

$$\left.\frac{\partial u(r)}{\partial r}\right|_k \approx \frac{u_{k+1}-u_{k-1}}{2\Delta r} \tag{3.84}$$

$$\left.\frac{\partial^2 u(r)}{\partial r^2}\right|_k \approx \frac{u_{k+1}-2u_k+u_{k-1}}{(\Delta r)^2} \tag{3.85}$$

$$\left.\frac{\partial^3 u(r)}{\partial r^3}\right|_k \approx \frac{u_{k+2}-2u_{k+1}+2u_{k-1}-u_{k-2}}{2(\Delta r)^3} \tag{3.86}$$

$$\left.\frac{\partial^4 u(r)}{\partial r^4}\right|_k \approx \frac{u_{k+2}-4u_{k+1}+6u_k-4u_{k-1}+u_{k-2}}{(\Delta r)^4} \tag{3.87}$$

3.7.1 Governing Equations in Finite Difference

Substituting the approximated derivatives into the plate governing equation (Equation (3.28)) will lead to the desired governing equation expressed in finite difference scheme. The outcomes are as following

1. Solid Circular Plate

$$\begin{aligned}
&\left(1-\frac{\Delta r}{r_i}\right)w_{n,i-2}^{(s)}-\left(4-\frac{2\Delta r}{r_i}+(\Delta r)^2\left[\frac{1}{r_i^2}+\frac{2n^2}{r_i^2}\right]+\frac{(\Delta r)^3}{2r_i}\left[\frac{1}{r_i^2}+\frac{2n^2}{r_i^2}\right]\right)w_{n,i-1}^{(s)}\\
&+\left(6+2(\Delta r)^2\left[\frac{1}{r_i^2}+\frac{2n^2}{r_i^2}\right]-\frac{(\Delta r)^4 n^2}{r_i^2}\left[\frac{4}{r_i^2}-\frac{n^2}{r_i^2}\right]\right)w_{n,i}^{(s)}\\
&-\left(4+\frac{2\Delta r}{r_i}+(\Delta r)^2\left[\frac{1}{r_i^2}+\frac{2n^2}{r_i^2}\right]-\frac{(\Delta r)^3}{2r_i}\left[\frac{1}{r_i^2}+\frac{2n^2}{r_i^2}\right]\right)w_{n,i+1}^{(s)}+\left(1+\frac{\Delta r}{r_i}\right)w_{n,i+2}^{(s)}\\
&-(\Delta r)^2\frac{N}{D}\left(\left[1-\frac{\Delta r}{2r_i}\right]w_{n,i-1}^{(s)}-\left[2+\frac{(\Delta r)^2 n^2}{r_i^2}\right]w_{n,i}^{(s)}+\left[1+\frac{\Delta r}{2r_i}\right]w_{n,i+1}^{(s)}\right)\\
&-(\Delta r)^4\left(\frac{q}{D}+\frac{\omega^2\rho h}{D}w_{n,i}^{(s)}\right)=0
\end{aligned} \tag{3.88}$$

2. Annular Plate

$$\left(1-\frac{\Delta r}{r_i}\right)w_{n,i-2}^{(a)}-\left(4-\frac{2\Delta r}{r_i}+(\Delta r)^2\left[\frac{1}{r_i^2}+\frac{2n^2}{r_i^2}\right]+\frac{(\Delta r)^3}{2r_i}\left[\frac{1}{r_i^2}+\frac{2n^2}{r_i^2}\right]\right)w_{n,i-1}^{(a)}$$
$$+\left(6+2(\Delta r)^2\left[\frac{1}{r_i^2}+\frac{2n^2}{r_i^2}\right]-\frac{(\Delta r)^4 n^2}{r_i^2}\left[\frac{4}{r_i^2}-\frac{n^2}{r_i^2}\right]\right)w_{n,i}^{(a)}$$
$$-\left(4+\frac{2\Delta r}{r_i}+(\Delta r)^2\left[\frac{1}{r_i^2}+\frac{2n^2}{r_i^2}\right]-\frac{(\Delta r)^3}{2r_i}\left[\frac{1}{r_i^2}+\frac{2n^2}{r_i^2}\right]\right)w_{n,i+1}^{(a)}+\left(1+\frac{\Delta r}{r_i}\right)w_{n,i+2}^{(a)} \quad (3.89)$$
$$-(\Delta r)^2\left(\left[\frac{N_{11}}{D}-\frac{\Delta r}{2r_i}\frac{N_{22}}{D}\right]w_{n,i-1}^{(a)}-\left[2\frac{N_{11}}{D}+\frac{(\Delta r)^2 n^2}{r_i^2}\frac{N_{22}}{D}\right]w_{n,i}^{(a)}\right.$$
$$\left.+\left[\frac{N_{11}}{D}+\frac{\Delta r}{2r_i}\frac{N_{22}}{D}\right]w_{n,i+1}^{(a)}\right)-(\Delta r)^4\left(\frac{q}{D}+\frac{\omega^2\rho h}{D}w_{n,i}^{(a)}\right)=0$$

3.7.2 Boundary Conditions in Finite Difference

Substituting the derivatives that has been approximated by finite difference method into the derivative that appear in the boundary condition will give the boundary condition in finite difference expression. The following are the terms that are used in the boundary condition;

1. The slope dw_n/dr

$$\frac{dw_n}{dr}\approx\frac{w_{n,i+1}-w_{n,i-1}}{2\Delta r} \quad (3.90)$$

2. The radial bending moment, M_{11}

$$M_{11}=-D\left(\frac{d^2w_n}{dr^2}+\frac{\mu}{r}\left[\frac{dw_n}{dr}-\frac{n^2}{r}w_n\right]\right)$$
$$\approx-\frac{D}{(\Delta r)^2}\left(\left[1-\frac{\mu\Delta r}{2r_i}\right]w_{n,i-1}-\left[2+\frac{\mu n^2(\Delta r)^2}{r_i^2}\right]w_{n,i}+\left[1+\frac{\mu\Delta r}{2r_i}\right]w_{n,i+1}\right) \quad (3.91)$$

3. The radial effective shear force, V_1

$$
\begin{aligned}
V_1 &= -D\left(\frac{d^3w_n}{dr^3}+\frac{1}{r}\frac{d^2w_n}{dr^2}-\left[\frac{1}{r^2}+\frac{(2-\mu)n^2}{r^2}\right]\frac{dw_n}{dr}+\frac{(3-\mu)n^2}{r^3}w_n\right)+N_{11}\frac{dw_n}{dr}\\
&\approx -\frac{D}{2(\Delta r)^3}\left(-w_{n,i-2}+\left[2+\frac{2\Delta r}{r_i}+(\Delta r)^2\left(\frac{1}{r_i^2}+\frac{(2-\mu)n^2}{r_i^2}\right)\right]w_{n,i-1}\right.\\
&\quad+\left[-\frac{4\Delta r}{r_i}+\frac{2(\Delta r)^3(3-\mu)n^2}{r_i^2}\right]w_{n,i}\\
&\quad-\left[2-\frac{2\Delta r}{r_i}+(\Delta r)^2\left(\frac{1}{r_i^2}+\frac{(2-\mu)n^2}{r_i^2}\right)\right]w_{n,i+1}+w_{n,i+2}\\
&\quad\left.+(\Delta r)^2\frac{N_{11}}{D}\left[-w_{n,i-1}+w_{n,i+1}\right]\right)
\end{aligned}
\tag{3.92}
$$

Close look at the boundary conditions revealed that there are nodes outside the plate mesh involved in the formulation. This is due to the derivatives approximation using central different. These nodes outside plate region nodes are called phantom nodes. This conditions may be avoid by using backward or forward different at the boundary but with a cost of accuracy. To maintain good accuracy, central different is used for any finite difference formulation in this thesis. For the plate with two regions such as the circular plate with annular plate surrounds it, the phantom nodes for annular plate will fall on the circular plate. The phantom nodes of annular plates will exactly equal to the nodes on the circular plates if the nodes spacing of annular and circular plates is the same. The similar explanation holds for the circular plates. In current study the mesh spacing is set to be equal.

3.7.3 Treatment at Center of Circular Plate

Solving differential equation, such as the plate governing equation for disk, which use a polar coordinate pose a problem at the origin or the center of the plate since it is singular at that point. Some researchers proposed extra condition for the origin which would give a non- singular solution at the origin (Mohseni & Colonius, 2000). Lai

(2002) has proposed a very simple way to treat this problem. Lai recognize that the numerical boundary condition at the origin (or the pole) in the traditional finite difference is needed only in the discretization of the transformed equation in the polar coordinate system. There is no need to impose any conditions from the rectangular coordinate point of view. He proposed a special mesh point locations so that this numerical boundary condition can be avoided. The special mesh points is achieved by shifting a grid a half mesh away from the origin and incorporating the symmetry constraint of Fourier coefficients. This approach also does not need to use one sided difference approximation (i.e. backward difference approximation) at the origin. The similar approach also reported by Mohseni and Colonius (2000).

At the origin, although there are no needs to impose any pole condition, it still need a numerical boundary value to make the linear system is closed beside the boundary condition at the edge of the plate. This is done by incorporating the symmetry constraint of Fourier coefficients which is derived as follows. The transformation between Cartesian and polar coordinates can be written as $x = r\cos\theta$ and $y = r\sin\theta$. When we replace r with $-r$, and θ with $\theta + \pi$, the Cartesian coordinates of a point remain the same. Therefore, any scalar function $w(r,\theta)$ satisfies $w(-r,\theta) = w(r,\theta+\pi)$. Using this equality, we have

$$w(-r,\theta) = w_n(-r)\cos n(\theta) = w_n(-r)\cos n(\theta+\pi) = (-1)^n w_n(r)\cos n(\theta)$$

Thus, when the domain of a function is extended to a negative value of r, the nth Fourier coefficient of this function satisfies $w_n(-r) = (-1)^n w_n(r)$ Using this equality, one obtained

$$w_n(r_0) = w_n\left(-\frac{\Delta r}{2}\right) = (-1)^0 w_n\left(\frac{\Delta r}{2}\right) = w(r_1) \qquad (3.93)$$

Therefore, with the plate edge condition the linear system now is a closed one and ready to be solved.

3.7.4 Finite Difference Implementation On Annular Plate

The problem of annular thin plate is actually a 2-D problems involving two independent variables namely radius, r and circumferential, θ. However, in the present analysis the dependent variable (the deflection W) is expand using the harmonic function. This reduce the problem into a 1-D problem involving one independent variables, the radius r. The governing equation for isotropic annular plate is given by Equation (3.88). The boundary condition for current analysis is the outer edge is free while the inner edge is simply supported but moveable in radial direction. The load case divided into two cases, first is where the annular plate is compressed at both edges and second is the plate is tensioned only at the inner edge.

In the present analysis, the boundary conditions is considered to be extra equations to be solved linearly. Arrange the governing equations and the boundary conditions in a matrix form will lead to a matrix consist of the coefficients of the unknown multiply with a set of unknown vectors equal to another vectors which are normally consists of external forces. This can be illustrated as the following matrix:

$$\begin{bmatrix} B.C. & B.C. & B.C. & B.C. & B.C. & B.C. & B.C. & B.C. & B.C. & B.C. \\ B.C. & B.C. & B.C. & B.C. & B.C. & B.C. & B.C. & B.C. & B.C. & B.C. \\ a_0 & b_0 & c_0 & d_0 & e_0 & 0 & 0 & \cdots & \cdots & 0 \\ 0 & a_1 & b_1 & c_1 & d_1 & e_1 & 0 & 0 & \cdots & 0 \\ \vdots & \ddots & \ddots & \ddots & \ddots & \ddots & \ddots & \ddots & \ddots & \vdots \\ \vdots & \ddots & \ddots & \ddots & \ddots & \ddots & \ddots & \ddots & \ddots & \vdots \\ 0 & \cdots & 0 & 0 & a_{i-1} & b_{i-1} & c_{i-1} & d_{i-1} & e_{i-1} & 0 \\ 0 & \cdots & \cdots & 0 & 0 & a_i & b_i & c_i & d_i & e_i \\ B.C. & B.C. & B.C. & B.C. & B.C. & B.C. & B.C. & B.C. & B.C. & B.C. \\ B.C. & B.C. & B.C. & B.C. & B.C. & B.C. & B.C. & B.C. & B.C. & B.C. \end{bmatrix} \begin{Bmatrix} w_{-2} \\ w_{-1} \\ w_0 \\ w_1 \\ \vdots \\ \vdots \\ w_{i-1} \\ w_i \\ w_{i+1} \\ w_{i+2} \end{Bmatrix} = \begin{Bmatrix} B.C. \\ B.C. \\ q_0 \\ q_1 \\ \vdots \\ \vdots \\ q_{i-1} \\ q_i \\ B.C. \\ B.C. \end{Bmatrix}$$

$$[A]\{w\} = \{q\} \tag{3.94}$$

where $[A]$, $\{w\}$ and $\{q\}$ are the coefficients matrix, deflection vector and external force vector, respectively. The first two and the last two unknowns are the phantom nodes. The first two lines and the last two lines are corresponding to the equations of the boundary conditions with the first two lines are inner edge conditions and the last two lines are from outer edge conditions. Everything between these four lines are corresponds to the governing equations. It is to be noted that the coefficient matrix is a pentadiagonal.

For a static problem which the desired solution is the deflection or the unknowns vector, the inverse of coefficients matrix multiply with the right hand side vector will results the solutions. However, for buckling eigenvalue problems of free vibration eigenvalue problems, while the deflection is unknown, the buckling load or the frequency also an unknown. In this eigenvalue problem, the determinant of the coefficient matrix is set to zero which give the so-called transcendental equations. The roots of this equation is the desired eigenvalues. The deflection is off interest in this type of problem. Though the deflection may be compute for each eigenvalue after computing the eigenvalues.

In the present problem, the space between two nodes is defined by

$$\Delta r = \frac{2\left(r_1 - r_0\right)}{2m+1} \tag{3.95}$$

where m is the number of nodes between nodes at inner edge and outer edge.

3.7.5 Finite Difference Implementation on Circular Plate Attached with Annular Plate

In similar approach to problem of annular plate buckling, a 1-D problem is considered here. The differences are there are no inner edge boundary conditions, and there are matching conditions that need to be included. In the problem of 1-D circular plate, one may model the plate from one outer edge to another, but here one modeled half of the plate (i.e. modeled the plate from the center of the plates to the outer edge of the plates). This may reduce the number of nodes and thus reduce the cost of calculation time. Therefore, as discussed in subsection 3.3.3, instead of inner edge condition, this condition is used.

At the interface of circular and annular plate, the matching condition is imposed. A mentioned earlier, in application of central difference, there exists phantom nodes outside the physical region. For finite different problem involving two different regions such as this problem, the phantom nodes of one region fell into another region. The phantom nodes one region will equal to nodes on another region if the meshing is equal in both regions. In the present study, the mesh is set to equal. In the present problem, the space between two nodes is defined by Equation (3.95).

$$\begin{bmatrix}
B.C. & B.C. & B.C. & B.C. & B.C. & B.C. & B.C. & B.C. & B.C. & B.C. \\
B.C. & B.C. & B.C. & B.C. & B.C. & B.C. & B.C. & B.C. & B.C. & B.C. \\
a_0 & b_0 & c_0 & d_0 & e_0 & 0 & 0 & \cdots & \cdots & 0 \\
0 & a_1 & b_1 & c_1 & d_1 & e_1 & 0 & 0 & \cdots & 0 \\
\vdots & \ddots & \ddots & \ddots & \ddots & \ddots & \ddots & \ddots & \ddots & \vdots \\
\vdots & \ddots & \ddots & \ddots & \ddots & \ddots & \ddots & \ddots & \ddots & \vdots \\
B.C. & B.C. & B.C. & B.C. & B.C. & B.C. & B.C. & B.C. & B.C. & B.C. \\
B.C. & B.C. & B.C. & B.C. & B.C. & B.C. & B.C. & B.C. & B.C. & B.C. \\
B.C. & B.C. & B.C. & B.C. & B.C. & B.C. & B.C. & B.C. & B.C. & B.C. \\
B.C. & B.C. & B.C. & B.C. & B.C. & B.C. & B.C. & B.C. & B.C. & B.C. \\
\vdots & \ddots & \ddots & \ddots & \ddots & \ddots & \ddots & \ddots & \ddots & \vdots \\
\vdots & \ddots & \ddots & \ddots & \ddots & \ddots & \ddots & \ddots & \ddots & \vdots \\
0 & \cdots & 0 & 0 & a_{i-1} & b_{i-1} & c_{i-1} & d_{i-1} & e_{i-1} & 0 \\
0 & \cdots & \cdots & 0 & 0 & a_i & b_i & c_i & d_i & e_i \\
B.C. & B.C. & B.C. & B.C. & B.C. & B.C. & B.C. & B.C. & B.C. & B.C. \\
B.C. & B.C. & B.C. & B.C. & B.C. & B.C. & B.C. & B.C. & B.C. & B.C.
\end{bmatrix}
\begin{Bmatrix}
w_{-2} \\ w_{-1} \\ w_0 \\ w_1 \\ \vdots \\ \vdots \\ B.C. \\ B.C. \\ B.C. \\ B.C. \\ \vdots \\ \vdots \\ w_{i-1} \\ w_i \\ w_{i+1} \\ w_{i+2}
\end{Bmatrix}
=
\begin{Bmatrix}
B.C. \\ B.C. \\ q_0 \\ q_1 \\ \vdots \\ \vdots \\ B.C. \\ B.C. \\ B.C. \\ B.C. \\ \vdots \\ \vdots \\ q_{i-1} \\ q_i \\ B.C. \\ B.C.
\end{Bmatrix}$$

$$[A]\{w\} = \{q\} \tag{3.96}$$

where $[A]$, $\{w\}$ and $\{q\}$ are the coefficients matrix, deflection vector and external force vector, respectively. The first two and the last two unknowns (W_{-1}, W_{-2} W_{i+1} and W_{i+2}) are the phantom nodes. The first two lines, the last two lines and 4 lines in the middle of the matrix (denotes by columns that contains *B.C.*) are corresponding to the equations of the boundary conditions with the first two lines are inner edge conditions, the last two lines are from outer edge conditions and the four lines corresponding to matching conditions between the two plates. Everything between these lines are corresponds to the coefficients derived from governing equations in finite different equation.

3.8 SUMMARY

This chapter provided the explanations and derivations to all general equations that are going to be used in the following chapters. The chapter starts with basic assumptions of Kirchhoff's hypothesis for thin plate and additional assumptions related to piezoceramic plate. Since the circular structure that is going to be analyze here may be divided two segments which are the isotropic circular segment and piezoceramic annular segment, the formulation for both segments was provided. Lastly, as one use FDM to solve the problem, the governing equations and the boundary conditions are formulated into FDM formulation. The formulations are then converted into matrix form which later coded into MATLAB.

CHAPTER FOUR

BUCKLING ANALYSIS OF ISOTROPIC CIRCULAR PLATE WITH ANNULAR PIEZOCERAMIC PLATE

4.1 OVERVIEW

Current thesis focus on the analysis of resonant frequency tuning by applying intermediate radial load. The maximum limit of the applied intermediate radial load is the first buckling load. While buckling is not the main issue in current analysis, proving that the FDM code can work well for buckling problem will strengthen the statement that the FDM code able to use for study of influence of in-plane load to plate vibration. Since the final analysis involving analysis where the in-plane load is varied radially, the verification that the FDM code may handle problem involving radially dependent in-plane load is important. Although current problem involve full circular plate, the verification of buckling with radial load varied radially is compared with wrinkling problem of annular plate reported by Coman and Haughton (2006)

Current chapter starts with the plate buckling due to compression which is solved by FDM code and compare with analytical results from Aung and Wang (2004). Secondly, the buckling problem of annular plate is solve and compared with Couman and Houghton (2006). Later the buckling due to intermediate radial load is done and compared with the ABAQUS (FEM software) results.

4.2 FORMULATIONS

4.2.1 In-plane Load Distribution for Isotropic Annular Plate with Uniform Compressive Load at Its Edges

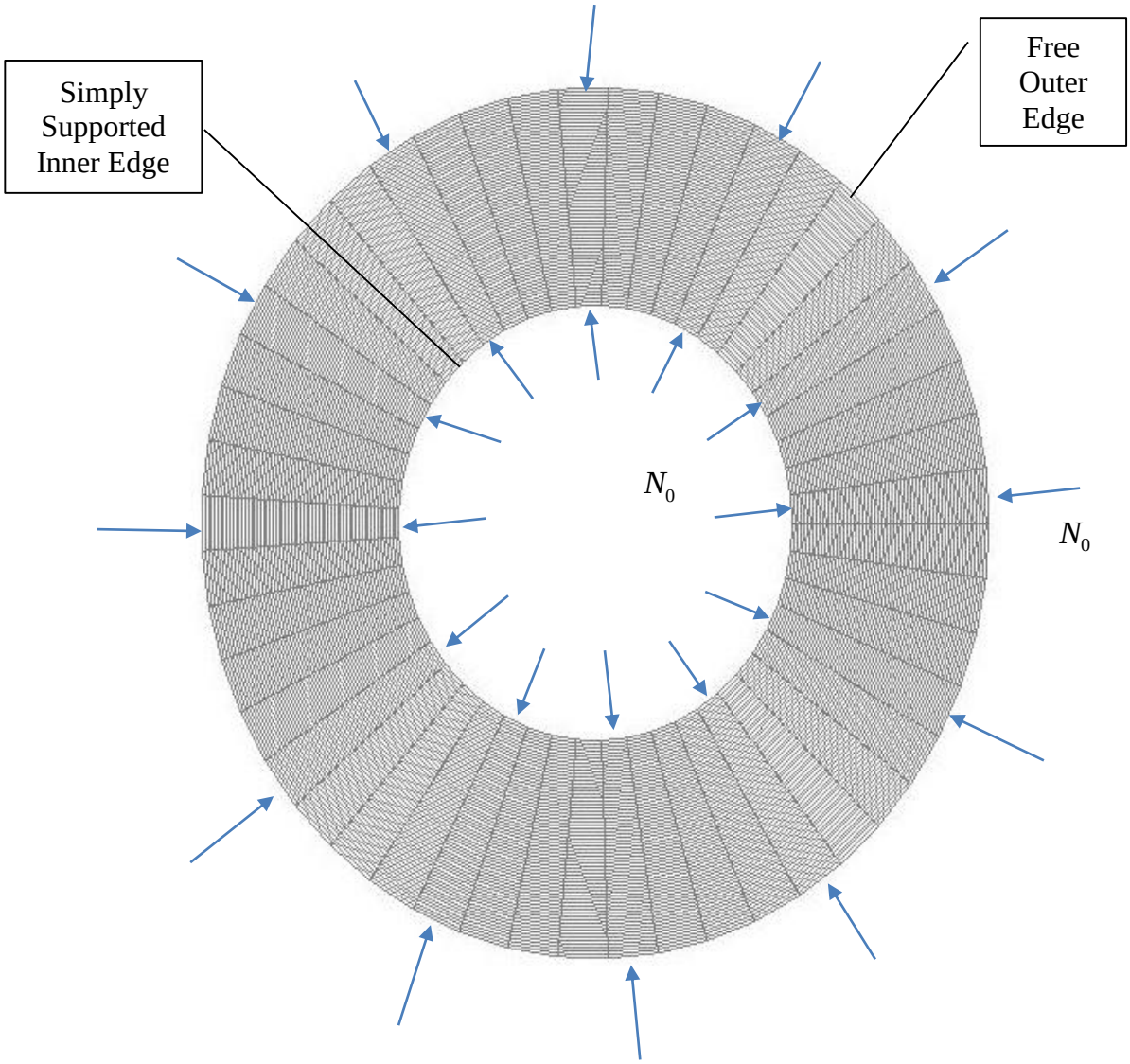

Figure 4.1 Annular plate is applied with compressive load at its both edges

In this case, the annular plate is applied with compressive load (N_0) at its both edges. The inner edge is simply supported while outer edge is a free edge. The constants for in-plane load may be determined by using the load conditions at the edges;

$$
\begin{aligned}
N_{11}^{(ac)}\Big|_{r=r_i} &= \frac{Eh}{\left(1-\mu^2\right)}\left(e_{11}^0\Big|_{r=r_i} + \mu e_{22}^0\Big|_{r=r_i}\right) \\
&= \frac{Eh}{\left(1-\mu^2\right)}\left(\frac{du_a}{dr}\Big|_{r=r_i} + \mu\frac{u_a}{r}\Big|_{r=r_i}\right) \\
&= A_{11}^{(s)}\frac{du_a}{dr}\Big|_{r=r_i} + A_{12}^{(s)}\frac{u_a}{r}\Big|_{r=r_i} \\
&= A_{11}^{(s)}\left(-\frac{C_1}{r_i^2}+C_2\right) + A_{12}^{(s)}\left(\frac{C_1}{r_i^2}+C_2\right) \\
&= -\frac{C_1}{r_i^2}\left(A_{11}^{(s)}-A_{12}^{(s)}\right) + C_2\left(A_{11}^{(s)}+A_{12}^{(s)}\right) \\
&= -\frac{C_1}{r_i^2}A_{11}^{(s)}\left(1-\mu\right) + C_2A_{11}^{(s)}\left(1+\mu\right) = -N_0
\end{aligned}
\tag{4.1}
$$

$$
\begin{aligned}
N_{22}^{(ac)}\Big|_{r=r_o} &= \frac{Eh}{\left(1-\mu^2\right)}\left(\mu e_{11}^0\Big|_{r=r_o} + e_{22}^0\Big|_{r=r_o}\right) \\
&= \frac{Eh}{\left(1-\mu^2\right)}\left(\mu\frac{du_a}{dr}\Big|_{r=r_o} + \frac{u_a}{r}\Big|_{r=r_o}\right) \\
&= A_{12}^{(s)}\frac{du_a}{dr}\Big|_{r=r_o} + A_{11}^{(s)}\frac{u_a}{r}\Big|_{r=r_o} \\
&= A_{12}^{(s)}\left(-\frac{C_1}{r_o^2}+C_2\right) + A_{11}^{(s)}\left(\frac{C_1}{r_o^2}+C_2\right) \\
&= \frac{C_1}{r_o^2}\left(A_{11}^{(s)}-A_{12}^{(s)}\right) + C_2\left(A_{11}^{(s)}+A_{12}^{(s)}\right) \\
&= \frac{C_1}{r_o^2}A_{11}^{(s)}\left(1-\mu\right) + C_2A_{11}^{(s)}\left(1+\mu\right) = -N_0
\end{aligned}
\tag{4.2}
$$

Superscript (ac) denoting for annular plate with compressed edge load. For these two equations to be satisfied constant C_1 has to be zero, therefore the second constant C_2 is

$$
C_2 = -\frac{N_0}{\left(A_{11}^{(s)}+A_{12}^{(s)}\right)} = -\frac{N_0}{A_{11}^{(s)}\left(1+\mu\right)} \tag{4.3}
$$

Therefore, the expression for in-plane load for this condition are

$$
N_{11}^{(ac)} = -N_0 \tag{4.4}
$$

$$N_{22}^{(ac)} = -N_0 \tag{4.5}$$

One can conclude that for compressive (or tensional) load applied at both edges of an annular plate will yield a uniform distributions of in-plane load (thus the stresses) throughout the plate as can be seen in above calculation.

4.2.2 In-plane Load Distribution for Isotropic Annular Plate with Inner Edge Applied Tension, Simply Supported and Free Outer Edge

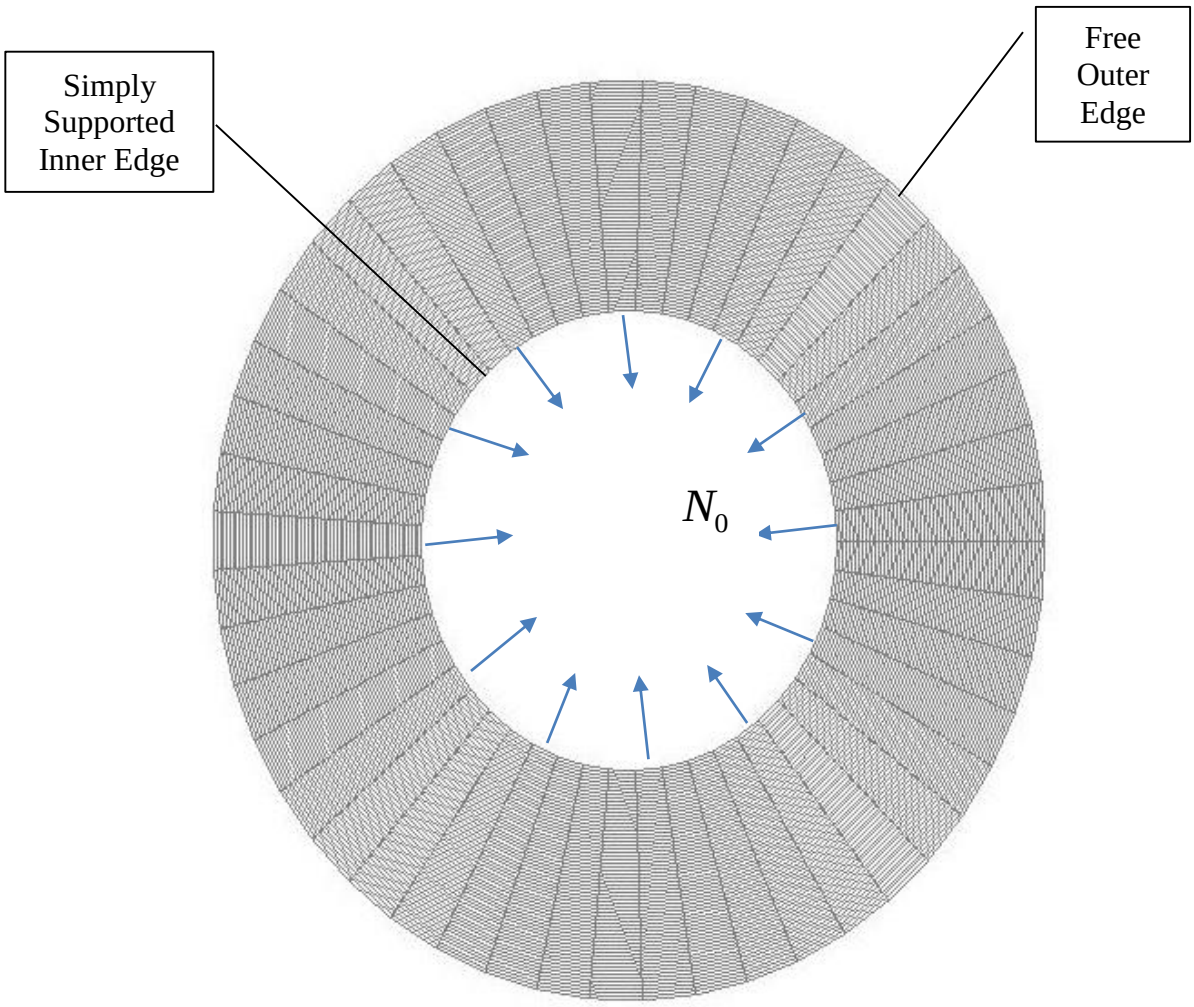

Figure 4.2 Annular plate is applied with tensional load at its inner edge

In this case, the annular plate is simply supported but radially movable, applied with tensional load at its inner edge while free at outer edge. At inner edge, the in-plane load must equal to the applied load N_0

$$
\begin{aligned}
N_{11}^{(it)}\Big|_{r=r_i} &= \frac{Eh}{\left(1-\mu^2\right)}\left(e_{11}^0\Big|_{r=r_i} + \mu e_{22}^0\Big|_{r=r_i}\right) \\
&= \frac{Eh}{\left(1-\mu^2\right)}\left(\frac{du_a}{dr}\Big|_{r=r_i} + \mu\frac{u_a}{r}\Big|_{r=r_i}\right) \\
&= A_{11}^{(s)}\frac{du_a}{dr}\Big|_{r=r_i} + A_{12}^{(s)}\frac{u_a}{r}\Big|_{r=r_i} \\
&= A_{11}^{(s)}\left(-\frac{C_1}{r_i^2}+C_2\right) + A_{12}^{(s)}\left(\frac{C_1}{r_i^2}+C_2\right) \\
&= -\frac{C_1}{r_i^2}\left(A_{11}^{(s)}-A_{12}^{(s)}\right) + C_2\left(A_{11}^{(s)}+A_{12}^{(s)}\right) \\
&= -\frac{C_1}{r_i^2}A_{11}^{(s)}\left(1-\mu\right) + C_2A_{11}^{(s)}\left(1+\mu\right) = N_0
\end{aligned}
\tag{4.6}
$$

while for outer edge condition the in-plane load is equal to zero,

$$
\begin{aligned}
N_{11}^{(it)}\Big|_{r=r_o} &= \frac{Eh}{\left(1-\mu^2\right)}\left(\mu e_{11}^0\Big|_{r=r_o} + e_{22}^0\Big|_{r=r_o}\right) \\
&= \frac{Eh}{\left(1-\mu^2\right)}\left(\mu\frac{du_a}{dr}\Big|_{r=r_o} + \frac{u_a}{r}\Big|_{r=r_o}\right) \\
&= A_{12}^{(s)}\frac{du_a}{dr}\Big|_{r=r_o} + A_{11}^{(s)}\frac{u_a}{r}\Big|_{r=r_o} \\
&= A_{12}^{(s)}\left(-\frac{C_1}{r_o^2}+C_2\right) + A_{11}^{(s)}\left(\frac{C_1}{r_o^2}+C_2\right) \\
&= \frac{C_1}{r_o^2}\left(A_{11}^{(s)}-A_{12}^{(s)}\right) + C_2\left(A_{11}^{(s)}+A_{12}^{(s)}\right) \\
&= \frac{C_1}{r_o^2}A_{11}^{(s)}\left(1-\mu\right) + C_2A_{11}^{(s)}\left(1+\mu\right) = 0
\end{aligned}
\tag{4.7}
$$

Supercript (it) denoting annular plate with tensional force at inner edge only. After some mathematical manipulation on Equation 4.6 and Equation 4.7, the constant C_1 and C_2 can be obtained,

$$C_1 = \frac{N_0 r_i^2 r_o^2}{A_{11}^{(s)}(1-\mu)\left(r_o^2 - r_i^2\right)} \tag{4.8}$$

$$C_2 = \frac{N_0 r_i^2 r_o^2}{A_{11}^{(s)}(1+\mu)\left(r_o^2 - r_i^2\right)} \tag{4.9}$$

Therefore, the expression for in-plane load for this condition are

$$N_{11}^{(it)} = \frac{N_0 r_i^2 r_o^2}{\left(r_o^2 - r_i^2\right)}\left(\frac{1}{r^2} - \frac{1}{r_o^2}\right) \tag{4.10}$$

$$N_{22}^{(it)} = \frac{N_0 r_i^2 r_o^2}{\left(r_o^2 - r_i^2\right)}\left(\frac{1}{r^2} + \frac{1}{r_o^2}\right) \tag{4.11}$$

4.2.3 In-plane Load Distribution for Clamped Circular Plate with Intermediate Radial Load

The intermediate radial load may be realized by heating some annular portion of the plate or attaching with piezoelectric part. For present analysis, a circular plate is attached with an annular plate which surrounds it therefore by applying voltage on the annular plate will produce tensional or compressed force to the circular plate. The boundary condition that being considered here is clamped outer edge while at interface between circular and annular plate, a matching condition is imposed. From clamped outer edge condition,

$$u^{(a)}\Big|_{r=r_o} = 0 \tag{4.12}$$

At interface circular - annular, the matching condition requires the radial in-plane load and radial displacement for both plate to be equal,

$$u^{(s)}\Big|_{r=r_i} = u^{(a)}\Big|_{r=r_i} \quad \text{and} \quad N_{11}^{(s)}\Big|_{r=r_i} = N_{11}^{(a)}\Big|_{r=r_i} \tag{4.13}$$

The general expression of the in-plane loads distributions are given by Equation (3.75) and (3.76) for annular plate and Equation (3.36) - (3.37) for solid circular plate.

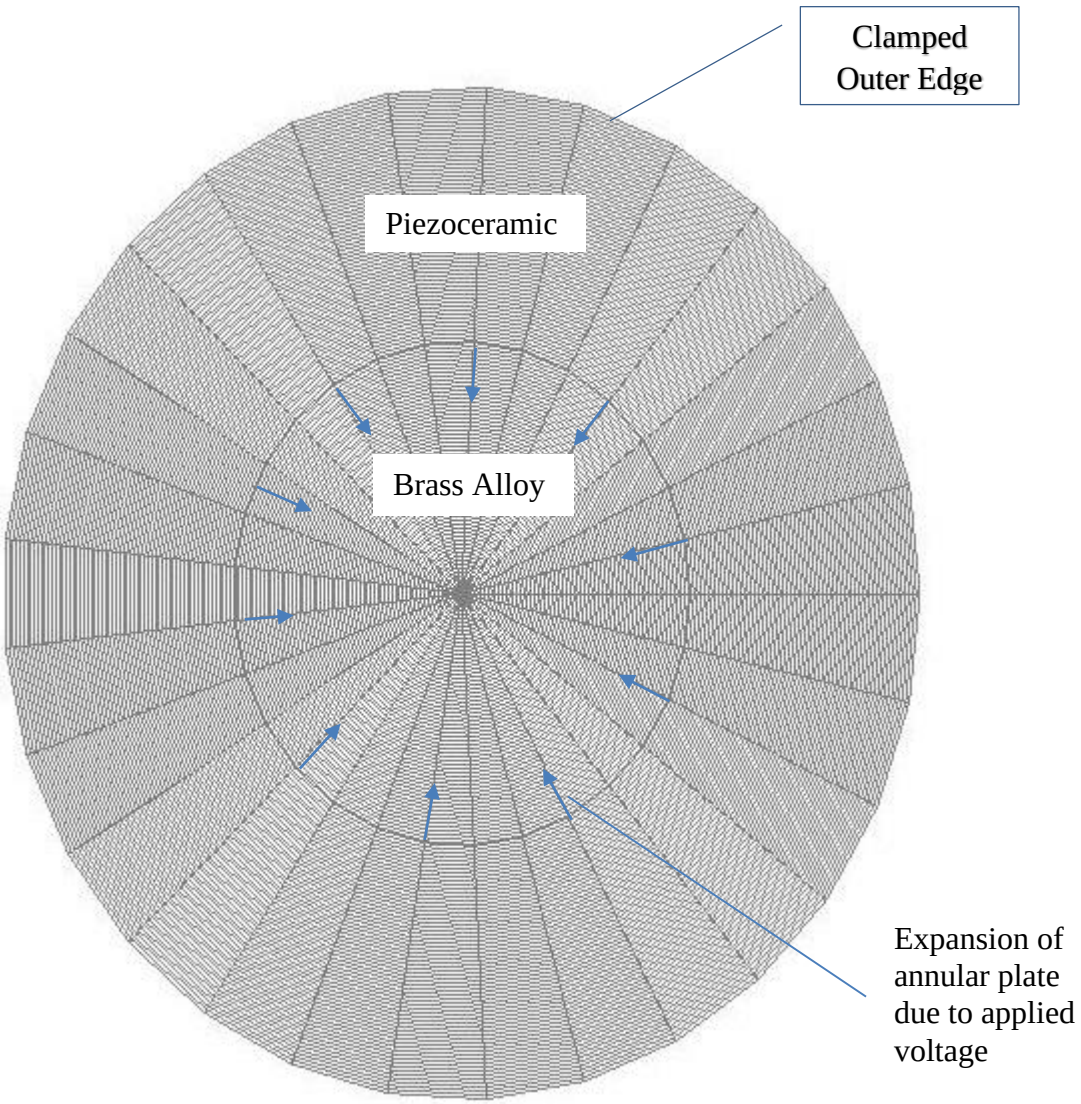

Figure 4.3 Circular plate with applied intermediate radial load due to expansion of piezoceramic annular region

Mathematically manipulate Equation (4.12) and (4.13) will give the constants C_1, C_2 and C_4 as

$$C_1 = \frac{N_p r_i^2 r_o^2}{\left(\left(A_{11}^{(s)} + A_{12}^{(s)}\right)\left(r_o^2 - r_i^2\right) + r_o^2\left(A_{11}^{(a)} - A_{12}^{(a)}\right) + r_i^2\left(A_{11}^{(a)} + A_{12}^{(a)}\right)\right)} \tag{4.14}$$

$$C_2 = -\frac{C_1}{r_o^2} \tag{4.15}$$

$$C_4 = \frac{C_1\left(r_o^2 - r_i^2\right)}{r_i^2 r_o^2} \tag{4.16}$$

Therefore the in-plane load distribution are,

$$N_{11}^{(a)} = \frac{N_p r_i^2 r_o^2}{\left(\left(A_{11}^{(s)} + A_{12}^{(s)}\right)\left(r_o^2 - r_i^2\right) + r_o^2\left(A_{11}^{(a)} - A_{12}^{(a)}\right) + r_i^2\left(A_{11}^{(a)} + A_{12}^{(a)}\right)\right)} \times\left(\frac{A_{11}^{(a)} - A_{12}^{(a)}}{r^2} + \frac{A_{11}^{(a)} + A_{12}^{(a)}}{r_o^2}\right) - N_p \tag{4.17}$$

$$N_{22}^{(a)} = -\frac{N_p r_i^2 r_o^2}{\left(\left(A_{11}^{(s)} + A_{12}^{(s)}\right)\left(r_o^2 - r_i^2\right) + r_o^2\left(A_{11}^{(a)} - A_{12}^{(a)}\right) + r_i^2\left(A_{11}^{(a)} + A_{12}^{(a)}\right)\right)} \times\left(\frac{A_{11}^{(a)} - A_{12}^{(a)}}{r^2} + \frac{A_{11}^{(a)} + A_{12}^{(a)}}{r_o^2}\right) - N_p \tag{4.18}$$

$$N_{11}^{(s)} = N_{22}^{(s)} = \frac{N_p\left(A_{11}^{(s)} + A_{12}^{(s)}\right)\left(r_o^2 - r_i^2\right)}{\left(\left(A_{11}^{(s)} + A_{12}^{(s)}\right)\left(r_o^2 - r_i^2\right) + r_o^2\left(A_{11}^{(a)} - A_{12}^{(a)}\right) + r_i^2\left(A_{11}^{(a)} + A_{12}^{(a)}\right)\right)} \tag{4.19}$$

For simplicity, from here $N_{11}^{(s)}$ and $N_{22}^{(s)}$ will be denoted as N_s unless stated otherwise.

4.2.4 Governing Equation for Buckling Problems

The general governing equation for circular plate buckling is given by Equation (3.26) with the inertia term and distributed load, q is dropped. Although in the present problem there are two region which are the annular and solid circular, they are basically governed by the similar governing equation except that the stiffness and the in-plane loads need to be specified for their respective regions. The in-plane load distribution has been

derived in the preceding section. The related bending stiffness are referred to Chapter 3. Here one rewrite the general equation of circular plate buckling

$$D\nabla_r^4 w - N_{11}\frac{\partial^2 w}{\partial r^2} - N_{22}\left(\frac{1}{r}\frac{\partial w}{\partial r} - \frac{1}{r^2}\frac{\partial^2 w}{\partial \theta^2}\right) = 0 \tag{4.20}$$

where ∇_r^4 is the polar biharmonic operator which defined by Equation (3.27) and, D and N_{ij} are representing the stiffnesses and the in-plane loads. Note that the N_{12} is assumed to be negligible and there are no lateral forces acting on the plates surfaces. Let $w = w_n \cos(n\theta)$ thus after dividing by bending stiffness D

$$\begin{aligned}&\frac{\partial^4 w_n}{\partial r^4} + \frac{2}{r}\frac{\partial^3 w_n}{\partial r^3} - \left(\frac{1}{r^2} + \frac{2n^2}{r^2}\right)\frac{\partial^2 w_n}{\partial r^2} + \left(\frac{1}{r^3} + \frac{2n^2}{r^3}\right)\frac{\partial w_n}{\partial r} + \left(\frac{n^4}{r^4} + \frac{4n^2}{r^4}\right)w_n \\ &\quad - \frac{N_{11}}{D^{(s)}}\frac{\partial^2 w_n}{\partial r^2} - \frac{N_{22}}{D^{(s)}}\left(\frac{1}{r}\frac{\partial w_n}{\partial r} - \frac{n^2}{r^2}w_n\right) = 0\end{aligned} \tag{4.21}$$

where n is the nodal diameter. For axisymmetric problems, the nodal diameter is zero $(n = 0)$. Equation (4.20) is the general governing equations that govern a circular plate buckling problems, thus either solid circular or annular plate is govern by Equation (4.20). However, in the present analysis, the different appear in the definition of the in-plane load. For the annular region, the in-plane load may varies in radial direction (Equation (4.17) and (4.18)) but for solid circular region they are constant throughout the region (Equation (4.19)).

To make it clear, here the governing equation is shown for each regions. The governing equation for solid circular plate where the in-plane loads is constant through the plate region is given by;

$$\frac{\partial^4 w_n^{(s)}}{\partial r^4}+\frac{2}{r}\frac{\partial^3 w_n^{(s)}}{\partial r^3}-\left(\frac{1}{r^2}+\frac{2n^2}{r^2}\right)\frac{\partial^2 w_n^{(s)}}{\partial r^2}+\left(\frac{1}{r^3}+\frac{2n^2}{r^3}\right)\frac{\partial w_n^{(s)}}{\partial r}+\left(\frac{n^4}{r^4}+\frac{4n^2}{r^4}\right)w_n^{(s)} - \frac{N_s}{D^{(s)}}\left(\frac{\partial^2 w_n^{(s)}}{\partial r^2}+\frac{1}{r}\frac{\partial w_n^{(s)}}{\partial r}-\frac{n^2}{r^2}w_n^{(s)}\right)=0 \tag{4.22}$$

and for the annular plate, the equation is

$$\frac{\partial^4 w_n^{(a)}}{\partial r^4}+\frac{2}{r}\frac{\partial^3 w_n^{(a)}}{\partial r^3}-\left(\frac{1}{r^2}+\frac{2n^2}{r^2}\right)\frac{\partial^2 w_n^{(a)}}{\partial r^2}+\left(\frac{1}{r^3}+\frac{2n^2}{r^3}\right)\frac{\partial w_n^{(a)}}{\partial r}+\left(\frac{n^4}{r^4}+\frac{4n^2}{r^4}\right)w_n^{(a)} - \frac{N_{11}^{(a)}}{D^{(a)}}\frac{\partial^2 w_n^{(s)}}{\partial r^2}-\frac{N_{22}^{(a)}}{D^{(a)}}\left(\frac{1}{r}\frac{\partial w_n^{(a)}}{\partial r}-\frac{n^2}{r^2}w_n^{(a)}\right)=0 \tag{4.23}$$

where $D^{(s)}$ and $D^{(a)}$ are the isotropic solid circular plate's bending stiffness and annular plate bending stiffness, respectively and, N_s and $N_{ij}^{(a)}$ are the in-plane loads defined in the preceding section.

4.3 RESULTS AND DISCUSSIONS

In this section 3 problems will be presented and discussed. The first two problems are mainly contributed for validating FDM code with existing problem in literatures. The third problem is the study of buckling due to intermediate load where results are compared with FEM results. The properties of piezoceramic material and the isotropic alloy that are used in these three problems are summarized in Table 4.1.

Table 4.1
Material Properties of Piezoceramic PIC-151 and Brass Alloy

PIC-151 piezoceramics		Brass Alloy	
s_{11}^E (10^{-12} m^2/N)	16.83	E (10^9 N/m^2)	110
d_{31} (10^{-10} m/V)	-2.14	ν	0.34
ε_{33}^T(10^{-9} F/m)	18.665	ρ (kg/m^3)	8400
ρ_p (kg/m^3)	7800		

4.3.1 Buckling of Annular Plate

In the present section, buckling problem of an isotropic annular plate which is simply supported at one edge and free at other edge is done. In the present analysis, the annular plate has outer radius of 40 mm and thickness of 0.3 mm. Three inner radius is used in the analysis which are 12 mm, 20 mm, and 28 mm which corresponds to inner to outer radius ratio of 0.3, 0.5 and 0.7, respectively. The results are compared to the works of Coman and Haughton (Coman & Haughton, 2006a, 2006b) and results available in e-book by Wang et. al. (2004).

4.3.1.1 Compressed Annular Plate

The annular plate is simply supported at inner edge, while free at outer edge. A uniform pressure is applied at inner and outer edge. The analysis is done through finite difference method and compared with results from finite element method via ABAQUS software and analytical results (Wang et. al., 2004). The sole purpose of validating the FDM code with current problem is to show that the code are able to handle standard buckling problem where in-plane load distributed constantly throughout the plate. The results are tabulated in Table 4.2.

Table 4.2
Annular plate with compression load at its edge

r_i / r_o	Critical Buckling Load [N]			Error (%)
	FD	FEM	Analytical	
0.3	303.57 ($n=1$)	300.44 ($n=1$)	314.06 ($n=1$)	3.3394

0.5	300.52 ($n=0$)	299.58 ($n=0$)	304.76 ($n=0$)	1.3911
0.7	220.43 ($n=0$)	219.39 ($n=0$)	227.31 ($n=0$)	3.0269

The error calculation is follow the following formula:

$$\frac{(\text{Analytical} - \text{FDM})}{\text{Analytical}} \times 100\% \tag{4.24}$$

The results showed a good agreement between the result from FDM code, FEM and analytical results. This positive results indicate that current code have no problems in solving standard buckling problems. This may extends its application to circular plate since the only different between the two is only the boundary conditions.

4.3.1.2 Tension Applied at Inner Edge

Now, one attempt to validate the FDM code for problem involving distributed in-plane load (radially distributed in-plane load). To one knowledge, such problem are yet to be solved analytically, thus no closed form solution exist. Therefore the results are compared to the results available from works of other researchers (obtained through perturbation method).

The annular plate is simply supported at inner edge, while free at outer edge. A tensional load is applied at inner edge while outer edge is free from any load. The analysis is done through finite difference method. The results are compared with the results reported by Couman and Haughton (Coman & Haughton, 2006a, 2006b) and is tabulated in Table 4.3. The error calculation is follow the following formula:

$$\text{Error } 1 = \frac{(\text{Literature} - \text{FDM})}{\text{Literature}} \times 100\% \tag{4.25}$$

$$\text{Error } 2 = \frac{(\text{FDM} - \text{FEM})}{\text{FDM}} \times 100\% \tag{4.26}$$

The results showed a good agreement with FEM and Coman and Haughton's results. Therefore one believed that, by this results, it is enough to conclude that the FDM code is able to handle problem involving distributed in-plane load.

As further evidence for annular plate having difference loading at its two edge (i.e. tensional at inner and free at outer edge) that its stress distribution is a function of its radius, the stresses distribution is compared between analytical based on Equation (4.10) and FEM analysis done via ABAQUS. The comparison is shown in Figure 4.4.

Table 4.3
Annular plate with tensional load at its inner edge while free at outer edge

r_o / r_i	Critical Buckling Load [$\times 10^3$ N]			Error 1 [%] (FD-FEM)	Error 2 [%] (FD-(Coman & Haughton, 2006a))
	FD	FEM	(Coman & Haughton, 2006a)		
0.3	7.1125 ($n=2$)	7.0321 ($n=2$)	7.0740 ($n=2$)	-1.1433	-0.5441
0.5	5.0145 ($n=3$)	4.9551 ($n=3$)	5.0426 ($n=3$)	-1.1988	0.5557
0.7	5.1915 ($n=4$)	5.0921 ($n=4$)	5.3085 ($n=4$)	-1.9520	2.2029

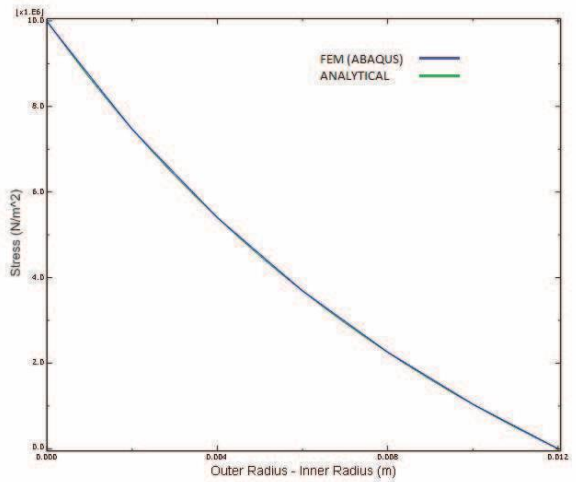

Figure 4.4 Stress distribution across radial direction for annular plate with tension at inner edge

4.3.2 Buckling of Circular Plate due to Intermediate Buckling Load

Aung and Wang (2005) has reported a circular plate buckling problems due to intermediate radial edge. However in their report, the stress distribution at annular plate is assumed either uniform throughout the annular plate or stress free. This is not the case if the annular plate is constrained with two different conditions along its two edges. For the stress to be uniform throughout the annular plate, the in-plane load has to be equal at both of its edge and for the annular plate to be stress free, it has to be constrained so that the annular plate behave like a rigid body. Figure 4.5 shows the comparison of the determined stress variation (Equation (4.17)) with the one obtained from FEM analysis. The results shows excellent agreement between the two results except at very narrow region at the annular-circular interface. The authors believe this is due to the boundary layer effects at an interface of two different regions with different properties.

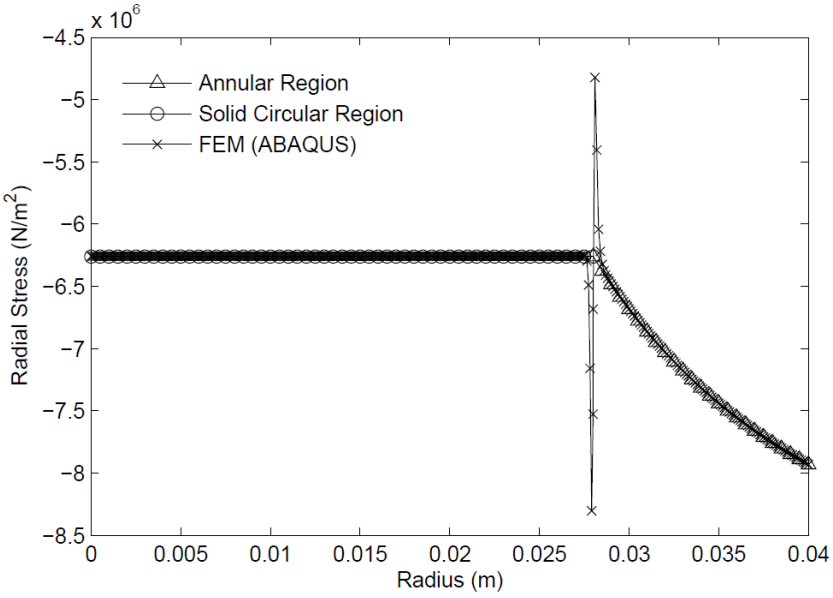

Figure 4.5 Radial stress distribution with applied voltage is 200V

In the present case, which the author believe to be the case for many practical cases due to intermediate radial load, the stress is varied with radius. This is due to the fact that the radial lo The FEM analysis is done by using FEM software (ABAQUS) where the plate is modeled by using axisymmetric element (8-node biquadratic axisymmetric quadrilateral, reduced integration (CAX8R) for isotropic alloy region and 8-node biquadratic axisymmetric piezoelectric quadrilateral, reduced integration (CAX8RE) is used for piezoceramic region. The FDM is formulated as discussed in Section 3.7 and coded in MATLAB. The results in Table 4.4 - Table 4.6 shows a good agreement of results obtained from FDM and FEM. The error calculation is follow the following formula:ad is different for both inner and outer edge.

$$\text{Error} = \frac{(\text{FDM} - \text{FEM})}{\text{FDM}} \times 100\% \tag{4.27}$$

Table 4.4
Critical buckling voltage for circular and annular plates having equal thickness

Mode (Nodal Circle)	FDM (V)	FEM (V)	Error (%)
1 (1)	245.93	235.00	4.44
2 (2)	844.10	825.27	2.23
3 (3)	1747.10	1713.60	1.92
4 (4)	2987.10	2945.30	1.40

Table 4.5
Critical buckling voltage for annular plate is thicker than circular plate

Mode (Nodal Circle)	FDM (V)	FEM (V)	Error (%)
1 (1)	742.20	725.85	2.20
2 (2)	2366.20	2296.30	2.95
3 (3)	4397.70	4239.20	3.60
4 (4)	6860.60	6703.40	2.29

Table 4.6
Critical buckling voltage for annular plate is thinner than circular plate

Mode (Nodal Circle)	FDM (V)	FEM (V)	Error (%)
1 (1)	671.00	650.90	3.00
2 (2)	1654.50	1602.60	3.14
3 (3)	4398.80	4324.30	1.69
4 (4)	6862.10	6804.20	0.84

Apart from the results comparison of current FDM code and FEM results, one may also deduced that it took significant amount of voltage to buckle current plate. Therefore, one may say that it is almost impossible the plate to buckle under current applied in-plane load unless one able to supply such huge voltage. Since the practical voltage that may be applied is lower than the critical buckling value, it can be said that it is safe to use the plate without concerning on buckling due to the applied voltage.

4.4 SUMMARY

As a step towards analysis of influence of radial load to circular plate resonant frequency, an analysis of plate buckling is done to show that the code running well for problem involving in-plane radial load. The chapter starts with buckling problem of annular plate where there is no radial variation of in-plane load. This follows with annular plate buckling problem which verified that current code handle problem involving in-plane load that vary with radius. The FDM code compared well for both annular problems. Lastly, the buckling analysis of circular plate with piezoceramic annular segment is performed. The results compared with the analysis via ABAQUS and the results shows good agreement. Therefore one may conclude that current FDM code handle problem involving in-plane load well. One also conclude that buckling of plate with piezoceramic annular segment is not a concern since the critical buckling load (voltage) is far from practical applicable voltage to the piezoceramic annular segment.

CHAPTER FIVE

VIBRATION ANALYSIS OF ISOTROPIC CIRCULAR PLATE WITH ANNULAR PIEZOCERAMIC PLATE

5.1 OVERVIEW

Current chapter will ultimately discussed on influence of intermediate radial load to circular plate resonant frequency. As progress from chapter 4 which focus on analysis involving solving problem involving influence of radial load in circular plate strength (which is buckling problem), current chapter starts with verification of FDM code for vibration of clamped circular plate. This follows on the code validation for vibration problem involving radial edge load. The results of both problems will be compared with NASA reports of Leissa (1969). Lastly, analysis of circular plate vibration under influence of intermediate load is performed and the results compared with results from ABAQUS. A parametric study also included in this chapter.

5.2 Formulations

5.2.1 Governing Equation for Out-of-Plane Vibrations

The general governing equation for circular plate free vibration is given by Equation (3.28). Although in the present problem there are two region which are the annular and solid circular, they are basically governed by the similar governing equation except that the stiffness and the in-plane loads need to be specified for their respective regions. The in-plane load distribution have been derived in the preceding section. The related bending stiffness are referred to Chapter 3. Here one rewrite the general equation of circular plate buckling

$$D\nabla_r^4 w - N_{11}\frac{\partial^2 w}{\partial r^2} - N_{22}\left(\frac{1}{r}\frac{\partial w}{\partial r} - \frac{1}{r^2}\frac{\partial^2 w}{\partial \theta^2}\right) + I_0\frac{\partial^2 w}{\partial t^2} = 0 \tag{5.1}$$

where ∇_r^4 is the polar biharmonic operator which defined by Equation (3.27) and, D and N_{ij} are representing the stiffnesses and the in-plane loads. Note that the N_{12} is assumed to be negligible and there are no lateral forces, q acting on the plates surfaces. Let $w = w_n\cos(n\theta)\cos(\omega t)$, thus after dividing by bending stiffness D

$$\begin{aligned}&\frac{d^4 w_n}{dr^4} + \frac{2}{r}\frac{d^3 w_n}{dr^3} - \left(\frac{1}{r^2} + \frac{2n^2}{r^2}\right)\frac{d^2 w_n}{dr^2} + \left(\frac{1}{r^3} + \frac{2n^2}{r^3}\right)\frac{dw_n}{dr} + \left(\frac{n^4}{r^4} + \frac{4n^2}{r^4}\right)w_n \\ &\quad - \frac{N_{11}}{D^{(s)}}\frac{d^2 w_n}{dr^2} - \frac{N_{22}}{D^{(s)}}\left(\frac{1}{r}\frac{dw_n}{dr} - \frac{n^2}{r^2}w_n\right) - \frac{\omega^2 I_0}{D}w_n = 0\end{aligned} \tag{5.2}$$

where n is the nodal diameter and ω is the angular frequency (rad/s) and w_n is a function of radius only. For axisymmetric problems, the nodal diameter is zero $(n = 0)$. Equation (5.1) is the general governing equations that govern a circular plate free vibration problems, thus either solid circular or annular plate is govern by Equation (3.28). However, in the present analysis, the different appear in the definition of the in-plane load. For the annular region, the in-plane load may varies in radial direction (Equation (4.17) and (4.18)) but for solid circular region they are constant throughout the region (Equation (4.19)).

To make it clear, here the governing equation is shown for each regions. The governing equation for solid circular plate where the in-plane loads is constant through the plate region is given by;

$$\frac{d^4w_n^{(s)}}{dr^4}+\frac{2}{r}\frac{d^3w_n^{(s)}}{dr^3}-\left(\frac{1}{r^2}+\frac{2n^2}{r^2}\right)\frac{d^2w_n^{(s)}}{dr^2}+\left(\frac{1}{r^3}+\frac{2n^2}{r^3}\right)\frac{dw_n^{(s)}}{dr}+\left(\frac{n^4}{r^4}+\frac{4n^2}{r^4}\right)w_n^{(s)}$$
$$-\frac{N_s}{D^{(s)}}\left(\frac{d^2w_n^{(s)}}{dr^2}+\frac{1}{r}\frac{dw_n^{(s)}}{dr}-\frac{n^2}{r^2}w_n^{(s)}\right)-\frac{2\omega^2\rho h}{D^{(s)}}w_n^{(s)}=0 \tag{5.3}$$

and for the annular plate, the equation is

$$\frac{d^4w_n^{(a)}}{dr^4}+\frac{2}{r}\frac{d^3w_n^{(a)}}{dr^3}-\left(\frac{1}{r^2}+\frac{2n^2}{r^2}\right)\frac{d^2w_n^{(a)}}{dr^2}+\left(\frac{1}{r^3}+\frac{2n^2}{r^3}\right)\frac{dw_n^{(a)}}{dr}+\left(\frac{n^4}{r^4}+\frac{4n^2}{r^4}\right)w_n^{(a)}$$
$$-\frac{N_{11}^{(a)}}{D^{(a)}}\frac{d^2w_n^{(s)}}{dr^2}-\frac{N_{22}^{(a)}}{D^{(a)}}\left(\frac{1}{r}\frac{dw_n^{(a)}}{dr}-\frac{n^2}{r^2}w_n^{(a)}\right)-\frac{2\omega^2\rho_p h_a}{D^{(a)}}w_n^{(a)}=0 \tag{5.4}$$

where $D^{(s)}$ and $D^{(a)}$ are the isotropic solid circular plate's bending stiffness and annular plate bending stiffness, respectively and, N_s and N_{ij} are the in-plane loads defined in Section 5.2.1. ρ and ρ_p are the density of isotropic and piezoceramic plate, respectively.

In this chapter, there will be three vibration problem will be described and discuss. The first two problem serve as validation of FDM code in Matlab for vibration problem while the third problem is main problem of the thesis. In the first problem, vibration of clamped isotropic circular plate is done. Second problem is analysis of the influence of radial edge load to the vibration of clamped circular plate. Lastly, the third problem is the analysis of the influence of intermediate radial load to the vibration of clamped circular plate. The intermediate radial load is realized by having annular piezoceramic plate segment as part of the circular plate.

5.3 Results and Discussions

Table 4.1 shows the material properties of the plate that is going to be used in this vibration analysis. The first two problems, only properties of brass alloy is used while

piezoceramic material is used in the third problem only. Table 5.1 lists the geometric properties that are going to be used for first and second problem. However, in the third problem where a parametric study also shown, some of the parameter may be changed to see how its influence to the resonant frequency.

Table 5.1
Geometric properties of circular structure

Parameter	Unit
Outer radius, r_o	40 mm
Inner radius, r_i	20 mm
Thickness, 2h	0.3 mm
Annular Thickness, $2h_a$	0.3 mm

For all three cases presented here, the same FDM code is used. The only different is that, for first two cases, both annular segment and circular segment are defined to have similar material properties which is the brass alloy while the third case the annular segment is defined as piezoceramic while circular is defined as brass alloy.

5.3.1 Free Vibration of Clamped Circular Plate

In the present section, vibration problem of clamped isotropic circular plate is done. The results is compared to the works of Leissa (1969). From Table 5.2, it can be seen that current FDM code compared well for free vibration problem when there is no influence of radial in-plane load.

The error calculation is follow the following formula:

$$\frac{(\text{Analytical} - \text{FDM})}{\text{Analytical}} \times 100\% \tag{5.5}$$

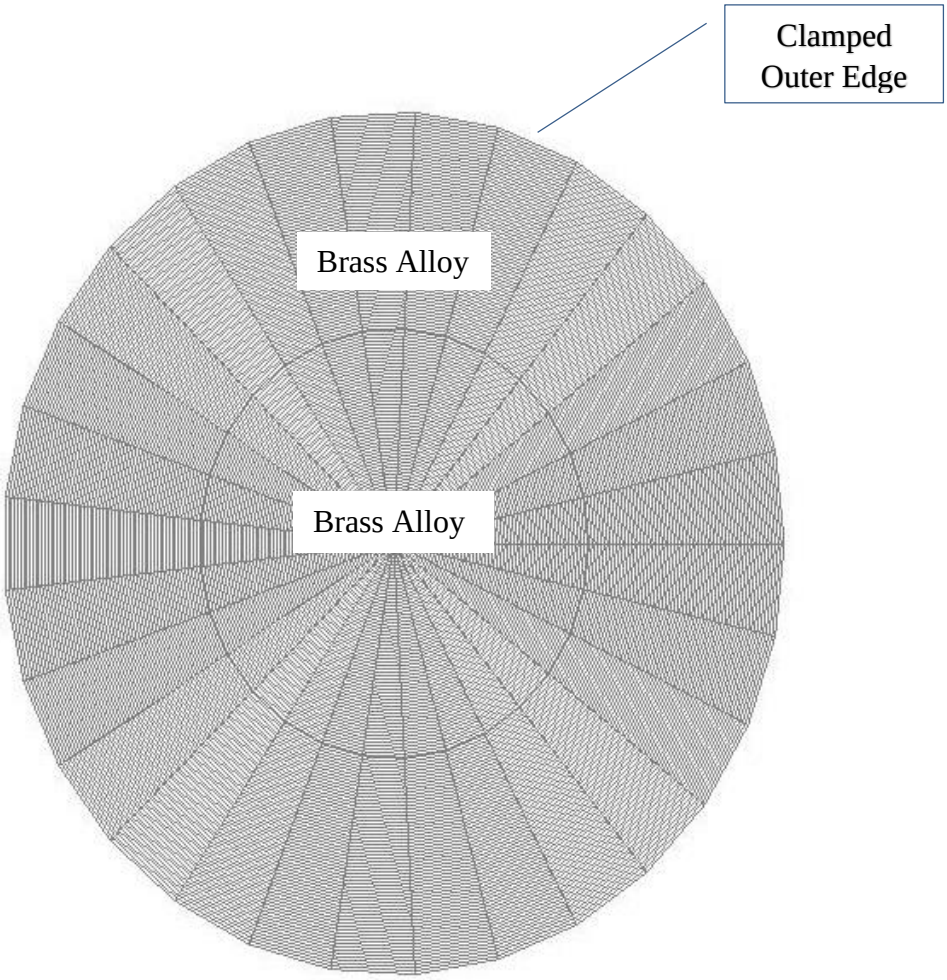

Figure 5.1 Circular plate with both annular region and solid circular region are brass alloy

Table 5.2
Frequency Parameter $\omega r_o^2\sqrt{\rho/D}$ of Clamped Circular Plate

Nodal circle, S	FDM	Leissa (1969)	Error
0	10.2905	10.2158	-0.7312
1	40.0515	39.771	-0.7053
2	89.7451	89.104	-0.7195
3	159.2742	158.183	-0.6898
4	248.6052	247.005	-0.6478

5.3.2 Influence of Radial Edge Load to Resonant Frequency of Clamped Circular Plate

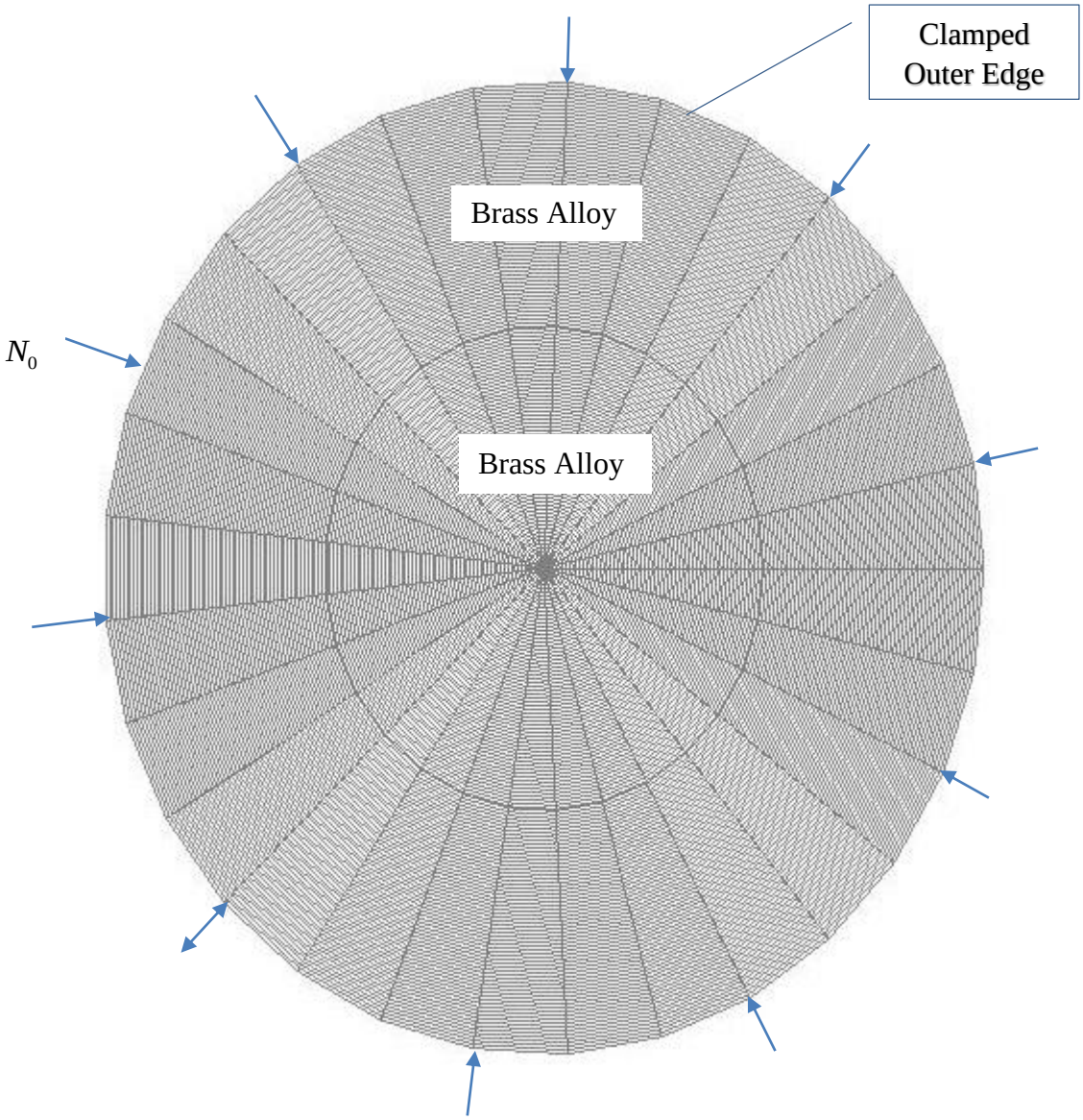

Figure 5.2 Circular plate with applied radial compression load at outer edge

In the present section, vibration problem of clamped isotropic circular plate with radial load applied at the edge of the circular plate is done. The results is compared to the works of Leissa (1969). Error calculation follows Equation 5.5.

Table 5.3
Influence of Radial Edge Load to the Resonant Frequency of Clamped Circular Plate

Radial Load, N_0 [N/m]	Frequency Parameter $\omega r_o^2\sqrt{\rho/D}$		
	FDM	Leissa (1969)	Error (%)
0	10.2905	10.215	-0.7391
r_o^2/D	9.9477	9.8712	-0.7749
$4r_o^2/D$	8.8319	8.7460	-0.9821
$9r_o^2/D$	6.5267	6.4129	-1.7745

The results shown in Table 5.3 shows an excellent agreement between results determined by FDM code and analytical results presented in Leissa (1969). As well as the trend of the resonant frequency that is decreasing due to compressing in-plane load agrees as one would expect.

5.3.3 Influence of Some Geometric Parameter to Resonant Frequency of Clamped Circular Plate

For this case the configuration of the circular plate structure is as shown in Figure 4.3 except that there is no voltage applied. Table 5.4 –Table 5.6 shows the first four eigen-frequency determined by FDM compared to the one found by FEM analysis for three different configuration of the plates which are:

a. the annular plate thickness (0.3 mm) is the same as the circular plate thickness (0.3 mm),
b. the annular plate thickness (0.6 mm) is larger than the circular plate thickness (0.3 mm) and,

c. the annular plate thickness (0.3 mm) is the smaller than the circular plate thickness (0.6 mm).

Table 5.4
Resonance Frequency for circular and annular plates having equal thickness

Mode (Nodal Circle)	FDM (Hz)	FEM (Hz)	Error (%)
1 (1)	305.91	323.28	5.37
2 (2)	1231.00	1298.40	5.19
3 (3)	2673.60	2906.50	8.01
4 (4)	4915.20	5175.70	5.03

Table 5.5
Resonance frequency for annular plate is thicker than circular plate

Mode (Nodal Circle)	FEM (Hz)	FDM (Hz)	Error (%)
1 (1)	534.32	548.00	2.50
2 (2)	1687.20	1726.40	2.27
3 (3)	3412.10	3463.20	1.48
4 (4)	6237.60	6327.60	1.42

Table 5.6
Resonance frequency for annular plate is thicker than circular plate

Mode (Nodal Circle)	FEM (Hz)	FDM (Hz)	Error (%)
1 (1)	415.86	421.20	1.27
2 (2)	1789.50	1810.50	1.16
3 (3)	4589.40	4640.00	1.09
4 (4)	8113.60	8257.50	1.74

For all three cases the outer radius and inner radius are 40 mm and 28 mm, respectively. The FEM analysis is done by using FEM software (ABAQUS) where the plate is modeled by using axisymmetric element (8-node biquadratic axisymmetric quadrilateral, reduced integration (CAX8R) for isotropic alloy region and 8-node biquadratic axisymmetric piezoelectric quadrilateral, reduced integration (CAX8RE) is used for piezoceramic region). The FDM is formulated as discussed in Section 3.3 and

coded in MATLAB. The number of nodes at the annular regions, m is 150 nodes. The number of nodes at the circular region varies as the inner edge varies. The results in Table 5.4 – Table 5.6 shows a good agreement of results obtained from FDM and FEM. Error calculation follows Equation 4.27.

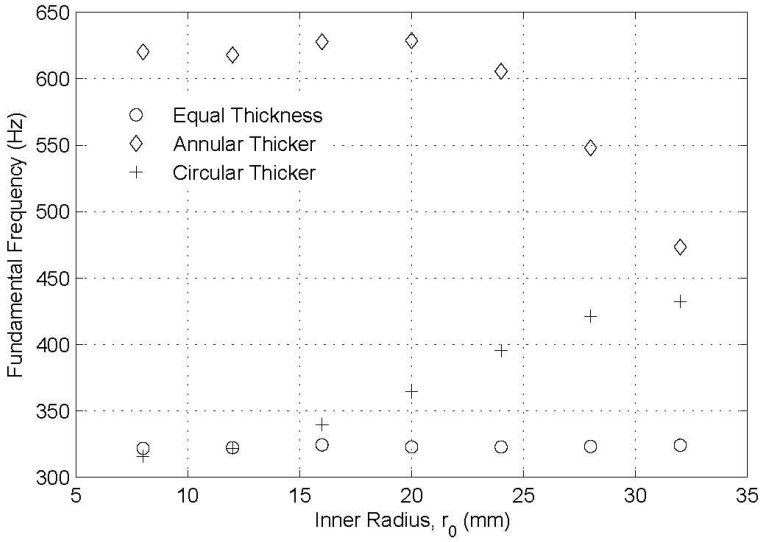

Figure 5.3 Fundamental frequency change due to inner radius

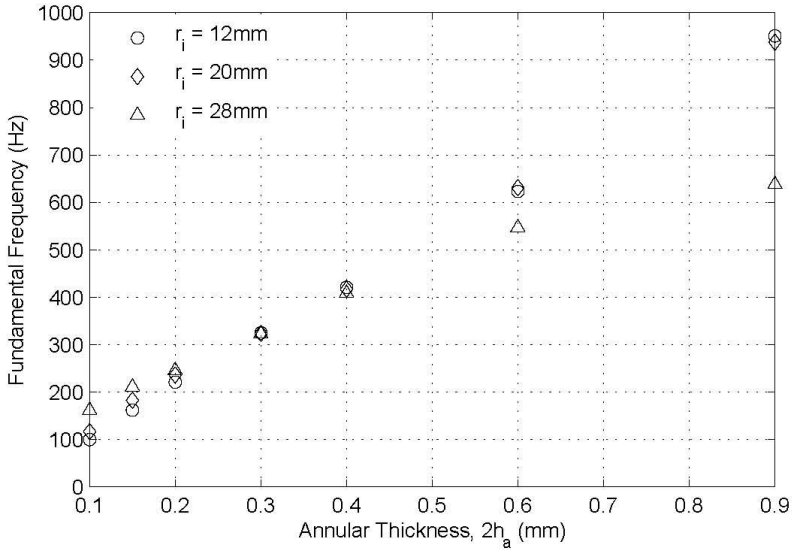

Figure 5.4 Fundamental frequency change due to annular thickness

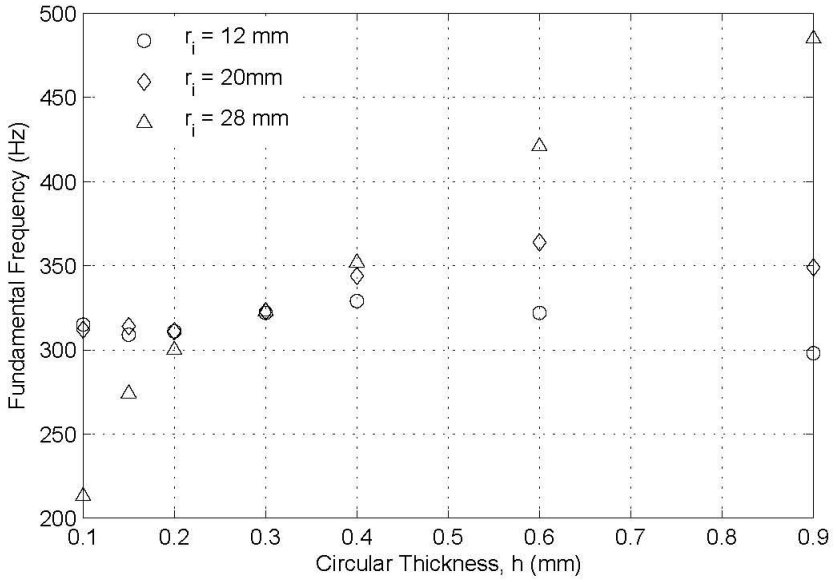

Figure 5.5 Fundamental frequency change due to circular thickness

Figure 5.3 - Figure 5.5 shows some of the parametric study. Figure 5.3 shows how the fundamental frequency change with the inner radius. Other parameters is fixed.

Outer radius, r_o is fixed at 40 mm while the annular and circular thicknesses are divided into 3 cases,

a. same thickness at 0.3 mm,

b. annular (0.6 mm) thicker than circular thickness (0.3 mm) and,

c. circular (0.6 mm) thicker than annular thickness (0.3 mm).

The results shows that the fundamental frequency is independent of the radius if the annular plate has equal thickness as the circular plate. For inner radius is less than half of the outer radius, the results shows similar behavior which the fundamental frequency is almost independent of the inner radius changes. The fundamental frequency reduces rapidly as the inner radius became larger than half of the outer radius.

While it is the opposite for the case where the annular plate is thinner than the circular plate.

Figure 5.4 shows how the fundamental frequency change with the annular thickness. The outer radius and circular thickness for this case are fixed at 40 mm and 0.3 mm, respectively. The inner radius are divided for 3 cases which are 12 mm, 20 mm and 28 mm, respectively. For this configuration the results shows that, for any inner radius, the fundamental frequency is increases as the annular thickness increases. Note that annular thickness more than 0.3 mm refers to annular plate is thicker than the circular thickness. It is worth to note also that for inner radius 28 mm, the annular plate thickness influence became lesser after certain thickness, which in the present case is 0.6 mm (twice the circular plate thickness).

Figure 5.5 shows how the fundamental frequency change with the solid circular thickness. The outer radius and annular thickness for this case are fixed at 40 mm and 0.3 mm, respectively. The inner radius are divided for 3 cases which are 12 mm, 20 mm and 28 mm. It can be seen that for inner radius 12 mm and 20 mm, the circular thickness play less influence on the fundamental frequency. However, it is interesting to see that for both cases the fundamental frequency has its maximum point, at circular thickness is 0.4 mm for inner radius 12 mm and 0.6 mm for inner radius is 20 mm. For the case of inner radius is 28 mm, the circular thickness plays a significant role in changing the fundamental frequency. The result shows that the fundamental frequency increases as the circular thickness increases.

Based on these three graphs, one may conclude that in design a plate structure which the annular region is piezoceramic, the parameter that one should pay attention is the thickness of the annular region since it gave significant changes in the fundamental frequency of the plate structure.

5.3.4 Influence of Intermediate Radial Load to Resonant Frequency of Clamped Circular Plate

For this case the configuration of the circular plate structure is as shown in Figure 4.3. While in Chapter 4, the aim is to see the limit of the applied voltage before the plate buckle, this section is aim to determine the effect of the intermediate radial load to the resonant frequency. Figure 5.6 - Figure 5.8 shows the effects of the intermediate radial loads to the fundamental frequency to the circular plate. It is known that the fundamental frequency reduces to zero when the applied in-plane load approaches its buckling loads. However, it is also a fact that for a piezoceramic structure, there is a limit of applied voltage's value called coercive voltage, V_c. At coercive voltage where the electric field switch its polarisation from remanent polarisation (the value of the polarisation that remains after an applied electric field is removed) to zero polarisation. For PIC-151, the coercive electric fields, E_c is 850 kV/m. The coercive voltage is defined as $2h_a E_c$. Therefore, one would avoid to apply this limit voltage.

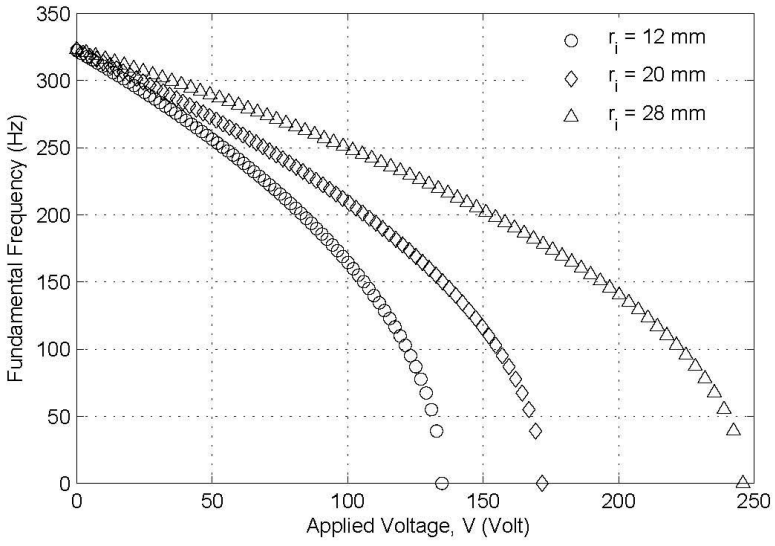

Figure 5.6 Fundamental frequency change due to applied voltage for annular and circular thickness is 0.3 mm

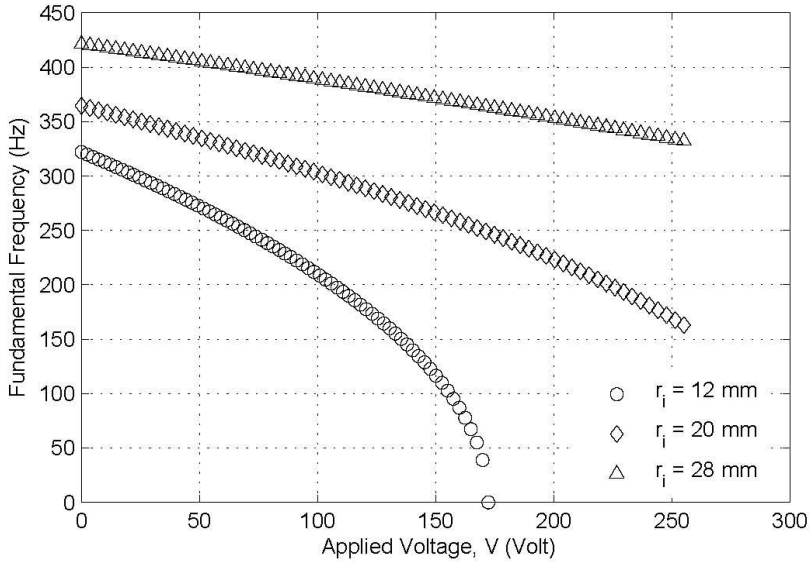

Figure 5.7 Fundamental frequency change due to applied voltage for annular and circular thickness is 0.6 mm and 0.3 mm, respectively

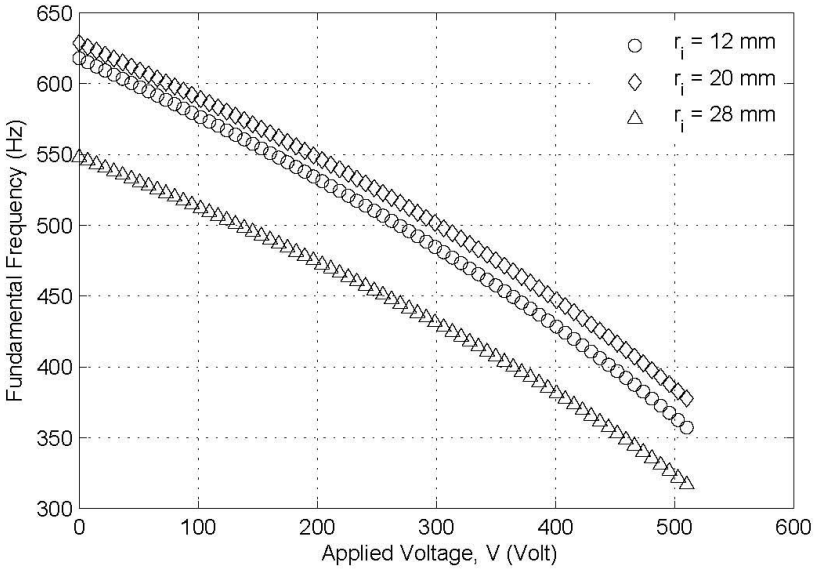

Figure 5.8 Fundamental frequency change due to applied voltage for annular and circular thickness is 0.3 mm and 0.6 mm, respectively

Figure 5.6 shows the effects of the intermediate radial load to the fundamental problem for annular thickness (0.3 mm) is equal to the circular thickness (0.3 mm). The

outer radius is 40 mm while inner radius is divided for three cases of 12, 20 and 28 mm. As can be seen for any inner radius, the fundamental frequency may be tuned up until near zero frequency which is at buckling point. Note that the fundamental frequency drop quicker at smaller inner radius.

Figure 5.7 shows the effects of the intermediate radial load to the fundamental problem for annular thickness (0.6 mm) is thicker than the circular thickness (0.3 mm). The outer radius is 40 mm while inner radius is divided for three cases of 12, 20 and 28 mm. For this configuration, the fundamental frequency may be tuned around 30 to 40 % of its frequency at free vibrations. It is known that the fundamental frequency decreases to zero as the applied in-plane load becomes near the critical buckling load.

Figure 5.8 shows the effects of the intermediate radial load to the fundamental problem for annular thickness (0.3 mm) is thinner than the circular thickness (0.6 mm). The outer radius is 40 mm while inner radius is divided for three cases of 12, 20 and 28 mm. For this configuration, the fundamental frequency tuning is depending on the inner radius. The intermediate radial load became more effective for the smaller inner radius.

The overall results shows the possibility of tuning around 40-50% of the resonant frequency for each case except case where annular thicker than circular segment and the inner radius is 28mm (70% of outer radius). However, the amount of voltage that need to be applied are impractical to apply. In addition, for application such as energy harvester such large amount would pose a problem since it required energy just for tuning. It is useless to tune frequency while the net energy harvested is similar to situation the frequency is not tuned. For other application of actuator, although such setback is not fatal but the use of large energy may give a disadvantage for such design. However, current structure is still useful if it is combined with other resonant frequency tuning method such as shunt circuit. Shunt circuit may tuned the resonant frequency for

around 20%. Close look at some situation such as when the thickness of annular segment and circular segment is equal, there is possibility to tune the resonant frequency of about 7% if one apply voltage around 25V to the annular piezoceramic segment. If double the voltage applied, the resonant frequency may be tuned up until around 23% (for case equal thickness and inner radius is 12 mm).

5.4 SUMMARY

The FDM code is verify for two cases of free vibration analysis. First, free vibration of isotropic circular plate is done, then followed by free vibration of clamped circular plate with influence of radial load at its outer edge. Both cases shows good agreement with the compared results from Leissa's report (Leissa, 1969).

An axisymmetric vibration analysis has been done for an isotropic circular plate with an annular piezoceramic plate attached at its edge (Figure 3.1). The annular plate is used as the source for the radial load applied to the circular plate. The free vibration analysis is done for three configurations which are

a. annular plate thickness (0.3 mm) is equal to the circular plate (0.3 mm),
b. annular plate (0.6 mm) has thickness larger than the circular plate (0.3 mm), and
c. annular plate (0.3 mm) has thickness smaller than the circular plate thickness (0.6 mm).

The results shows that results obtained from FDM have a good agreement with the results obtained from FEM analysis. An analysis of the effects of the intermediate in-plane load through application of piezoceramic material has been shown. It shows that the applied load give a significant range of frequency tuning for most configuration reported (at least 40-50%).

The possibility of broad range of frequency came at price of high amount of voltage that needed to be applied. However, the results indicate that at relatively low voltage, the frequency may be tuned for around 7% of the original frequency. Therefore, this may open broader range of tunable resonant frequency, particularly when combine with other method such as shunt circuit.

CHAPTER SIX

CONCLUSIONS AND FUTURE RESEARCH

6.1 OVERVIEW

A circular plate vibrational behavior under influence of in-plane load have been discussed throughout this thesis. The in-plane loads are applied through application of annular piezoceramic plate. Therefore, the plate structure consists of a solid circular plate that an annular piezoceramic plate is attached at its edge. By applying voltage, the annular piezoceramic plate may stretch or contract thus resulting either compressive or tensile load to the solid circular plate attached at its inner edge. In this thesis the solid circular plate is assumed to be homogeneous.

6.2 CONCLUSIONS

The main research question for this study is the possibility of tuning a circular plate resonant frequency through application of in-plane load without complicated mechanical parts. This may achieve by using piezoceramic material as source of the in-plane load. The results indicated that the proposed structure' resonant frequency may be tuned without complicated mechanical part, but the applied voltage needed is high. However, there are results that indicate that at relatively low voltage (about 25V) the resonant frequency may be tuned to 7% of its resonant frequency.

The other contributions that have been discussed in this thesis are:

i. **Formulation of circular plate governing equations in finite different form.** In Chapter 3 we have formalized the governing equation for general circular plate problems. Later the set of equations is transformed into the

finite different formulation for circular plate problems. The general in-plane load distribution as well as the electric field distribution also defined for current problem.

ii. **Buckling of circular plate via intermediate radial load.** Chapter 4 is concerned about buckling of circular plate due to intermediate radial load. In this chapter, the problem discussed as the buckling of isotropic solid circular plate with annular piezoelectric annular plate which the intermediate radial load is served by the voltage applied to the piezoelectric annular plate. In such a problem the stresses in the region of annular plate are showed to be radial dependent while in the region of solid circular plate the stresses are constants. The chapter served as part of FDM code validation for problem involving in-plane load. The results shows the code is able to handle problem involving in-plane load that vary with radius. Besides, one may conclude that buckling of circular plate with piezoceramic annular segment is not a concern since the critical buckling load (voltage) is far from practical applicable voltage to the piezoceramic annular segment.

iii. **Effects of intermediate radial load to fundamental frequency.** Chapter 5 is concerned about vibration problems of solid circular plate with annular plate attached to it at the edge. The free vibration of such structures is presented in this chapter. The earlier part of the chapter shows validation of FDM code on free vibration clamped circular plate as well as free vibration involving edge in-plane load. In both cases, the results shows that the FDM code run well when compared to analytical results. However, the main contributions of the chapter shows the effects of the intermediate radial load to the fundamental frequency of the structure. The intermediate radial load

is provided by the annular piezoelectric plate. The results indicate that at relatively low voltage, the frequency may be tuned for around 7% of the original frequency.

6.3 FUTURE RESEARCH

i. For plates used as vibrating diaphragm of devices such as synthetic jet actuator, the pressure on the plate played significant role in its application. In the present thesis, such effect is omitted. Therefore to provide better insights to the design of such plates, further research to address the problem is needed.

ii. In the present analysis, the governing equations are solved through application of numerical methods, i.e. finite different methods. It is interesting to look into asymptotic solutions for current problem by using asymptotic method such as perturbation methods.

iii. The present research developed a plate structure that its frequency may be tuned via electrical means alone. However, in applications such as energy scavenging devices or aircraft related adaptive devices total energy used by the device may not be too costly. In energy scavenging devices, if the total energy consume by the device is equal or more that it harvests, the device will not meet it purpose to harvest energy. While for aircraft related adaptive devices such as SJA for flow control, the overall energy consume and weight of the device should not be a disadvantage that overshadow the benefit of the devices. Since the energy consume and weight addition will add more fuel consumption which is not desired by aircraft designer.

Therefore, an overall study on the energy consumption of the structure is desired.

REFERENCES

Adams, S. G., Bertsch, F. M., A.Shaw, K., & MacDonald, N. C. (1998). Independent tuning of linear and nonlinear stiffness coefficients. *Journal of Microelectromechanical Systems, 7*(2), 172-180.

Adelman, N. T., & Stavsky, Y. (1980). Flexural-extensional behavior of composite piezoelectric circular plates. *Journal of Acoustical Society of America, 67*(3), 819-822.

Ahmadian, M., & DeGuilio, A. P. (2001). Recent advances in the use of piezoceramics for vibration suppression. *Shock and Vibration Digest, 33*(1), 15-22.

Aksu, G., & Ali, R. (1976). Free vibration analysis of stiffened plates using finite difference method. *Journal of Sound and Vibration, 48*(1), 15-25.

Almeida, S. F. M. d. (1999). Shape control of laminated plates with piezoelectric actuators including stress-stiffening effects. *AIAA Journal, 37*(8), 1017-1019.

Amitay, M., & Glezer, A. (2002). Role of actuation frequency in controlled flow reattachment over a stalled airfoil. *AIAA Journal, 40*(2), 209-216.

Amitay, M., Honohan, A., Trautman, M., & Glezer, A. (1997). Modification of the aerodynamic characteristics of bluff bodies using fluidic actuators. *AIAA Paper 97-2004*.

Arafat, H. N., Nayfeh, A. H., & Faris, W. F. (2004). Natural frequencies of heated annular and circular plates. *International Journal of Solids and Structures, 41*, 3031-3051.

Aung, T. M., & Wang, C. (2005). Buckling of circular plates under intermediate and edge radial loads. *Thin-Walled Structures, 43*, 1926-1933.

Bodaghi, M., & Saidi, A. R. (2011). Buckling behavior of standing laminated mindlin plates subjected to body force and vertical loading. *Composite Structures, 93*, 538-547.

Bokaian, A. (1988). Natural frequencies of beams under compressive axial loads. *Journal of Sound and Vibration, 126*(1), 49-65.

Brighenti, R., & Carpinteri, A. (2011). Buckling and fracture behaviour of cracked thin plates under shear loading. *Materials and Design, 32*, 1347-1355.

Brissaud, M. (2006). Theoretical modelling of non-symmetric circular piezoelectric bimorphs. *Journal of Micromechanics and Microengineering, 16*, 875-885.

Brown, C. J. (1991). Elastic buckling of plates subjected to distributed tangential loads. *Computers & Structures, 41*(1), 151-155.

Brunelle, E. J., & Robertson, S. R. (1976). Vibrations of an initially stressed thick plate. *Journal of Sound and Vibration, 45*(3), 405-416.

Brunner, A. J., Birchmeier, M., Melnykowycz, M. M., & Barbezat, M. (2009). Piezoelectric fiber composites as sensor elements for structural health monitoring and adaptive material systems. *Journal of Intelligent Material Systems and Structures, 20*, 1045-1055.

Carrera, E. (1997). An improved Reissner-Mindlin-type model for the electromechanical analysis of multilayered plates including piezo-layers. *Journal of Intelligent Material Systems and Structures, 8*, 232-248.

Cattafesta III, L. N., & Sheplak, M. (2011). Actuators for active flow control. *Annual Review of Fluid Mechanics*, 43, 247-272.

Chattopadhyay, A., & Seeley, C. E. (1997). A higher order theory for modeling composite laminates with induced strain actuators. *Composites Part B: Engineering, 28*(3), 243-251.

Chen, X. R., Yang, T. Q., Wang, W., & Yao, X. (2012). Vibration energy harvesting with a clamped piezoelectric circular diaphragm. *Ceramics International*, 38, S271-S274.

Cheng, Z.-Q., Reddy, J. N., & Xiang, Y. (2005). Buckling of a thin circular plate loaded by in-plane gravity. *Journal of Applied Mechanics, 72*(2), 296-298.

Chirica, I., & Beznea, E.-F. (2011). Buckling analysis of the composite plates with delaminations. *Computational Materials Science, 50*, 1587-1591.

Cohen, J. M. (1992). Elastic buckling coefficients for long, unstiffened plates. [Technical Note]. *Journal of Engineering Mechanics, 118*(12), 2491-2496.

Coman, C. D., & Haughton, D. M. (2006a). Localized wrinkling instabilities in radially stretched annular thin films. *Acta Mechanica, 185*, 179-200.

Coman, C. D., & Haughton, D. M. (2006b). On some approximate methods for the tensile instabilities of thin annular plates. *Journal of Engineering Mathematics, 56*, 79-99.

Corr, L. R., & Clark, W. W. (2006). Similarities between variable stiffness springs and piezoceramic switching shunts. *AIAA Journal, 44*(11), 2797-2800.

Correia, V. M. F., Gomes, M. A. A., Suleman, A., Soares, C. M. M., M., C. A., & Soares. (2000). Modelling and design of adaptive composite structures. *Computer Methods in Applied Mechanics and Engineering, 185*, 325-346.

Crawley, E. F., & Anderson, E. H. (1990). Detailed models of piezoceramic actuation of beams. *Journal of Intelligent Material Systems and Structures, 1*, 4-25.

Crook, A., Sadri, A. M., & Wood, N. J. (1999). *The development and implementation of synthetic jets for the control of separated flow*. Paper presented at the 17th AIAA Applied Aerodynamics Conference.

Darus, I. Z. M., & Tokhi, M. O. (2004). Finite difference simulation of a flexible plate structure. *Journal of low frequency noise, vibration and active control, 23*(1), 27-46.

Davis, C. L., & Lesieutre, G. A. (2000). An actively tuned solid-state vibration absorber using capacitive shunting of piezoelectric stiffness. *Journal of Sound and Vibration, 232*(3), 601-617.

Deolasi, P. J., & Datta, P. K. (1997). Experiments on the parametric vibration response of plates under tensile loading. *Experimental Mechanics, 37*(1), 56-61.

Doong, J.-L., Chen, T.-J., & Chen, L.-W. (1987). Vibration and stability of an initially stressed laminated plate based on a higher-order deformation theory. *Composite Structures, 7*, 285-310.

Ebrahimi, F., & Rastgoo, A. (2011). Nonlinear vibration analysis of piezo-thermo-electrically actuated functionally graded circular plates. *Archive of Applied Mechanics, 81*, 361-383.

Ergun, A., & Kumbasar, N. (2011). A new approach of improved finite difference scheme on plate bending analysis. *Scientific Research and Essays, 6*(1), 6-17.

Fallah, A. S., Johnson, H. E., & Louca, L. A. (2011). Experimental and numerical investigation of buckling resistance of marine composite panels. *Journal of Composite Materials, 45*, 907-922.

Faris, W. F. (2003). *Nonlinear Dynamics of Annular and Circular Plates under Thermal and Electrical Loadings.* Unpublished Dissertation, Virginia Polytechnic Institute and State University, Blacksburg, Virginia.

Farshad, M., & Flueler, P. (1996). On internal satbility problems in structured materials. *Journal of Computer-Aided Materials Design, 3*, 303-310.

Fauconneau, G., & Marangoni, R. D. (1971). Natural frequencies and elastic stability of a simply-supported rectangular plate under linearly varying compressive loads. *International Journal of Solids and Structures, 7*, 473-493.

Fernandes, A., & Pouget, J. (2001a). Accurate modelling of piezoelectric plates: Single-layered plate. *Archive of Applied Mechanics, 71*, 509-524.

Fernandes, A., & Pouget, J. (2001b). Two-dimensional modelling of laminated piezoelectric composites: Analysis and numerical results. *Thin-Walled Structures, 39*, 3-22.

Fernandes, A., & Pouget, J. (2002). An accurate modelling of piezoelectric multi-layer plates. *European Journal of Mechanics A/Solids, 21*, 629-651.

Fernandes, A., & Pouget, J. (2003). Analytical and numerical approaches to piezoelectric bimorph. *International Journal of Solids and Structures, 40*, 4331-4352.

Ferreira, A., Castro, L., Roque, C., Reddy, J., & Bertoluzza, S. (2011). Buckling analysis of laminated plates by wavelets. *Computers and Structures, 89*, 626-630.

Ferreira, A., Roque, C., Neves, A., Jorge, R., Soares, C., & Liew, K. (2011). Buckling and vibration analysis of isotropic and laminated plates by radial basis functions. *Composites Part B: Engineering, 42*, 592-606.

Fraser, W. B. (1975). Bending of a radially prestressed annular plate by tilting a central rigid inclusion. *Journal of Elasticity, 5*(2), 129-140.

Fu-ru, J. (1982). Unsymmetrical bending annular and circular thin plates under various supporting conditions (i). *Applied Mathematics and Mechanics (English Edition), 3*(5), 683-695.

Fu-ru, J. (1984). Unsymmetrical bending annular and circular thin plates under various supports (ii). *Applied Mathematics and Mechanics (English Edition), 5*(2), 1173-1184.

Fu, L., & Waas, A. M. (1992). Buckling of polar and rectilinearly orthotropic annuli under uniform internal or external pressure loading. *Composite Structures, 22*, 47-57.

Gallas, Q., Holman, R., Nishida, T., Carrol, B., Sheplak, M., & Cattafesta, L. (2003). Lumped element modeling of piezoelectric-driven synthetic jet actuators. *AIAA Journal, 41*(2), 240-247.

Gallas, Q., Wang, G., Papila, M., Sheplak, M., & Cattafesta, L. (2003). *Optimization of synthetic jet actuators*. Paper presented at the 41st Aerospace Sciences Meeting & Exhibit.

Geymonat, G., Licht, C., & Weller, T. (2011). Plates made of piezoelectric materials: When are they really piezoelectric? *Applied Mathematical Modelling, 35*, 165-173.

Glezer, A., & Amitay, M. (2002). Synthetic jets. *Annual Review of Fluid Mechanics*, 34(1), 503-529.

Glezer, A. (2011). Some aspects of aerodynamic flow control using synthetic-jet actuation. *Philosophical Transactions of the Royal Society of London A: Mathematical, Physical and Engineering Sciences*, 369(1940), 1476-1494.

Gomes, L. D., Crowther, W. J., & Wood, N. J. (2006, 5-8 June 2006). *Toward a practical piezoceramic diaphragm based synthetic jet actuator for high subsonic applications - effect of chamber and orifice depth on actuator peak velocity*. Paper presented at the 3rd AIAA Flow Control Conference, San Francisco, California.

Greenblatt, D., & Wygnanski, I. J. (2000). The control of flow separation by periodic excitation. *Progress in Aerospace Sciences, 36*, 487-545.

Greenblatt, D., & Wygnanski, I. J. (2000). The Control of Flow Separation by Periodic Excitation. *Progress in Aerospace Sciences, 36*(7), 487-545.

Gregory, J. W., Sullivan, J. P., Raman, G., & Raghu, S. (2004, 28 June - 1 July 2004). *Characterization of a micro fluidic oscillator for flow control.* Paper presented at the 2ND AIAA Flow Control Conference, Portland, Oregon.

Hagood, N. W., & Flotov, A. V. (1991). Damping of structural vibrations with piezoelectric materials and passive electrical networks. *Journal of Sound and Vibration, 146*(2), 243-268.

Hak, M. G.-e., & Bushnell, D. M. (1991). Separation control: Review. *Journal of Fluids Engineering, 113*, 5-30.

Haojiang, D., Rongqiao, X., & Weiqiu, C. (2000). Exact solutions for free vibration of transversely isotropic piezoelectric circular plates. *Acta Mechanica Sinica (English Series), 16*(2), 142-147.

Hebert, C. A., & Lesieutre, G. A. (1998). Flexural piezoelectric transducers with frequency agility obtained via membrane loads. *Journal of Intelligent Material Systems and Structures, 9*, 1030-1037.

Heyliger, P., & Brooks, S. (1995). Free vibrations of piezoelectric laminates in cylindrical bending. *International Journal of Solids and Structures, 32*(20), 2945-2960.

Hinton, E. (1978). Buckling of initially stressed Mindlin plates using a finite strip method. *Computers & Structures, 8*, 99-105.

Hosseini-Hashemi, S., Khorshidi, K., & Amabili, M. (2008). Exact solution for linear buckling of rectangular Mindlin plates. *Journal of Sound and Vibration, 315*, 318-342.

Hu, Y., Xue, H., & Hu, H. (2007). A piezoelectric power harvester with adjustable frequency through axial preloads. *Smart Material and Structures, 16*, 1961-1966.

Huang, C. H. (2005). Free vibration analysis of the piezoceramic bimorph with theoretical and experimental investigation. *IEEE Transactions on Ultrasonics, Ferroelectrics, and Frequency Control, 52*(8), 1393–1403.

Huang, C. H., Lin, Y. C., & Ma, C. C. (2004). Theoretical analysis and experimental measurement for resonant vibration of piezoceramic circular plates. *IEEE Transaction on Ultrasonics, Ferroelectrics, and Frequency Control, 51*(1), 12-24.

Jia-qi, M., & Bing-guo, S. (1981). Perturbation method for thin plate bending problems. *Applied Mathematics and Mechanics (English Edition), 2*(5), 567-574.

Jillella, N., & Peddieson, J. (2012). Modeling of wrinkling of thin circular sheets. *International Journal of Non-Linear Mechanics*, 47(1), 85-91.

Kang, J.-H., & Leissa, A. W. (2005). Exact solutions for the buckling of rectangular plates having linearly varying in-plane loading on two opposite simply supported edges. *International Journal of Solids and Structures, 42*, 4220-4238.

Kaplevatsky, I. D., & Shestopal, V. O. (1982). Bending and buckling of multilayer thin plates. *Acta Mechanica, 43*, 169-176.

Kiang, F.-r. (1980). Some applications of perturbation method in thin plate bending problems. *Applied Mathematics and Mechanics (English Edition), 1*(1), 35-53.

Lai, M.-C. (2002). A simple compact fourth-order poisson solver on polar geometry. *Journal of Computational Physics, 182*, 337-345.

Laura, P. A., Ficcadenti, G. M., & Grossi, R. O. (1981). Comments on "natural frequencies of simply supported circular plates". *Journal of Sound and Vibration, 76*(1), 143-145.

Lee, G. H. C., P.Ha, Q., & Mallinson, S. G. (2003). Piezoelectrically actuated micro synthetic jet for active flow control. *Sensors and Actuators, 108*, 168-174.

Leissa, Arthur W. (1969). Vibration of plates. Washington : Scientific and Technical Information Division, National Aeronautics and Space Administration

Leissa, A. W., & Kang, J.-H. (2002). Exact solutions for vibration and buckling of an ss- c-ss-c rectangular plate loaded by linearly varying in-plane stresses. *International Journal of Mechanical Sciences, 44*, 1925-1945.

Leissa, A. W., & Narita, Y. (1980). Natural frequencies of simply supported circular plates. *Journal of Sound and Vibration, 70*(2), 221-229.

Lesieutre, G. A. (1998). Vibration damping and control using shunted piezoelectric materials. *Shock and Vibration Digest, 30*(3), 187-195.

Lesieutre, G. A., & Davis, C. L. (1997). Can a coupling coefficient of a piezoelectric device be higher than those of its active material? *Journal of Intelligent Material Systems and Structures, 8*, 859-867.

Li, D., Or, S. W., Chan, H. L. W., Choy, P. K., & Liu, P. C. K. (2006). Tunable vibration absorber incorporating piezoceramic sensoriactuator. *Japanese Journal of Applied Physics, 45*(5B), 4787-4792.

Li, T., Chen, Y. H., & Ma, J. (2009). Static and dynamic high voltage limitation of series and parallel bimorph actuators. *Mechatronics, 19*, 520-528.

Liao, L., & Yu, W. (2009). An electromechanical Reissner-Mindlin model for laminated piezoelectric plates. *Composite Structures, 88*, 394-402.

Lo, K. H., Christensen, R. M., & Wu, E. M. (1977). A high-order theory of plate deformation - part 1: Homogeneous plates. *Journal of Applied Mechanics, 44*(4), 663-668.

Lumentut, M. F., & Howard, I. M. (2009). *Theoretical study of piezoelectric bimorph beams with two input base-motion for power harvesting.* Paper presented at the 4th World Congress on Engineering Asset Management, Athens, Greece.

Luo, Z., Xia, Z., & Liu, B. (2006). New generation of synthetic jet actuators. *AIAA Journal, 44*(10), 2418-2419.

Luo, Z. B., Xia, Z. X., & Xie, Y. G. (2007). Jet vectoring control using a novel synthetic jet actuator. *Chinese Journal of Aeronautics, 20*, 193-201.

Mane, P., Mossi, K., & Bryant, R. (2008). Experimental design and analysis for piezoelectric circular actuators in flow control applications. *Smart Materials and Sructures, 17*(1).

Mane, P., Mossi, K., Rostami, A., Bryant, R., & Castro, N. (2007). Piezoelectric actuators as synthetic jets: Cavity dimension effects. *Journal of Intelligent Material Systems and Structures, 18*(11), 1175-1190.

Mansfield, E. H. (1960). On the buckling of an annular plate. *Quarterly Journal of Mechanical Applied Mathematics, 13*(1), 16-23.

Maugin, G. A., & Attou, D. (1990). An asymptotic theory of thin piezoelectric plates. *Quarterly Journal of Mechanical Applied Mathematics, 43*(3), 347-362.

Mauritsson, K. (2009). Modelling of finite piezoelectric patches: Comparing an approximate power series expansion with exact theory. *International Journal of Solids and Structures, 46*, 1053-1065.

Mazzoni, D., & Kristiansen, U. (1999). Finite difference method for the acoustic radiation of an elastic plate excited by a turbulent boundary layer: A spectral domain solution. *Flow, Turbulent and Combustion, 61*, 133-159.

Mirzavand, B., & Eslami, M. R. (2010). A closed-form solution for thermal buckling of piezoelectric fgm rectangular plates with temperature-dependent properties. *Acta Mechanica, 218*, 87-101.

Mitchell, J. A., & Reddy, J. N. (1995). A refined hybrid plate theory for composite laminates with piezoelectric laminae. *International Journal of Solids and Structures, 32*(16), 2345-2367.

Mittal, R., Rampunggoon, P., & Udaykumar, H. S. (2001, 11-14 June 2001). *Interaction of a Synthetic Jet with a Flat Plate Boundary Layer.* Paper presented at the 31st AIAA FLuid Dynamics Conference & Exhibit, Anaheim, CA.

Moheimani, S. O. R. (2003). A survey of recent innovations in vibration damping and control using shunted piezoelectric transducers. *IEEE Transaction on Control Systems Technology, 11*(4), 482-494.

Mohseni, K., & Colonius, T. (2000). Numerical treatment of polar coordinate singularities. *Journal of Computational Physics, 157*, 787-795.

Mukhopadhyay, M. (1978). A semi-analytic solution for free vibration of rectangular plates. *Journal of Sound and Vibration, 60*(1), 71-85.

Mukhopadhyay, M. (1989a). Vibration and stability analysis of stiffened plates by semi-analytic finite difference method, part I: Consideration of bending displacements only. *Journal of Sound and Vibration, 130*(1), 27-39.

Mukhopadhyay, M. (1989b). Vibration and stability analysis of stiffened plates by semi-analytic finite difference method, part II: Consideration of bending and axial displacements. *Journal of Sound and Vibration, 130*(1), 41-53.

Muriuki, M. G., & Clark, W. W. (2007). Analysis of a technique for tuning a cantilever beam resonator using shunt switching. *Smart Materials and Structures, 16*, 1527-1533.

Nali, P., Carrera, E., & Lecca, S. (2011). Assessments of refined theories for buckling analysis of laminated plates. *Composite Structures, 93*, 456-464.

Nguyen-Thanh, N., Rabczuk, T., H.Nguyen-Xuan, & S.Bordas. (2011). An alternative alpha finite element method with discrete shear gap technique for analysis of isotropic Mindlin-Reissner plates. *Finite Elements in Analysis and Design, 47*, 519-535.

Niezrecki, C., Brei, D., Balakrishnan, S., & Boskalik, A. (2001). Piezoelectric actuation: State of the art. *Shock and Vibration Digest, 33*(4), 269-280.

Nosier, A., & Reddy, J. N. (1992a). On vibration and buckling of symmetric laminated plates according to shear deformation theories: Part I. *Acta Mechanica, 94*, 123-144.

Nosier, A., & Reddy, J. N. (1992b). On vibration and buckling of symmetric laminated plates according to shear deformation theories: Part II. *Acta Mechanica, 94*, 145-169.

Ottman, G. K., Hofmann, H. F., Bhatt, A. C., & Lesieutre, G. A. (2002). Adaptive piezoelectric energy harvesting circuit for wireless remote power supply. *IEEE Transaction on Power Electronics, 17*(5), 669-676.

Papila, M., Sheplak, M., & Cattafesta-III, L. N. (2008). Optimization of clamped circular piezoelectric composite actuators. *Sensors and Actuators A: Physical, 147*(1), 310-323.

Pawlus, D. (2006). Solution to the static stability problem of three-layered annular plates with a soft core. *Journal of Theoretical and Applied Mechanics, 44*(2), 299-322.

Pawlus, D. (2011). Solution to the problem of axisymmetric and asymmetric dynamic instability of three-layered annular plates. *Thin-Walled Structures, 49*, 660-668.

Pierson, J. K., & Roorda, J. (1994). Delamination buckling in circular plates. *Thin-Walled Structures, 18*, 161-175.

Polit, O., & Bruant, I. (2006). Electric potential approximations for an eight node plate finite element. *Computers and Structures, 84*, 1480-1493.

Prasad, S. A. N., Gallas, Q., Horowitz, S., Homeijer, B., Sankar, B. V., Cattafesta, L. N., et al. (2006). Analytical electroacoustic model of a piezoelectric composite circular plate. *AIAA Journal, 44*(10), 2311-2318.

Raju, B. B. (1966). Vibration of thin elastic plates of linearly variable thickness. *International Journal of Mechanical Sciences, 8*(2), 89-100.

Raju, R., Mittal, R., & Cattafesta, L. (2008). Dynamics of airfoil separation control using zero-net mass-flux forcing. *AIAA journal*, 46(12), 3103-3115.

Ramaiah, G. K., & Vijayakumar, K. (1974). Elastic stability of annular plates under uniform compressive forces along the outer edge. *AIAA Journal, 13*(6), 832.

Ramkumar, R. L., Kamat, M. P., & Nayfeh, A. H. (1977). Vibrations of highly prestressed anisotropic plates via a numerical-perturbation technique. *International Journal of Solids Structures, 13*, 1037-1044.

Rammerstorfer, F. G. (1977). Increase of the first natural frequency and buckling load of plates by optimal fields of initial stresses. *Acta Mechanica, 27*, 217-238.

Reddy, J. N. (1999). *Theory and Analysis of Elastic Plates*: Taylor & Francis.

Rosen, A., & Libai, A. (1976). Stability and behavior of an annular plate under uniform compression. *Experimental Mechanics, 16*(12), 461-467.

Roundy, S., Wright, P. K., & Rabaey, J. (2003). A study of low level vibrations as a power source for wireless sensor nodes. *Computer Communications, 26*, 1131-1144.

Saravanos, D. A., Heyliger, P. R., & Hopkins, D. A. (1997). Layerwise mechanics and finite element for the dynamic analysis of piezoelectric composite plates. *International Journal of Solids and Structures, 34*(3), 359-378.

Seifert, A., Greenblatt, D., & Wygnanski, I. J. (2004). Active separation control: An overview of Reynolds and Mach numbers effects. *Aerospace Science and Technology, 8*, 569-582.

Sekouri, E. M., Hu, Y.-R., & Ngo, A. D. (2004). Modeling of a circular plate with piezo-electric actuators. *Mechatronics, 14*, 1007-1020.

Sheng-li, Q., & Ai-shu, Z. (1984). On the problems of buckling of an annular thin plate. *Applied Mathematics and Mechanics (English Edition), 6*(2), 169-183.

Shi-rong, L. (1992). Nonlinear vibration and thermal-buckling of a heated annular plate with a rigid mass. *Applied Mathematics and Mechanics (English Edition), 13*(8), 771-777.

Shibaoka, Y. (1956). On the buckling of an elliptic plate with clamped edge i. *Journal of the Physical Society of Japan, 11*(10), 1088-1091.

Singh, J. P., & Dey, S. S. (1990). Variational finite difference approach to buckling of plates of variable stiffness. *Computers & Structures, 3*(1), 39-45.

Spencer, H. H., & Surjanhata, H. (1986a). On plate buckling coefficients. *Journal of Engineering Mechanics, 112*(3), 249-259.

Spencer, H. H., & Surjanhata, H. (1986b). The simplified buckling criterion applied to plates with partial edge loading. *Applied Scientific Research, 43*, 79-90.

Stavsky, Y., & Friedland, S. (1971). Buckling of composite circular plates under radial compression. *Acta Mechanica, 11*(1), 87-98.

Tani, J., & Yamaki, N. (1981). Elastic instability of a uniformly compressed annular plate with axisymmetric initial deflection. *International Journal of Non-Linear Mechanics, 16*(2), 213-220.

Thai-Hoang, C., Nguyen-Thanh, N., Nguyen-Xuan, H., & Rabczuk, T. (2011). An alternative alpha finite element method with discrete shear gap technique for analysis of laminated composite plates. *Applied Mathematics and Computation, 217*, 7324-7348.

Thevendran, V., & Wang, C. M. (1996). Buckling of annular plates elastically restrained against rotation along edges. *Thin-Walled Structures, 25*(3), 231-246.

Tiersten, H. F. (1969). *Linear Piezoelectric Plate Vibrations*: Plenum Press.

Touratier, M. (1991). An efficient standard plate theory. *International Journal of Engineering and Science, 29*(8), 901-916.

Touratier, M. (1992). A refined theory of laminated shallow shells. *International Journal of Solids and Structures, 29*(11), 1401-1415.

Tylikowski, A. (2001). Control of circular plate vibrations via piezoelectric actuators shunted with a capacitive circuit. *Thin-Walled Structures, 39*, 83-94.

Varelis, D., & Saravanos, D. A. (2004). Coupled buckling and postbuckling analysis of active laminated piezoelectric composite plates. *International Journal of Solids and Structures, 41*, 1519-1538.

Veldhuis, L. L. M., & Jagt, M. v. d. (2010). *Separation Postponement by means of Periodic Surface Excitation.* Paper presented at the 27th International Congress of the Aeronautical Sciences.

Ven, A. A. F. V. D. (1978). Magnetoelastic buckling of thin plates in a uniform transverse magnetic field. *Journal of Elasticity, 8*(3), 297-312.

Vidoli, S., & dell'Isola, F. (2001). Vibration control in plates by uniformly distributed pzt actuators interconnected via electric networks. *European Journal of Mechanics A/Solids, 20*, 435-456.

Wang, C. M., Wang, C. Y., & Reddy, J. N. (2004). *Exact solutions for buckling of structural members*: CRC Press.

Wang, C. Y. (2010). Buckling of a heavy standing plate with top load. *Thin-Walled Structures, 48*, 127-133.

Wang, Q., Quek, S. T., Sun, C. T., & Liu, X. (2001). Analysis of piezoelectric coupled circular plate. *Smart Material and Structures, 10*, 229-239.

Wu, T., Wang, Y., & Liu, G. (2002). Free vibration analysis of circular plates using generalized differential quadrature rule. *Computer Methods in Applied Mechanics and Engineering, 191*(5365-5380), 5365.

Xiang, Y., Wang, C. M., & Kitipornchai, S. (2003). Exact buckling solutions for rectangular plates under intermediate and end uniaxial loads. *Journal of engineering mechanics*, 129(7), 835-838.

Xu, R. Q. (2008). Three-dimensional exact solutions for the free vibration of laminated transversely isotropic circular, annular and sectorial plates with unusual boundary conditions. *Archive of Applied Mechanics, 78*, 543-558.

Yalcin, H. S., Arikoglu, A., & Ozkol, I. (2009). Free vibration analysis of circular plates by differential transformation method. *Applied Mathematics and Computation, 212*, 377-386.

Yang, I. H., & Shieh, J. A. (1987). Vibrations of initially stressed thick, rectangular, orthotropic plates. *Journal of Sound and Vibration, 119*(3), 545-558.

Yang, J. S., & Batra, R. C. (1995). Equations for the extension and flexure of relatively thin thermopiezoelectric plates subjected to large electric fields. *Defence Technical Information Center: Contemporary Research in Engineering Science*, 654-669.

You, D., & Moin, P. (2007). Study of flow separation over an airfoil with synthetic jet control using large-eddy simulation. *Center for Turbulent Research, Annual Research Briefs*.

Yu, C. (2003). Buckling of rectangular plates under intermediate and end loads. Unpublished Dissertation, National University of Singapore

Yu, L. H., & Wang, C. Y. (2009). Fundamental frequency of standing heavy plate with vertical simply-supported edges. *Journal of Sound and Vibration, 321*, 1-7.

Zhang, X. D., & Sun, C. T. (1999). Analysis of a sandwich plate containing a piezoelectric core. *Smart Material and Structures, 8*, 31-40.

Zheng, B., Chang, C.-J., & Gea, H. C. (2009). Topology optimization of energy harvesting devices using pieozelectric materials. *Structural and Multidisciplinary Optimization, 38*, 17-23.

Zhou, M. D., & Wygnanski, I. (2001). The response of a mixing layer formed between parallel streams to a concomitant excitation at two frequencies. *Journal of Fluid Mechanics, 441*, 139-168.

Zhu, D., Tudor, M. J., & Beeby, S. P. (2010). Strategies for increasing the operating frequency range of vibration energy harvesters: a review. *Measurement Science and Technology*, 21(2), 022001.

APPENDIX A: SAMPLE OF MATLAB CODE

A-1 MAIN CODE

```
clear all
close all
clc

%#####################################################################
% Material Definition ----------------------------------------------

% PIC151
s11=16.83e-12; %compliance
s33=19.0e-12;
s12=-5.656e-12;
s13=-7.107e-12;
s44=50.96e-12;
s66=44.97e-12;
d31=-2.14e-10; %piezoelectric constant
d33=4.23e-10;
d15=6.1e-10;
e11=17.134e-9; % dielectric coefficient
e33=18.665e-9;
rhop=7800; % density

nup=-s12./s11; % planar Poisson's ratio
kp=sqrt((2.*d31.^2)./(e33.*s11.*(1-nup))); %coupling coefficient

% brass alloy
muiso=0.34; %Poisson's ratio
E=110e9; %Young modulus
rho=8400; %density
alpha=19e-6; %thermal expansion
% ------------------------------------------------------------------

% Geometric Properties ---------------------------------------------

isothk=0.15e-003;
annthk=0.15e-003;
r_outer=40e-003;
r_inner=0.5*r_outer;
bendstiff=2*E*isothk^3/(3*(1-muiso^2)); %bending stiffness

% Material Properties
nu=0.346;              % poisson ratio
Famp=10;               % surface load
DA11=bendstiff;
DS11=DA11;
%-------------------------------------------------------------------

N11=5e3:2e2:2e6;
lambda=-1e3:2e3:5e11;
%#####################################################################
% Finite Difference Meshing ----------------------------------------
```

```
%   Setting for meshing
nlevels = input(' No. of grid levels = ');
k=nlevels;

% number of unknown for annular region
ka=k;                   % number of unknown for annular region
ks=ka;                  % number of unknown for solid region
% ka=input(' No. of grid levels ann = ');
% ks=input(' No. of grid levels circ = ');

if k==1
    na=5;
    ns=5;
else
    na = 2*2^ka - 1;         %  No. of interior grid points -
annular.
    ns = 2*2^ks - 1;         %  No. of interior grid points - solid.
end

% r_center=0.0013;
ha = (r_outer-r_inner)/(na+1);    % Grid spacing - annular.
hs = r_inner/(ns+1);                    % Grid spacing - solid.
ra = r_inner:ha:r_outer;                % Grid points - annular.
rs = hs/2:hs:r_inner;                     % Grid points - solid.
ra_interior = ra(1:na+1);               % Interior grid points -
annular
rs_interior = rs(1:ns+1);               % Interior grid points -
solid
r=[rs,ra];                              % radius (ammend annular
radius to solid circular radius)
theta=linspace(0,2*pi,30);              % angular direction

[row_rs,colomn_rs]=size(rs_interior);
[row_ra,colomn_ra]=size(ra_interior);
N = colomn_ra+colomn_rs+8; % size of matrix A (no. of interior nodes
+ no. of B.C)

% ------------------------------------------------------------------
%##################################################################
% Problems Analysis by FDM ----------------------------------------
% *** Setting-------------------------------------------------------
n=0; % axisymmetric
% n=1 % non-axisymmetric
F = Famp*ones(N,1); % load per node <--- use for static problem

% *** Static problem-----------------------------------------------
%  Solve linear system.
[matrixAh,bh]=subplate_static(n,N,na,hs,ha,r_inner,...
    rs_interior,ra_interior,DS11,DA11,nu,F);
% uh = matrixAh\bh;
[LA,UA] = lu(matrixAh);
uh = UA\(LA\bh);

% calculated deflection by FDM
Uh=[uh(3:colomn_rs+2);uh(N-2-na:N-1)];

% Theoretical Results Deflections - Static-------------------------
```

```
% analytical deflection (Reddy)
U_exact=Famp*(r_outer^4/(64*DS11)*(1-(r.^2)/r_outer^2).^2);
Utheory=U_exact';
Ucenter_th=U_exact(1)
Ucenter_FD=Uh(1)
Err_center_defl=(U_exact(1)-Uh(1))./U_exact(1)*100

% ***Buckling Load-----------------------------------------------------

% maxroots=1;
% fhandle=@(N11) subplate_buck(N11,n,N,na,hs,ha,r_inner,...
%     rs_interior,ra_interior,DS11,DA11,nu,F);
% [NbuckFD]=findroots(fhandle,N11,maxroots)
% buckfactorFD=NbuckFD*((r_outer^2)/DS11)

% % Theoretical Results
Nbuckclamped=14.682*DS11/(r_outer^2);
% Err_Nbuck=(Nbuckclamped-NbuckFD)/Nbuckclamped*100

% % applied at 0.7outerrad - ref: Aung Wang (2005), Buckling of
circular
% % plates under intermediate and edge load
% Nbuckintermediate=17.5866*DS11/(r_outer^2)

% ***Eigenfrequencies-------------------------------------------------
maxroots=1; % number of roots (nodal circle)
N11=0; % no influence from in-plane load
% N11=-0.25*Nbuckclamped; % under influence from in-plane load
fhandle=@(lambda) subplate_vibra(lambda,n,N,na,hs,ha,r_inner,...
    rs_interior,ra_interior,DS11,DA11,nu,F,N11);
[NatfreqFD]=findroots(fhandle,lambda,maxroots)

% % *** Natural Frequency - theoretical
lambdsqr=(r_outer^2)*sqrt(NatfreqFD)
% Err_lambd=(10.2158-lambdsqr)/10.2158*100

% omega=sqrt(NatfreqFD*DS11/(2*rho*isothk));
% omegaclamped=((10.2158)/(r_outer^2))*(sqrt(DS11/(2*rho*isothk)))

% freq=2*pi*omega;

%#####################################################################
% Plotting results ----------------------------------------------------

% *** for static problem ----------------------------------------------
% 1-D deflections result. Half Plate. Comparing analytical to FDM
result

figure(1)
% plot(r,Uh,'-^r',r,U_exact,'-ob')
plot(rs_interior(1:ns+1),uh(3:colomn_rs+2),'-sr',ra,uh(N-2-na:N-1),'-
^k',r,U_exact,'-ob')
hleg1 = legend('Uctr_{FD}','Uctr_{exact}');
xlabel('Radius, r (mm)')
xlabel('Radius, r (mm)')
ylabel('Deflection, w (mm)')
title('FD Solution')
```

A-2 DEFINING MATRIX COEFFICIENT

```
function [Det_matrixA]=subplate_vibra(lambda,n,N,na,hs,ha,r_inner,...
    rs_interior,ra_interior,DS11,DA11,nu,F,N11)

%#####################################################################
% Constructing matrix A of Ax=b

% defining matrix coefficients
% # solid circular
adiag_sol =
6+2*(hs^2)*(1./(rs_interior.^2)+(2*n^2)./(rs_interior.^2))...
    -((hs^4).*(n^2)./(rs_interior.^2)).*(4./(rs_interior.^2)-
(n^2)./(rs_interior.^2));
asub1_sol = -(4-2*hs./rs_interior...
    +(hs^2).*(1./(rs_interior.^2)+(2.*n^2)./(rs_interior.^2))...

+((hs^3)./(2.*rs_interior)).*(1./(rs_interior.^2)+2*(n^2)./(rs_interi
or.^2)));
asub2_sol = 1-hs./rs_interior;
asuper1_sol = -(4+2*hs./rs_interior...
    +(hs^2).*(1./(rs_interior.^2)+(2*n^2)./(rs_interior.^2))...
    -
((hs^3)./(2*rs_interior)).*(1./(rs_interior.^2)+2*(n^2)./(rs_interior
.^2)));
asuper2_sol = 1+hs./rs_interior;

% # annular
adiag_ann =
(hs^4/ha^4)*(DA11/DS11).*(6+2*(ha^2).*(1./(ra_interior.^2)+(2*n^2)./(
ra_interior.^2))...
    -((ha^4).*(n^2)./(ra_interior.^2)).*(4./(ra_interior.^2)-
(n^2)./(ra_interior.^2)));
asub1_ann = -(hs^4/ha^4)*(DA11/DS11)*(4-2.*ha./ra_interior...
    +(ha^2).*(1./(ra_interior.^2)+(2*n^2)./(ra_interior.^2))...

+((ha^3)./(2.*ra_interior)).*(1./(ra_interior.^2)+2*(n^2)./(ra_interi
or.^2)));
asub2_ann = (hs^4/ha^4)*(DA11/DS11).*(1-ha./ra_interior);
asuper1_ann = -(hs^4/ha^4)*(DA11/DS11).*(4+2.*ha./ra_interior...
    +(ha^2).*(1./(ra_interior.^2)+(2.*n^2)./(ra_interior.^2))...
    -
((ha^3)./(2.*ra_interior)).*(1./(ra_interior.^2)+2.*(n^2)./(ra_interi
or.^2)));
asuper2_ann = (hs^4/ha^4)*(DA11/DS11).*(1+ha./ra_interior);

%$$$$$$$$$$$$$$$$$$$$$$$$$$$$$$$$$$$$$$$$$$$$$$$$$$$$$$$$$$$$$$$$$$$
%     the following is used during construction of Matrix A, to make
sure
%     the correct value of radius enter the correct row

%     adiag_sol = rs_interior;
%     asub1_sol = rs_interior;
%     asub2_sol = rs_interior;
%     asuper1_sol = rs_interior;
%     asuper2_sol = rs_interior;
%
%     adiag_ann = ra_interior;
%     asub1_ann = ra_interior;
```

```
%     asub2_ann = ra_interior;
%     asuper1_ann = ra_interior;
%     asuper2_ann = ra_interior;

% raddiag_sol = rs_interior;
% raddiag_ann = ra_interior;
% raddiag = [0,0,raddiag_sol,0,0,0,0,raddiag_ann,0,0]';
%$$$$$$$$$$$$$$$$$$$$$$$$$$$$$$$$$$$$$$$$$$$$$$$$$$$$$$$$$$$$$$$$

Adiag = [0,0,adiag_sol,0,0,0,0,adiag_ann,0,0]';
Asub1 = [0,asub1_sol,0,0,0,0,asub1_ann,0,0,0]';
Asuper1 = [0,0,0,asuper1_sol,0,0,0,0,asuper1_ann,0]';
Asub2 = [asub2_sol,0,0,0,0,asub2_ann,0,0,0,0]';
Asuper2 = [0,0,0,0,asuper2_sol,0,0,0,0,asuper2_ann]';

%     Ah = spdiags([Asub6,Asub5,Asub4,Asub3,Asub2,Asub1,Adiag,...
%         Asuper1,Asuper2,Asuper3,Asuper4,Asuper5,Asuper6],...
%         [-(2*na) -(na+1) -(na) -(na-1) -2 -1 0 1 2 na-1 na na+1
2*na],N,N);
Ah = spdiags([Asub2,Asub1,Adiag,Asuper1,Asuper2],[-2 -1 0 1 2],N,N);
matrixA=full(Ah);

%#########################################################################
% **** In-plane Load

% In-plane load distribution
N11=-N11;
N22=N11;

nsub1_sol = -(hs^2)*(N11/DS11-(hs./(2.*rs_interior)).*N22/DS11);
ndiag_sol = -(-
(hs^2)*(2*N11/DS11+((n^2)*(hs^2)./(rs_interior.^2))*N22/DS11));
nsuper1_sol = -(hs^2)*(N11/DS11+(hs./(2.*rs_interior)).*N22/DS11);

nsub1_ann = -(hs^4)/(ha^2)*(N11/DS11-
(ha./(2.*ra_interior)).*N22/DS11);
ndiag_ann = -(-
(hs^4)/(ha^2)*(2*N11/DS11+((n^2)*(ha^2)./(ra_interior.^2))*N22/DS11))
;
nsuper1_ann = -
(hs^4)/(ha^2)*(N11/DS11+(ha./(2.*ra_interior)).*N22/DS11);

Ndiag = [0,0,ndiag_sol,0,0,0,0,ndiag_ann,0,0]';
Nsub1 = [0,nsub1_sol,0,0,0,0,nsub1_ann,0,0,0]';
Nsuper1 = [0,0,0,nsuper1_sol,0,0,0,0,nsuper1_ann,0]';

Nsparse = spdiags([Nsub1,Ndiag,Nsuper1],[-1 0 1],N,N);
matrixN=full(Nsparse);

%#########################################################################
% **** Vibration Term
[rrs,crs]=size(adiag_sol);
[rra,cra]=size(adiag_ann);

omdiag_sol = -(hs^4)*lambda*ones(1,crs); %lambda=(angular
freq)^2*density*thickness/DS11
omdiag_ann = -(hs^4)*lambda/DS11*ones(1,cra);
```

```
Omdiag = [0,0,omdiag_sol,0,0,0,0,omdiag_ann,0,0]';
matrixVib = diag(Omdiag);

%#####################################################################
%   Include the boundary condition

BCdiag      = zeros(N,1);
BCsub1      = zeros(N,1);
BCsuper1    = zeros(N,1);
BCsub2      = zeros(N,1);
BCsuper2    = zeros(N,1);

BCh = spdiags([BCsub2,BCsub1,BCdiag,BCsuper1,BCsuper2],[-2 -1 0 1
2],N,N);

% for static analysis
% BCh(N-5-na,:)=matrixA(N-7-na,:);
% for buckling analysis
% BCh(N-5-na,:)=matrixA(N-7-na,:)+matrixN(N-7-na,:);
% for free vibration
BCh(N-5-na,:)=matrixA(N-7-na,:)+matrixVib(N-7-na,:);
% for free vibration under influence of in-plane load
% BCh(N-5-na,:)=matrixA(N-7-na,:)+matrixN(N-7-na,:)+matrixVib(N-7-
na,:);

%%% Center of plate ---------------------------------------------------
BCh(1,1)=1.0*(hs^4);
BCh(1,4)=-((-1.0)^n)*(hs^4);
BCh(2,2)=1.0*(hs^4);
BCh(2,3)=-((-1.0)^n)*(hs^4);
%%%-------------------------------------------------------------------

%%% Matching condition ------------------------------------------------
% deflection - solid circular
BCh(N-7-na,N-7-na)=1.0*(hs^4);
% deflection - annular
BCh(N-7-na,N-7-na+5)=-1.0*(hs^4);

% slope - solid circular
BCh(N-6-na,N-6-na-2)=-(hs^3)*1.0/2.0;
BCh(N-6-na,N-6-na)=(hs^3)*1.0/2.0;
% slope - annular
BCh(N-6-na,N-6-na+3)=(hs^4/ha)*1.0/2.0;
BCh(N-6-na,N-6-na+5)=-(hs^4/ha)*1.0/2.0;

% effective shear force - solid circular
BCh(N-4-na,N-4-na-5)=-0.5*hs*(-1.0);
BCh(N-4-na,N-4-na-4)=-0.5*hs*(2.0+2.0*hs/r_inner+...
    (hs^2)*(1/(r_inner^2)+((2-nu)*n^2)/(r_inner^2))-(hs^2)*N11/DA11);
BCh(N-4-na,N-4-na-3)=-0.5*hs*(-4.0*hs/(r_inner)...
    +(2*(hs^3)*(3-nu)*n^2)/(r_inner^2));
BCh(N-4-na,N-4-na-2)=-0.5*hs*(-1.0)*(2.0-2.0*hs/r_inner+...
    (hs^2)*(1/(r_inner^2)+((2-nu)*n^2)/(r_inner^2))-(hs^2)*N11/DA11);
BCh(N-4-na,N-4-na-1)=-0.5*hs*(1.0);
% effective shear force - annular
BCh(N-4-na,N-4-na)=-(DA11/DS11)*(hs^4/ha^3)*(-0.5*(-1.0));
BCh(N-4-na,N-4-na+1)=-(DA11/DS11)*(hs^4/ha^3)*(-
0.5*(2.0+2.0*ha/r_inner+...
```

```
    (ha^2)*(1/(r_inner^2)+((2-nu)*n^2)/(r_inner^2))-
(ha^2)*N11/DA11));
BCh(N-4-na,N-4-na+2)=-(DA11/DS11)*(hs^4/ha^3)*(-0.5*(-
4.0*ha/(r_inner)...
    +(2*(ha^3)*(3-nu)*n^2)/(r_inner^2)));
BCh(N-4-na,N-4-na+3)=-(DA11/DS11)*(hs^4/ha^3)*(-0.5*((-1.0)*(2.0-
2.0*ha/r_inner+...
    (ha^2)*(1/(r_inner^2)+((2-
nu)*n^2)/(r_inner^2)))+(ha^2)*N11/DA11));
BCh(N-4-na,N-4-na+4)=-(DA11/DS11)*(hs^4/ha^3)*(-0.5*(1.0));

% bending moment - solid circular
BCh(N-3-na,N-3-na-5)=-(hs^2)*(1-(nu*hs)/(2*r_inner));
BCh(N-3-na,N-3-na-4)=-(hs^2)*(-(2+(nu*(n^2)*(hs^2))...
    /(r_inner^2)));
BCh(N-3-na,N-3-na-3)=-(hs^2)*(1+(nu*hs)/(2*r_inner));
% bending moment - annular
BCh(N-3-na,N-3-na)=-(-(hs^4/ha^2)*(DA11/DS11)*(1-
(nu*ha)/(2*r_inner)));
BCh(N-3-na,N-3-na+1)=-(-(hs^4/ha^2)*(DA11/DS11)*(-
(2+(nu*(n^2)*(ha^2))...
    /(r_inner^2))));
BCh(N-3-na,N-3-na+2)=-(-
(hs^4/ha^2)*(DA11/DS11)*(1+(nu*ha)/(2*r_inner)));
%%%--------------------------------------------------------------------

%%% Outer edge of plate ----------------------------------------------
% displacement - annular
BCh(N-1,N-1)=(hs^4)*1.0;

% slope - annular
BCh(N,N-2)=(hs^4/ha)*(-1.0)/2.0;
BCh(N,N)=(hs^4/ha)*1.0/2.0;
%%%--------------------------------------------------------------------

matrixA(N-7-na,1:N)=zeros(1,N);
matrixN(N-7-na,1:N)=zeros(1,N);
matrixVib(N-7-na,1:N)=zeros(1,N);
matrixBC=full(BCh); % matrix with only Boundary Conditions

%####################################################################
% ***full matrix of coefficient matrix-------------------------------

% for static analysis
% matrixAh=matrixA+matrixBC*(1);

% for buckling analysis
% matrixAh=matrixA+matrixBC+matrixN;

% for free vibration analysis
% matrixAh=matrixA+matrixBC+matrixVib;

% for free vibration analysis under influence of in-plane load
matrixAh=matrixA+matrixBC+matrixN+matrixVib;

%####################################################################
% %  Set up r.h.s. vector b by stacking columns of h^4*F. This
corresponds to
```

```
% %  lexicographical column ordering of the grid points.
%
% bh = (hs^4)*F/DS11;
% bh(1)=0.0;
% bh(2)=0.0;
% bh(N-7-na)=0.0;
% bh(N-6-na)=0.0;
% bh(N-4-na)=0.0;
% bh(N-3-na)=0.0;
% bh(N-1)=0.0;
% bh(N)=0.0;

%#####################################################################
% Calculate the determinant of the coefficient matrix
Det_matrixA=det(matrixAh)

end
```